

# Minimization of the Effect of Cross Phase Modulation in a WDM Optical Transmission System

by

Kazi Abu Taher

A thesis submitted to the Department of Electrical and Electronic Engineering of  
Bangladesh University of Engineering and Technology  
in partial fulfillment of the requirement for the degree of

**MASTER OF SCIENCE IN ELECTRICAL AND ELECTRONIC ENGINEERING**



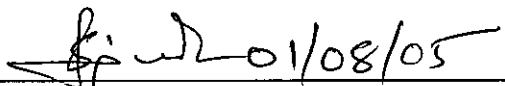


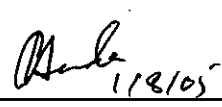
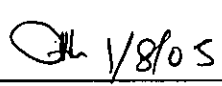
Department of Electrical and Electronic Engineering  
BANGLADESH UNIVERSITY OF ENGINEERING AND TECHNOLOGY

2005

## APPROVAL CERTIFICATE

The thesis titled " Minimization of the effect of Cross Phase Modulation in a WDM optical transmission system" Submitted by Kazi Abu Taher, Roll No:040306249F, Session: April 2003 has been accepted as satisfactory in partial fulfillment of the requirement for the degree of Master of Science in Electrical engineering of August 01, 2005.

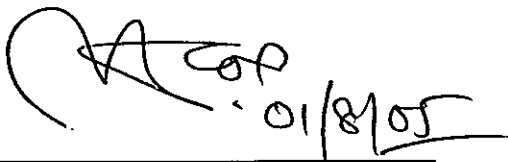
### BOARD OF EXAMINERS

1.   
\_\_\_\_\_
- Dr. Satya Prasad Majumder  
Professor  
Department of Electrical and Electronic Engineering  
BUET, Dhaka-1000, Bangladesh  
Chairman
  
2.   
\_\_\_\_\_
- Dr. S. Shahnawaz Ahmed  
Professor & Head  
Department of Electrical and Electronic Engineering  
BUET, Dhaka-1000, Bangladesh  
Member  
(Ex-Officio)
  
3.   
\_\_\_\_\_
- Dr. Md Saifur Rahman  
Professor  
Department of Electrical and Electronic Engineering  
BUET, Dhaka-1000, Bangladesh  
Member
  
4.   
\_\_\_\_\_
- Dr. Md. Quamrul Huda  
Associate Professor  
Department of Electrical and Electronic Engineering  
BUET, Dhaka-1000, Bangladesh  
Member
  
5.   
\_\_\_\_\_
- Mohammad Abdul Moqaddem  
Deputy General Manager  
Billing System  
Teletalk Bangladesh Ltd.  
Banana, Dhaka  
Member  
(External)

## DECLARATION

It is hereby declared that this thesis or any part of it has not been submitted elsewhere for the award of any degree or diploma.

Signature of the candidate



---

Kazi Abu Taher

**DEDICATED TO MY PARENTS**

## TABLE OF CONTENTS

Declaration	ii
Table of contents	iv
List of figures	vii
List of tables	xi
List of symbols	xii
List of abbreviation	xiii
Acknowledgements	xv
Abstract	xvi

### CHAPTER 1: Introduction

1.1	Communication System	1
1.2	Evolution of Optical Communication	2
1.3	Review of Previous Works	5
1.4	Research Aims	13
1.5	Outline of the Thesis	13

### CHAPTER 2: Optical Communication and Nonlinear Effects

2.1	Principles of Optical Communication	15
	2.1.1 Optical Transmitter	15
	2.1.2 Optical Fiber	16
	2.1.3 Optical Receiver	16
2.2	Wavelength Division Multiplexing (WDM) and Dense WDM (DWDM)	17
2.3	Fundamentals of Nonlinear Effects in Optical Fibers	18
	2.3.1 Stimulated Brillouin Scattering (SBS)	18
	2.3.2 Stimulated Raman Scattering (SRS)	19

2.3.3 Optical Kerr Effect	20
2.3.3.1 Self-Phase Modulation (SPM)	20
2.3.3.2 Cross-Phase Modulation (XPM)	21
2.3.3.3 Four-Wave Mixing (FWM)	23
2.4 Summary	25

## CHAPTER 3: Theoretical Analysis of Optical Line Coding

3.1 Introduction	26
3.2 Duobinary Line Code	27
3.2.1 Differential Encoding	29
3.2.2 Differential Encoder	30
3.2.3 Optical System for Duobinary Modulation	31
3.3 A Multi-Level Novel Optical Line Code	32
3.3.1 First Order Code	33
3.4 Summary	36

## CHAPTER 4: Theoretical Analysis of XPM on a WDM System

4.1 Introduction	37
4.2 Block System Diagram	37
4.3 Theoretical Analysis of XPM	39
4.3.1 Input and Output Power Representation	39
4.3.2 Bit Error Rate (BER) Derivation	43
4.4 Applying Line Coding Schemes	44
4.4.1 Applying Duobinary Line Coding Schemes	44
4.4.2 Applying Novel Optical Line Coding Schemes	45
4.5 Summary	45

## CHAPTER 5: Simulation Methods

5.1	Introduction	46
5.2	Split Step Fourier Method	46
5.2.1	Light Waves Beam Propagation Method using Split Step Model	47
5.2.2	Algorithm for the Split Step Model	50
5.3	Eye-opening Penalty	52
5.4	Filter Design	53
5.5	Summary	54

## CHAPTER 6: Simulation Results and Discussions

6.1	Introduction	55
6.2	Simulation Results for XPM in the DWDM System	55
6.3	Discussions	74
6.4	Summary	75

## CHAPTER 7: Conclusion and Recommendations for Future Work

7.1	Conclusion of this Study	76
7.2	Recommendations for Future Work	77
	References	78

## List of Figures

Figure 2.1:	Optical fiber communication system	15
Figure 2.2:	Block Diagram of an Optical Transmitter	16
Figure 2.3:	Block Diagram of an Optical Receiver	17
Figure 2.4:	Graphical Representation of a Point to Point WDM Optical System	17
Figure 2.5:	Experimental Setup to Demonstrate the Effects of XPM	22
Figure 2.6:	Illustration of Walk-off Distance	24
Figure 2.7:	Illustration of Side-Bands Generation due to FWM in Two-Channel Systems	25
Figure 3.1:	Duobinary Encoder	29
Figure 3.2:	Differential Encoder with an XOR Gate	30
Figure 3.3:	Differential Encoder with a Divide-by-2 Counter	30
Figure 3.4:	Effect of Dispersion on NRZ and Duobinary Sequences	31



Figure 3.5:	(a) An Example Showing the Transformation of Data in a Duobinary System and (b) NRZ and Duobinary Signal for Data Sequence [1 0 1 0 0 0 1 1 1 1 0 1 0 1 0 1]	32
Figure 3.6:	(a) Elementary Signals and (b) Code State Diagram for Novel Multilevel Optical Line Code of Order one [40].	33
Figure 3.7:	Transmitter Model of an optical system	34
Figure 3.8:	An Example Showing NRZ and Duobinary Signals for Data Sequence [0 1 1 0 0 0 1 1 1 1 0 1 0 1 0 1]	35
Figure 4.1:	System Block Diagram (IM-DD): (a) without line coder	38
Figure 4.2:	Direct detection system of a optical system.	39
Figure 5.1:	Schematic Illustration of Symmetrized Split Step Model	49
Figure 5.2:	(a) Frequency and (b) Magnitude Response of a Butterworth Low-pass Filter	54
Figure 6.1:	(a) Normalized IM index in dB and (b) phase response versus the pump modulation frequency for the channel separations of 0, 0.25 and 4 nm. The average power per channel is 0 dBm. Here $\lambda_1=1550$ nm, $D = 17$ ps/km-nm, $\gamma_1 = 1.18$ W <sup>-1</sup> . km <sup>-1</sup> , $\alpha = 0.21$ dB/km and $L = 80$ km.	56
Figure 6.2	Total XPM induced power in a lossless system with probe power $P_1 = 0$ dBm, bit rate = 10 GHz, channel spacing = 50 GHz and fiber length = 50, 100 and 150 km for pump power ( $P_2$ ) = (a) -20 to 20 and (b) -10 to 10 dBm	57

Figure 6.3	Total XPM induced power in a lossless system with pump power $P_2 = 0$ dBm, bit rate = 10 GHz, channel spacing = 50 GHz and fiber length = 50, 100 and 150 km for probe power ( $P_1$ ) = (a) -20 to 20 and (b) -10 to 10 dBm.	58
Figure 6.4	Total XPM induced power for a lossy system with probe power $P_1 = 0$ dBm, bit rate = 10 GHz, channel spacing = 50 GHz and fiber Length = 50, 100 and 150 km.	59
Figure 6.5	Total XPM power in dB for different (a) probe powers (0, -5 and -10 dBm) and (b) pump powers (-10, -5 and 0 dBm) at 100 km	60
Figure 6.6	Plot of BER for channel spacing 50, 60, & 75 and 100 GHz with $P_2 = 0$ dBm, fiber length = 100 km and bit rate = 10 GHz	61
Figure 6.7	XPM Power with line coding, (a) analytical result for pump power = -10 and 0 dBm and (b) simulated result for probe power = -10 and 0 dBm with fiber length = 100 km, bit rate = 10 GHz and channel spacing = 50 GHz.	63
Figure 6.8	(a) Analytical (b) Simulated BER for different probe powers -10, -5, 0, 5 and 10 dBm at 100 km with bit rate = 10 GHz and channel spacing = 50 GHz.	64
Figure 6.9	(a) Analytical (b) Simulated BER for different pump powers -10, -5, 0, 5 and 10 dBm at 100 km	65
Figure 6.10	Plot of (a) XPM induced power and (b) BER caused by XPM with NRZ data, Duobinary and Novel Order 1 Code for probe power -10, -5, 0, 5 and 10 dBm for 100 km fiber.	66

Figure 6.11	Plot of (a) XPM induced power and (b) BER caused by XPM with NRZ data, Duobinary and Novel Order 1 Code for pump power -10, -5, 0, 5 and 10 dBm for 100 km fiber.	67
Figure 6.12	Plot of allowable pump power for BER of $10^{-9}$ at 50, 100 and 150 k	68
Figure 6.13	Plot of allowable probe power for BER of $10^{-9}$ at 50, 100 and 150 km	69
Figure 6.14	Plot of 512 bit (PRBS) eye-power penalty of NRZ data for 25, 50, 75, 100, 125 and 150 km	70
Figure 6.15	Plot of 512 bit (PRBS) eye-power penalty of Duobinary coded data for 25, 50, 75, 100, 125 and 150 km	71
Figure 6.16	Plot of 512 bit (PRBS) eye-power penalty of Novel Optical coded data for 25, 50, 75, 100, 125 and 150 km	72
Figure 6.17	Plot of Theoretical normalized IM index in dB as a function of the pump modulation frequency in 10 and 20 fiber segment fiber links of DSF without DC and with distributed and lumped DC. The average power per channel at fiber input is 0 dBm and the channel separation is 0.8 nm.	74

## List of Tables

Table-3.1:	Encoding Rule of Novel Optical Line Code (Order 1)	34
Table 6.1:	Improvement in allowable pump power in dB by applying Novel line code in comparison with NRZ data for BER of $10^{-9}$ at different lengths	68
Table 6.2:	Improvement in allowable probe power in dB by applying Novel line code in comparison with NRZ data for BER of $10^{-9}$ at different lengths	69
Table 6.3:	Eye power penalty for pump power of 0 dBm and probe power of -10 dBm	73

## List of Symbols

$\alpha$	Attenuation constant
$\beta$	Propagation constant
$n$	Fiber refractive index
$\eta$	Efficiency of cross phase modulation
$\phi$	Propagation phase
$\omega$	Angular frequency
$\gamma$	Fiber nonlinear coefficient
$L$	Fiber length
$L_{eff}$	Effective length of fiber
$D$	Fiber chromatic dispersion
$A_{eff}$	Effective core area of fiber
$c$	Speed of light
$\lambda$	Wavelength
$R$	Photo-detector's responsivity
$\eta_q$	Quantum efficiency of photo-detector
$N_{th}$	Thermal noise
$N_{sh}$	Shot noise
$erfc$	Complementary error function
$\eta_{xpm}$	XPM efficiency
$B_e$	Electrical bandwidth of the receiver
$v_g$	Group velocity
$\varphi(\omega)$	Phase retardation
$\gamma_1$	Nonlinear coupling coefficient

## List of Abbreviations

ABI	Alternate-block-inversion
APD	Avalanche Photodiode
BER	Bit Error Rate
CCR	Carrier to crosstalk ratio
CW	Continuous Wave
DCF	Dispersion Compensating Fiber
DeMUX	Demultiplexer
DSF	Dispersion Shifted Fiber
DWDM	Dense Wavelength Division Multiplexing
EDFA	Erbium-Doped Fiber Amplifier
EOP	Eye-opening Penalty
FDM	Frequency Division Multiplexing
FIR	Finite impulse response
FWM	Four-Wave Mixing
GVD	Group velocity dispersion
ISI	Inter Symbol Interference
IM/DD	Intensity modulation/ direct detection
IrDI	Inter-domain interfaces
LASER	Light Amplification by Stimulated Emission of Radiation
LECAF	Large Effective Core Area Fiber
LED	Light Emitting Diode
MUX	Multiplexer
MMI	Monospaced-mark-inversion
MZ	Mach-Zehnder
NDSF	Non Dispersion Shifted Fiber
NLSE	Nonlinear Schrödinger equation
NRZ	Non-return to zero

NZ-DSF	Non Zero Dispersion Shifted Fiber
NZDSF	Non-Zero Dispersion Shifted Fiber
PASS	Phased amplitude-shift signaling
PM	Phase modulation
SBS	Stimulated Brillouin Scattering
SPM	Self Phase Modulation
SMF	Single Mode Fiber
SNR	Signal-to-Noise Ratio
SRS	Stimulated Raman Scattering
WDM	Wavelength Division Multiplexing
XPM	Cross Phase Modulation

## Acknowledgements

I am highly pleased to express my sincere and profound gratitude to my supervisor Dr. Satya Prasad Majumder, Professor, Department of Electrical and Electronic Engineering (EEE), Bangladesh University of Engineering and Technology, Dhaka, for providing me the opportunity to conduct graduate research in optical communications. I wish my hearty thanks to him for his continuous guidance, suggestions and wholehearted help throughout the course of the work.

I would like to express my special thanks to Muhammad Anisuzzaman Talukder, Assistant Professor, Department of EEE, BUET and Afreen Azhari, M. Sc. student, Department of EEE, BUET for their generous support by providing materials related to my research work.

I would also like to thank my colleague Lieutenant Colonel Akhteruzzaman Siddiqi, pse, te, Signals, Commanding Officer, 5 Signal Battalion, Comilla Cantonment and Mohammd Quadrat-E-Maula, Assistant Professor, Department of Computer Science and Electronic, Jahangirnagar University, Dhaka for their support and continuous encouragement. I am also thankful to all personnel of departmental library, BUET reference library and Xerox section. As a member of IEEE, I received enormous support from the online Digital Library of IEEE. I would like to express my heartfelt gratitude to all the unseen contributors.

I like to express my deepest gratitude to my wife Rehana Akhter, my beloved daughters: Nidhi and Diya, and other family members for their invaluable encouragement and patience.

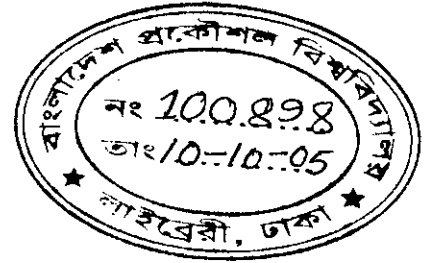
Finally, I am grateful to Almighty Allah for enabling me to complete the thesis.



## **Abstract**

Cross phase modulation (XPM) is the most serious effect that limits the allowable input power and system capacity by generating intensity modulated power causing more noise at the receiver in long-haul multi-channel light-wave DWDM transmission system. In this thesis line coding schemes are applied to combat the effect of XPM in a DWDM optical system. Multilevel line coding schemes like duobinary and Novel optical line codes are analyzed in detail to get an insight to their effect in data transmission. The XPM effect is also analyzed to quantify its effect in terms of realizable parameters. Performance criteria are expressed in terms of bit error rate (BER) and eye-opening penalty (EOP). Performances of line coding are evaluated for different parameters like different fiber lengths, channel spacing and input powers. Analytical and simulated results show 1.89 dB improvements in terms of input power.

## CHAPTER 1 INTRODUCTION



### 1.1 Communication System

A communication system transmits information or message like voice, video, text, etc. from one place to another. Communication systems exchange signals between two or more entities in a form suitable to process and manipulate most economically. The basic principle of a communication system remains the same for different types of systems. The basic principle of a communication system is to bridge two entities at different locations. A communication system consists of many components which take part in the system activity and perform its part in a definite sequence. The function of each component of a communication system is to assist transmit the information from the source to the destination over the transmission medium with least possible distortion and attenuation. However, in any communication system with the best possible design parameters, the received signal will fall short of the true duplication of the transmitted signal.

A typical communication system consists of three basic components; transmitter, transmission medium and receiver. A transmitter receives the information from the source and transforms it into suitable form conforming to the transmission medium. The transformed information is called signal. The design parameters of the transmitter mainly takes into consideration of the facts like power, distance, type of data, bandwidth, type of the transmission medium, operating frequency, etc.

The transmission medium bridges the distance between the source and the receiver. It is the component of a communication system that determines many important aspects of the transmitter, the receiver and signal flow. As signal propagates through the medium it gets attenuated due to interaction between the signal and the

medium. The signal also gets distorted due to nonlinear characteristics of the medium and other interferences. The transmission medium may be of various types. It includes physical and non-physical media. Physical media includes copper wire, coaxial cable, optical fiber, etc. The non-physical media includes links at various frequencies like high frequency, very high frequency, microwave, etc.

The receiver transforms the signal into information that travels up to it through the transmission medium. The receiver performs all necessary steps to ensure that the received information is a faithful copy of the original information and provides required energy level to be passed to the destination.

Electrical communication systems became the first dominant modern communication method since the advent of telegraphy in the 1830s. Until the early 1980s, most of the fixed (non-radio) signal transmission was carried by metallic cable (twisted wire pairs and coaxial cable) systems. However, large attenuation and limited bandwidth of coaxial cable limited its capacity upgrade. The bit rate of the most advanced coaxial system which was put into service in 1975 was 274 Mb/s. At around the same time, there was a need of conversion from analogue to digital transmission to improve transmission quality, which requires further increase of transmission bandwidth. Many efforts were made to overcome the drawbacks of coaxial cable during the 1960s and 1970s. After the invention of wireless communication system, signals could be transmitted through the atmosphere using the suitable frequencies as carrier. But the available frequency bandwidth could not meet the growing demands of communication bandwidth.

## **1.2 Evolution of Optical Communication**

Even though an optical communication system had been conceived in the late 18th century by a French Engineer Claude Chappe who constructed an optical telegraph, electrical communication systems remained the dominant means of communication. In 1966, Kao and Hockham proposed the use of optical fiber as a guiding medium for the optical signal [2]. Four years later, a major breakthrough occurred when the fiber loss

was reduced to about 20 dB/km from previous values of more than 1000 dB/km by applying improved fiber manufacture design techniques. Since that time, optical communication technology has developed rapidly to achieve larger transmission capacity and longer transmission distance. The capacity of transmission has been increased about 100 fold in every 10 years.

There were several major technological breakthroughs during the past two decades to achieve such a rapid development. In 1980, the bit rate used was 45 Bb/s with repeater spacing of 10 km. The multimode fiber was used as the transmission medium and GaAs LED as the source of the system. In 1987 the bit rate was increased to 1.7 Gb/s with repeater spacing of 50 km. By 1990 the bit rate was increased to 2.5 Gb/s with repeater spacing further increased to 60-70 km. Dispersion shifted fibers are used to minimize the bit error rate and to increase the repeater spacing and the bit rate.

In 1996 the bit rate of the optical transmission system was increased to 5 Gb/s. The development of optical amplifiers brought another important break through in optical communication system. Optical amplifiers reduced the associated delay and power requirement of the electronic amplifiers. Wavelength division multiplexing (WDM) was also introduced at this time to increase the available bandwidth capacity in terms of the channels. By 2002, the bit rate of the optical system was increased to 10 Gb/s with repeater spacing of 70-80 km. The introduction of the dense DWDM (DWDM) system increased the channel capacity and the bit rate got increased to 40 GB/s.

The first generation of optical communication was designed with multi-mode fibers and direct band gap GaAs light emitting diodes (LEDs) which used to operate at the 0.8  $\mu\text{m}$ - 0.9  $\mu\text{m}$  wavelength range. Compared to the typical repeater spacing of coaxial system ( $\sim 1\text{km}$ ), the longer repeater spacing ( $\sim 10\text{km}$ ) was a major motivation. Large modal dispersion of multi-mode fibers and high fiber loss at 0.8  $\mu\text{m}$  ( $> 5\text{dB/km}$ ) limited both the transmission distance and bit rate. In the second generation, multi-mode fibers were replaced by single-mode fibers, and the center wavelength of light sources was shifted to 1.3  $\mu\text{m}$ , where optical fibers have minimum dispersion and lower loss of about 0.5 dB/km.

However, there was still a strong demand to increase repeater spacing further, which could be achieved by operating at 1.55  $\mu\text{m}$  where optical fibers have an intrinsic minimum loss around 0.2dB/km. Larger dispersion in the 1.55  $\mu\text{m}$  window delayed moving to a new generation until dispersion shifted fiber became available. Dispersion shifted fibers reduced the large amount of dispersion in the 1.55  $\mu\text{m}$  window by modifying the index profile of the fibers while keeping the benefit of low loss at the 1.55  $\mu\text{m}$  window. However, growing communication traffic and demand for larger bandwidth per user revealed a significant drawback of electronic regenerator systems. Because all the regenerators are designed to operate at a specific data rate and modulation format, all of them needed to be replaced to convert to a higher data rate.

The difficulty of upgradeability has finally been removed by optical amplifiers, which led to a completely new generation of optical communication. An important advance was that an erbium-doped single mode fiber amplifier (EDFA) at 1.55  $\mu\text{m}$  was found to be ideally suited as an amplifying medium for modern fiber optic communication systems. Invention of the EDFA had a profound impact especially on the design of long-haul undersea systems. Trans-oceanic systems installed like TAT (Transatlantic Telephone)-12/13 [3] and TPC (Transpacific Crossings)-5 [4] were designed with EDFAs, and the transmission distance reaches over 8000 km without electronic repeaters between terminals. The broad gain spectrum (3~4THz) of an EDFA also makes it practical to implement wavelength-division-multiplexing (WDM) systems.

It is highly likely that DWDM systems will bring another big leap of transmission capacity of optical communication systems. Some research groups have already demonstrated that it is possible to transmit almost a Tbits/s bit rate over thousands of kilometers. There are some important experimental results of DWDM systems [5-10]. In 1999, a channel system was simulated experimentally with bit rate of 20 Gb/s. The system could cover 10,000 km with amplifier spacing of 50 km. The signal format used here was of soliton type. Later the number of channels was increased to 20 with NRZ type signal format. In 1997 the number of the channels was increased 32 with 45 km amplifier spacing and the distance covered was 9,300 km. In this system NRZ and soliton type signal format were used. In 1998, the number of the channels was increased to 64

at the cost of reduced transmission distance of 500 km with 100 km amplifier spacing. However by 1999 the distance could be extended to 7,200 km with 64 channel system and 10 Gb/s bit rate at the cost of reduced amplifier spacing of 50 km. In 2004, the bit rate was increased to 40 Gb/s at the cost of reduced number of channels of 34 which could cover a distance of 6,380 km.

For example, N. Bergano et al. successfully demonstrated transmission of 640 Gb/s over 7200km using a re-circulating loop [9] while G. Vareille et al. demonstrated the transmission capacity of 340 Gb/s over 6380 km on a straight-line test bed [10]. These results indeed show that remarkable achievements have been made in recent years, and let us forecast that optical communication systems in the next generation will have a transmission capacity of a few hundreds of Gb/s.

### **1.3 Review of Previous Works**

In 1994 Chraplyvy described optical nonlinearities namely the stimulated Raman, stimulated Brillouin, four wave mixing (FWM) and carrier induced phase noise in the context of lightwave system limitations. In 1994 together with Marcuse and Tkach concluded that XPM did not limit the number of wavelength channels that a single optical fiber can support [11].

Chiang, Kagi, Fong, Marhic and Kazovsky (1994) and Chiang, Kagi, Marhic and Kazovsky (1996) have inspired many others for this research [12-13]. They presented a detailed investigation theoretically and experimentally of the impact of modulation frequency to XPM in dispersive fibers. In the case of fibers with multiple optical amplifiers, the XPM induced phase shift is smaller in system employing lumped dispersion compensation than in systems employing distributed dispersion compensation. They also concluded that in non-dispersive fibers XPM is frequency independent, while in dispersive fibers XPM frequency response is approximately inversely proportional to the product of frequency, fiber dispersion and wavelength separation.

With the application of Erbium-doped fiber amplifiers (EDFA), the fiber loss can be compensated periodically [14]. Hence, fiber loss is no longer a limiting factor in long-haul optical communication system. Fiber nonlinearities if not properly addressed, may adversely affect system performance. This reality stirs up research interests in this field, which leads to understanding nonlinear phenomenon, making attempts of quantifying and reducing their affects in DWDM optical communication. Marhic, Yang, Akasaka and Kazovsky (1999) proposed replacing EDFA by Distributed Raman Amplification (DRA) along the transmission fiber. They suggested using a Raman pump Modula at the transmitting end and reducing the transmitted power so that the received power remains the same. Hence lower transmitter powers would be possible and this would help reduce fiber nonlinear effects during transmission.

Cartaxo (1998 and 1999) accepted the pump-probe format investigating the impact of modulation frequency on XPM but extended it to IM/DD WDM systems [15-16]. At very low modulation frequency, the walk off effect does not affect the XPM-induced IM efficiency but at higher frequency it significantly reduced it. Kim, Han and Chung (2001) [17] reported the effect of SRS on hybrid WDM systems. Experimental results were compared with theoretical values and it was shown that the SRS induced crosstalk increased with wavelength separation. The results were used to estimate the scalability of hybrid WDM systems. The carrier to crosstalk ratio (CCR) was also presented for CATV systems taking SRS, XPM and Optical Kerr effect into account.

Djordjevic (2001) [18] derived simple expressions for maximum transmission length for dispersion compensated links using inline optical amplifiers, The non linearity's taken into consideration in the presence of ASE noise were FWM and SRS. Djordjevic investigated different dispersion compensation configurations and determined that the ZDSF and CF combination gives the maximum transmission distance while the CF and DCF could provide much denser packaging. He also showed that as the number of channels increase, the transmitting distance and the total bandwidth for optimum channels spacing decreases. He showed that the total transmitter distance is dependant on the bit rate.

Norimatsu and Yamamoto (2001) [19] studied the influence of SRS on wideband transmission systems taking into account the random modulation and the walk-off. It was shown that the power depletion due to SRS could be separated into the average power loss and the waveform distortion. Simple equations that described the GVD were derived and the waveform distortion due to SRS can be evaluated in short calculation for different system parameters such as channel allocation, bit rate, fiber input power, effective core area of fiber and so on. The evaluations were done on various types of fibers such as DSF, SMF, Large Effective Core Area Fiber (LECAF) and NZDSF and it was shown that the waveform distortion of the rectangular NRZ pulses in SMF were smaller than that in LECAF.

In 1998, Belloti, Varani, Francia and Bononi, made a new linear model for the XPM induced intensity distortion on a CW probe in a dispersion compensated transmission system [20]. The model succeeds in capturing the interaction between XPM and group velocity dispersion (GVD) hence giving an accurate prediction within the applicability model range. In this model, XPM induced intensity modulation can be treated as additive intensity noise giving allowance for SPM effects extensions. This model is of great value in the search for optimized dispersion maps. Bigo, Belloti and Chbat (1999) studied the impact of XPM on the transmission performance of a 2x10 Gb/s multiplex. They have characterized the impact over four types of fiber infrastructures namely NZDSF-, DSF, NZDSF+ and SMF+DCF. The outcome of their study concluded that dispersion-compensated single mode fiber is virtually not affected by XPM down to 50 GHz-channel spacing.

Kowalewski, Marciniak and Sedlin in 2000 [21] reported an investigation of optical crosstalk caused by nonlinear interactions in short and long haul WDM transmission systems called inter-domain interfaces (IrDI). IrDI is a 16-Channel WDM interface that is to be used to connect two sub-networks belonging to different administrative domains. By using the parameters proposed by ITU, simulations on various nonlinear effects (FWM, SPM, XPM, stimulated Raman, stimulated Brillouin and nonlinear interactions in EDFA) showed that XPM and FWM greatly influenced the efficiency of IrDI transmission systems.



However, dispersion management can be used to combat these effects effectively. For NRZ signal formats, estimates of the penalty can be obtained from calculations of the distortion of a CW probe channel, permitting the effect of XPM to be isolated from other impairments. The pump-probe technique allows rapid optimization of the link design to minimize XPM penalties.

In single mode fiber links, the pulse broadening effect of self phase modulation (SPM) severely affects the transmission distance. Lakoba and Agrawal (2000) [22] investigated the performance of dispersion maps for long haul soliton data. An effort was made to find the maximum allowed range of values for the average dispersion. They showed that positive residual dispersion can be used to counter the effects of pulse broadening. The use of positive residual dispersion effectively minimized XPM induced distortion and also reduces pulse broadening due to SPM.

Ten, Ennser, Grochosinski, Burtsev and Silva [23] compared the FWM and XPM impairments in a dense WDM system and examined the impact of different fiber dispersion slopes and effective areas. XPM and FWM were considered as noise like impairments. From the analysis done, they showed that XPM dominates FWM across the entire channel plan for all types of fibers. Increasing the fiber effective area decreases the FWM and XPM variance uniformly for all channels and reducing the dispersion slope allows for better XPM compensation resulting in smaller Q variations with wavelength.

Betti, Giaconi and Nardini (2003) [24], presented a statistical analysis that takes into account both the effect on the FWM inter-modulation products due to dispersive propagation, and the statistics of such inter-modulation terms, which are considered as random processes. The autocorrelation function of the FWM process was calculated for the independent wavelength division multiplexing optical channel. The fiber propagation of WDM signals affected by FWM was analyzed and it was shown that the penalty values due to the FWM effect result lower than the ones obtained by analytical models considering unmodulated optical signals.

Thiele, Killey and Bayvel (1999) [25] investigated the effects of pre and post compensation in high capacity WDM systems with large inter amplifier spacing. They measured spectral broadening by using a gated, scanning interferometer. It was shown that in the case of post compensation, the eye closure was more rapid in the post compensated case, where the SPM chirp acquired led to additional pulse broadening. With 4 channel transmission little change was kin the SPM penalty was observed. This was attributed to the XPM induced timing jitter and to crosstalk between channels at the receiver due to spectral broadening. For the case of precompensation in a 4 channel system, large broadening was observed due to high peak power of the compressed pulses at the start of each span increasing the effects of SPM and XPM. The limitation imposed by SPM in post compensated systems can be overcome by precompensated systems.

Keang (2002) [26] calculated the channel capacity of DWDM systems and demonstrated how constant intensity modulation formats such as phase or frequency modulation can be used to eliminate the phase shift caused by SPM and XPM. By using constant intensity modulation SPM and XPM cause only constant phase shifts thus eliminating both phase and intensity distortion. This in turn leads to a monotonic increase in channel capacity for increased powers. They observed that constant intensity techniques provide a higher efficiency than that of in the regime in which XPM dominates over FWM. This was attributed to the fact that FWM decreases more rapidly than XPM as channel spacing increases.

Hoon (2003) [27] investigated, theoretically and experimentally the SPM and XPM induced phase noise in a DPSK system and determined how much of this noise contributes to performance degradation. In order to accomplish this he calculated the rms intensity ratio of XPM induced noise to SPM induced noise for a two channel WDM system. The BER was then measured while varying the OSNR of the signals at the receiver. It was shown that the XPM induced phase noise becomes as large as SPM induced phase noise in a NZ-DSF link for channel spacing less than 100 GHz. BER degradation was also observed for a two channel systems as compared to a single channel system.

Sang, Hyun, Wanseok and Seung (2001) [28] suggested a SBS suppression method for WDM links based on XPM effect induced by an optical supervisory channel. It was found that the phases of the signal channels could be modulated through the XPM induced by the SV channel. The induced XPM broadened spectrum line widths of the signal by four times and effectively reduced the SBS induced error floors and power penalties in transmission. The demonstrated experimentally that this method could increase the SBS threshold and reduce the error floors irrespective of the bit rate, channel power, channel wavelength and channel spacing of the WDM channels.

Wang, Bodther and Jacobsen performed an analysis on crosstalk due to XPM in SCM-WDM video transmission systems in 1995 [29]. An analytical expression for XPM in a 2 channel system was derived. The effect of XPM for different channel spacing parameters was investigated and it was shown that the crosstalk level is smaller for larger channel spacing and larger for a higher sub-carrier frequency. The analysis was extended to a total of 16 optical channels it was found that the number of achievable optical channels is severely limited by XPM.

The same model mentioned above was improved upon by Belloti et al. in 1998 [30]. The first approach was based on the assumption of undistorted interfering channels. The new model assumes that the intensity noise in systems at 40 Gb/s. The model was used to evaluate XPM related transmission impairments in WDM transmission systems for different dispersion compensation schemes.

Hui, Demarest and Allen (1999) [31] reported the results of an experimental and theoretical study on the frequency response of XPM induced crosstalk in multi-span WDM optical systems, both with single fiber configurations. Interference between XPM induced crosstalk effects created in different amplified optical spans was found to have a strong impact on the overall spectral feature of XPM induced crosstalk. A simple analytical expression was obtained to describe the XPM induced crosstalk and it was found that crosstalk levels are strongly dependant on fiber dispersion and optical channel spacing. The crosstalk level between high and low bit rate channels was found to be similar to that between two low bit rate channels. The effect of dispersion compensation on XPM

crosstalk was also discussed. In uncompensated optical systems, a decrease in fiber dispersion will increase XPM induced phase modulation efficiency while an increase in fiber dispersion will increase phase to intensity noise conversion efficiency. Compared to lumped dispersion compensation, per span dispersion compensation was found to be the most effective way to minimize the impact of XPM and SPM crosstalk.

Cartaxo (1999) [16] also investigated the effect of XPM in IM/DD optical fiber links with multiple fiber segments with different fiber characteristics and optical amplifiers theoretically and numerically. A generalized model was simulated and its validity range was present. It was shown that XPM induced IM is approximately proportional to the square frequency when the walk off effect is weak. However, when the walk off is strong the XPM induced IM is approximately linearly proportional to the frequency and inversely proportional to the wavelength separation. Cartaxo proved theoretically and numerically that the effect of XPM could be reduced by properly arranging the dispersion characteristics in each fiber in a multiple fiber segments. In non-dispersion compensated amplifier link and for weak walk off effect, the total XPM induced IM increases approximately with the square of the number of fiber segments and of modulation frequency. It was also shown that in a multi segment fiber link the best way to compensate for dispersion was to place one dispersion compensator in each fiber segment.

Thiele, Killey and Bayvel (2000) [32] investigated the variation of XPM induced distortion with transmission for dispersion managed fiber links. The experimental set up used a recirculating loop and the build up of XPM induced distortion was measured as a function of the number of recirculations. Dispersion compensating fibers (DCF) were used to perfectly compensate 40km of standard single mode fiber. It was shown that the XPM induced distortion increases almost linearly with distance after compensation.

In 2002, R. Hui, Y. Wang, K. Demarest and C. Allen [33] analyzed the performance of a fiber optic SCM transmission system a 10-Gb/s SCM fiber optic system in which 4x2.5-Gb/s data streams were combined in one wavelength . OSSB modulation was used as it was deemed an effective method to reduce the impact of fiber chromatic

dispersion and increase the bandwidth efficiency. Receiver sensitivity was also evaluated and it was concluded that if a narrowband optical filter was used in front of the receiver, the signals' ASE beat noise will be reduced and an improvement in receiver sensitivity was seen. A comparison between ASK and PSK modulation formats was also made. Optical carrier suppression was suggested as a method to increase modulation efficiency. The effect of nonlinear crosstalk in fiber due to XPM and FWM were also analyzed. Analytical expressions were presented and it was found that XPM induced crosstalk decreases monotonically with increase in number of channels and decrease of channel data rate.

In a dispersive fiber, the input pulse get broaden causing inter-symbol interference (ISI) at the receiver. This effect is due to the nonlinear shape of the fiber phase response around the optical carrier frequency. A signal with narrow bandwidth should suffer less from chromatic dispersion. A way to reduce the signal bandwidth is to apply line coding [34]. NRZ line code is a preferred format for optical transmission. Duobinary code has been successfully implemented to reduce the spectral bandwidth. But duobinary code alone is not enough to combat the interference phenomenon occurring in practice between optical marks and spaces. For highly dispersive fibers, band limiting is a necessary requirement to have a benefit from duobinary coding. Recently, other line coding schemes, called phased amplitude-shift signaling (PASS) codes based on a modification of the duobinary one, have been proposed by Stark. According to the duobinary code, marks separated by an odd number of spaces are oppositely phased. The alternate-block-inversion (ABI) PASS code establishes that marks separated by any nonzero number of spaces be oppositely phased. In monospaced-mark-inversion (MMI) PASS code, only marks separated by a single space are oppositely phased. These codes have substantially different power spectra and the power spectrum alone is not a clear indicator of transmission performance. Novel Optical Line Codes tolerant to fiber chromatic dispersion is also introduced in [35] giving hints to try out the applicability of line codes to reduce the nonlinear effects like SPM and XPM.

All these works discussed various nonlinear phenomena with the aim to quantify and reduce their effects in optical communication system. The FWM effect could be

reduced effectively by dispersion management. But the Kerr effects remained as a problem for DWDM systems with high bit rates. The dispersion management could be found effective in reducing the effects caused by nonlinear phenomena like FWM, SPM and XPM. But there is no work reported that quantifies and reduces the effect of the XPM alone. This paper addresses the XPM effect with the aim to quantify and reduce its effect by applying line coding schemes.

#### **1.4 Research Aims**

The main objective of this research is to develop an approach to minimize the effects of XPM in a DWDM optical transmission system applying suitable optical line coding schemes. In particular, the objectives are to carryout analysis for phase and amplitude distortions in a DWDM system with different line-coding schemes like Miller code, duobinary code, Novel optical line codes, etc. and to evaluate the eye closer penalty due to XPM for the above systems by using computer simulation and further, to determine the effectiveness of the line coding schemes in minimizing the effect of XPM in a DWDM system compared to the system without line coding. It is expected that this research will be useful in designing DWDM optical transmission systems with reduced XPM effects

#### **1.5 Outline of the Thesis**

This introduction chapter presents the theoretical background covered in this study. At the beginning, a brief explanation of a simple optical transmission system is described. Then, an elaborate record of previous works on works related to nonlinear effects in optical transmission system is presented indicating huge research in this field. In Chapter 2, an insight on the factors deterring the performance of optical transmission is highlighted briefly. Emphasis was put on the nonlinear effects and particularly on the Kerr effects. This chapter is regarded as a starting point for understanding the subject matter.

Chapter 3 presents the theoretical analysis of various optical line codes. These line codes will be discussed here in detail. Chapter 4 is the backbone of this study. The system block diagram is depicted and the principles of system operation are described. The main discussion in this chapter revolves around the analytical formulations of XPM. Chapter 5 describes the simulation methods of this study focusing on split step Fourier method, eye-opening penalty and filter design. Following the above, the results obtained are discussed upon in Chapter 6. Finally, the summary of findings is presented in chapter 7. The author also provides recommendations for future research in this field at the end of this chapter.

## CHAPTER 2

### OPTICAL COMMUNICATION AND NONLINEAR EFFECTS

#### 2.1 Principles of Optical Communication

A typical point-to-point optical communication system consists of three major components: optical transmitter, optical fiber cable as the transmission medium and optical receiver as in Figure 2.1.

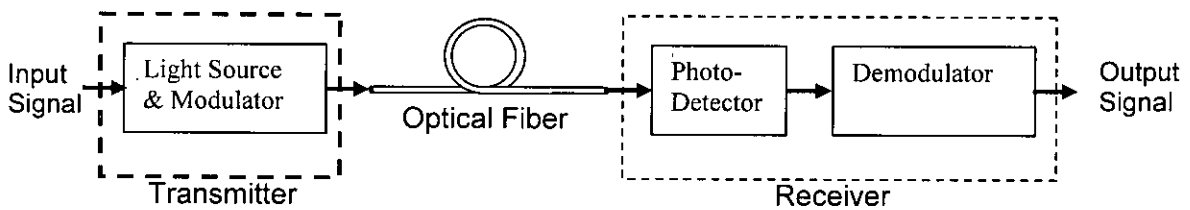


Figure 2.1: Optical fiber communication system

##### 2.1.1 Optical Transmitter

The function of an optical transmitter is to transform the electrical signal into optical form. The electrical signal is then launched into the optical fiber. Figure 2.2 shows the block diagram of an optical transmitter. It consists of an optical source, a modulator and a channel coupler. Semiconductor lasers or light emitting diodes are used as optical source. The main consideration in selecting a source is its ability in launching maximum power into the optical fiber in the suitable wavelength. The optical signal is generated after modulating the light wave by the input signal. The coupler is generally a micro-lens that focuses the optical signal onto the entrance plane of an optical fiber with the maximum possible efficiency. The amount of launched power is an important factor in designing the optical communication system.



### 2.1.2 Optical Fiber

The optical fiber bridges the distance between the optical transmitter and the optical receiver. The main consideration in designing the fiber is to ensure the propagation of the transmitted signal up to the receiver with acceptable level of attenuation and distortion so that the same information can be received at the receiver with minimum error. With the development in the field of optical fiber communication, the attenuation of the signal could be reduced to 0.2 dB/km. Factors that contributed to this reduction in the loss parameter are improved fiber design technique, low loss fiber window, dispersion compensation, etc [36]. Fiber loss, dispersion and nonlinear effects are main design considerations of optical fiber. Introduction of optical amplifiers and dispersion shifted fibers could successfully address the limitations imposed by fiber loss and dispersion. But many aspects of nonlinear characteristics of the fiber yet remained as the limitation of optical fibers.

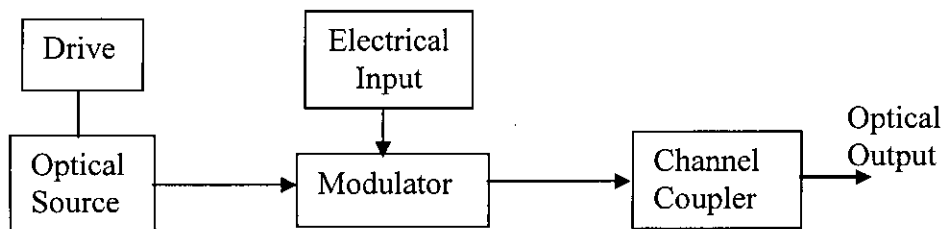


Figure 2.2: Block Diagram of an Optical Transmitter

### 2.1.3 Optical Receiver

The optical receiver converts the received optical signal from the fiber into the original electrical signal. Figure 2.3 shows the block diagram of an optical receiver. It consists of a coupler, a photo-detector and a demodulator. The coupler focuses the received optical signal onto the photo detector. Semiconductor photo diodes are used as photo-detectors because of their compatibility with the whole system. The design of the modulator depends on the modulation format used in the system. Receiver sensitivity is

one of the important design parameter. It is often designed to keep the system within a bit error rate of  $10^{-9}$ .

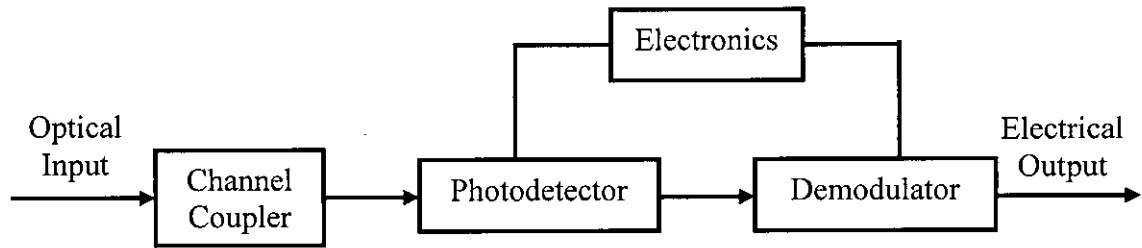


Figure 2.3: Block Diagram of an Optical Receiver

## 2.2 Wavelength Division Multiplexing (WDM) and Dense WDM (DWDM)

The development of WDM fiber links marks the advent of the 4<sup>th</sup> generation of light wave systems. It offers the technology to increase the bit rate and having in-line amplifiers in order to increase the transmission distance. WDM is essentially the same as frequency division multiplexing which has been used in radio systems. In DWDM, the wavelengths are selected with small channel separation like channel spacing of 100 GHz.

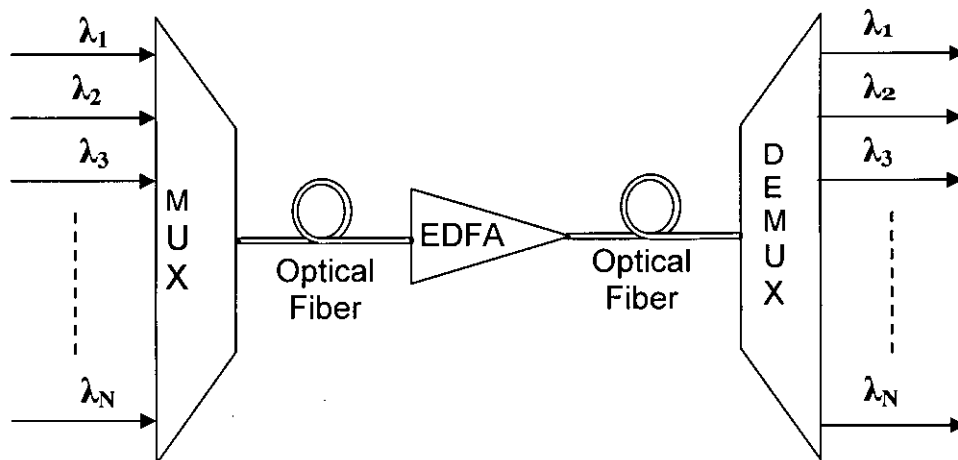


Figure 2.4: Graphical Representation of a Point to Point WDM Optical System

WDM makes use of the optical fiber's available intrinsic bandwidth by multiplexing many wavelengths of coherent light along a single mode fiber channel. Each wavelength of light can transmit encoded information at the optimum data rate. Therefore, multiplexing the distinct wavelengths of lights leads to a significant increase in the total throughput of information for the system. The key elements of a WDM optical system are: tunable semiconductor lasers, multiplexing components, electro-optical modulators, single mode optical fibers, Erbium doped fiber amplifiers (EDFA), semiconductor optical amplifier wavelength translators, demultiplexers and high speed photodetectors. Figure 2.4 shows a point to point WDM optical system.

## **2.3 Fundamentals of Nonlinear Effects in Optical Fibers**

The nonlinearities in optical fibers fall into two categories. One is stimulated scattering (Raman and Brillouin), and the other is the optical Kerr effect due to changes in the refractive index with optical power. While stimulated scatterings are responsible for intensity dependent gain or loss, the nonlinear refractive index is responsible for intensity dependent phase shift of the optical signal. One major difference between scattering effects and the Kerr effect is that stimulated scatterings have threshold power levels at which the nonlinear effects manifest themselves while the Kerr effect does not have such a threshold.

### **2.3.1 Stimulated Brillouin Scattering (SBS)**

Stimulated Brillouin scattering (SBS) may be defined as the light modulation through thermal molecular vibrations within the fiber. It generates acoustic phonon during the process. In SBS, a strong optical wave traveling in one direction (forward) provides narrow band gain for light propagating in the opposite direction (backward). Some of the forward-propagating signal is redirected to backward, resulting in power loss at the receiver. If the SBS threshold is defined as the input power at which the scattered power increases as large as the input power in the undepleted pump approximation, the SBS threshold power is proportional to [37-38],

$$P_B^{th} \approx \frac{1}{g_B} \left( 1 + \frac{\Delta V_S}{\Delta V_B} \right) \dots\dots\dots (2.1)$$

where  $g_B$  is the Brillouin gain coefficient,  $\Delta V_S$  is the line-width of the source and  $\Delta V_B$  is the Brillouin line-width. Equation (2.1) indicates that the threshold power will be increased as the line-width of the source increases. For optical fibers at 1550 nm, the Brillouin line-width is about 20 MHz, so optical signals modulated at higher bit rates will experience lesser effects of SBS. From a system point of view, the relatively narrow gain spectrum of SBS prevents interactions among channels in a WDM system, which makes SBS independent of channel number. Only each individual channel signal needs to be below the threshold power. Another characteristic of SBS which makes it less troublesome compared to other nonlinear effects is that the threshold of SBS does not decrease in a long amplified system because practical optical amplifiers have one or more optical isolators. The optical isolators prevent accumulations of the backscattered light from SBS. Therefore, although SBS could be a detrimental nonlinear effect in an optical communication system, system limitations are usually set by other nonlinear effects [39].

### 2.3.2 Stimulated Raman Scattering (SRS)

SRS is due to the interaction of photons with a fiber's molecular vibrations. High frequency optical phonons are generated in the process. Unlike SBS, SRS scatters light waves in both directions, forward and backward. However, the backward-propagating light can be eliminated by using optical isolators. Therefore, the forward scattered light is of more concern. The Raman gain coefficient is about three orders of magnitude smaller than the Brillouin gain coefficient and the SRS threshold is known to be around 1W for a single-channel system [37]. In a single-channel system, the large threshold power makes SRS a negligible effect. Also, the gain bandwidth of SRS is of the order of 12 THz, which is about 6 orders of magnitude greater than that of SBS. The large gain bandwidth of SRS enables it to couple different channels in a WDM system. On the other hand, it can cause performance degradation through crosstalk. Chraplyvy and Tkach estimated the worst case of signal-to-noise ratio (SNR) degradation in an amplified system due to SRS [40]. According to the estimate, the requirement to ensure an SNR degradation of less than 0.5 dB in the worst channel is that the product of total power, total bandwidth and

the total effective length of the system should be less than 10 THz-mW-Mm. Although it was assumed in their estimate that all the channels are transmitting mark states simultaneously, the probability of which is very low in a multi-channel system, it indicates that SRS may impose a fundamental limit on the capacity of future optical communication systems.

### 2.3.3 Optical Kerr Effect

The refractive index of silica fiber for communication is weakly dependent on optical intensity, and is given by [36],

$$n = n_0 + n_2 I(t) \dots\dots\dots (2.2)$$

where linear refractive index  $n_0 \approx 1.5$ , nonlinear-index coefficient  $n_2 \approx 2.6 \times 10^{-20} \text{ m}^2/\text{W}$ , and  $I(t)$  is the optical intensity. Although the refractive index is a very weak function of signal power, the higher power from optical amplifiers and long transmission distances make it no longer negligible in modern optical communication systems. In fact, phase modulation due to intensity dependent refractive index induces various nonlinear effects, namely, self-phase modulation (SPM), cross-phase modulation (XPM) and four-wave mixing (FWM).

#### 2.3.3.1 Self-Phase Modulation (SPM)

The dependence of the refractive index on optical intensity causes a nonlinear phase shift while propagating through an optical fiber. The nonlinear phase shift is given by

$$\phi_{NL} = \frac{2\pi}{\lambda} n_2 I(t) z \dots\dots\dots (2.3)$$

where  $\lambda$  is the wavelength of the optical wave and  $z$  is the propagation distance. Since the nonlinear phase shift is dependent on its own pulse shape, it is called self-phase modulation (SPM) [41-44]. When the optical signal is time varying, such as an intensity modulated signal, the time-varying nonlinear phase shift results in a broadened spectrum

of the optical signal. If the spectrum broadening is significant, it may cause cross talk between neighboring channels in a dense wavelength division multiplexing (DWDM) system. Even in a single channel system, the broadened spectrum could cause a significant temporal broadening of optical pulses in the presence of chromatic dispersion. However, under some circumstances SPM and chromatic dispersion can be beneficial. One extreme example is the soliton [45], which is known to be stable and dispersion-free. Even with non-return-to-zero (NRZ) pulses, it is known that pulse compression could be achieved partially in the anomalous dispersion region where the linear chirp induced by chromatic dispersion and the nonlinear one due to SPM have opposite signs. The anomalous dispersion region has a negative sign of  $\beta_2$ , the second order propagation constant. When a transmission system is designed to achieve the optimum compensation of the linear chirp and the nonlinear chirp, it is often called a nonlinear assisted transmission system.

### 2.3.3.2 Cross-Phase Modulation (XPM)

Another nonlinear phase shift originating from the Kerr effect is cross-phase modulation (XPM). While SPM is the effect of a pulse on its own phase, XPM is a nonlinear phase effect due to optical pulses in neighbouring channels. Therefore, XPM occurs only in multi-channel systems. In a multi-channel system, the nonlinear phase shift of the signal at the center wavelength  $\lambda_i$  is described by [36],

$$\phi_{NL} = \frac{2\pi}{\lambda_i} n_{2z} [I_i(t) + 2 \sum_{i \neq j}^M I_j(t)] \dots\dots\dots 2.4$$

where M is the number of co-propagating channels in the fiber. The first term is responsible for SPM, and the second term is for XPM. Equation (2.4) might lead to a speculation that the effect of XPM could be at least twice as significant as that of SPM. A pump-probe approach helps isolate the effect of XPM [32]. Referring to Figure 2.5, the pump channel generates a time varying intensity signal,  $\lambda_1$  while the probe generates a constant intensity continuous wave (CW) wave signal,  $\lambda_2$ . Then they are transmitted through two channels of a fiber. At the receiver, both signals are demultiplexed and

compared to the original condition at the transmitter. Both pump channel and probe channel signals experience amplitude variation. The amplitude variation in the pump channel is due to the SPM. On the other hand, the amplitude variations in the probe channel are caused by the XPM from the pump channel. This is because the signal in the probe has a constant intensity, which eliminates the effects of SPM.

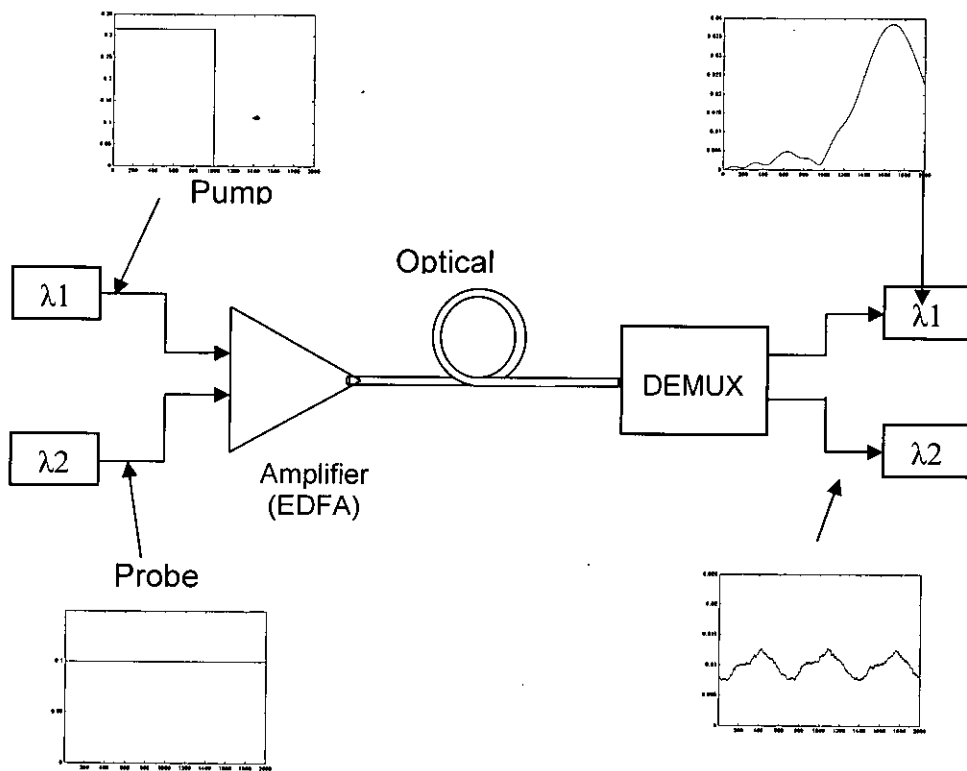


Figure 2.5 Experimental Setup to Demonstrate the Effects of XPM

However, XPM is effective only when pulses in the other channels are synchronized with the signal of interest. When pulses in each channel travel at different group velocities due to dispersion, the pulses slide past each other while propagating [15-16, 46]. Figure 2.6 illustrates how two isolated pulses in different channels collide with each other. When the faster traveling pulse has completely walked through the slower traveling pulse, the

XPM effect becomes negligible. The relative transmission distance for two pulses in different channels to collide with each other is called the walk-off distance,  $L_w$  [36].

$$L_w = \frac{T_0}{|v_g^1(\lambda_1) - v_g^1(\lambda_2)|} \approx \frac{T_0}{|D\Delta\lambda|} \dots\dots\dots (2.5)$$

where  $T_0$  is the pulse width,  $v_g$  is the group velocity, and  $\lambda_1, \lambda_2$  are the center wavelength of the two channels.  $D$  is the dispersion coefficient and  $\Delta\lambda = |\lambda_1 - \lambda_2|$ . When dispersion is significant, the walk-off distance is relatively short, and the interaction between the pulses will not be significant, which leads to a reduced effect of XPM. However, the spectrum broadened due to XPM will induce more significant distortion of temporal shape of the pulse when large dispersion is present, which makes the effect of dispersion on XPM complicated.

### 2.3.3.3 Four-Wave Mixing (FWM)

Four-wave mixing (FWM), also known as four-photon mixing, is a parametric interaction among optical waves, which is analogous to inter-modulation distortion in electrical systems [47-51]. In a multi-channel system, the beating between two or more channels causes generation of one or more new frequencies at the expense of power depletion of the original channels. When three waves at frequencies  $f_i, f_j,$  and  $f_k$  are put into a fiber, new frequency components are generated at  $f_{FWM}=f_i+f_j-f_k$ . In a simpler case here two continuous waves (CW) at the frequencies  $f_1$  and  $f_2$  are put into the fiber, the generation of side bands due to FWM is illustrated in Figure 2.6. The number of side bands due to FWM increases geometrically, and is given by,

$$M = \frac{1}{2} (N_{ch}^3 - N_{ch}^2) \dots\dots\dots (2.6)$$

where  $N_{ch}$  is the number of channels, and  $M$  is the number of newly generated sidebands. For example, eight channels can produce 224 side bands. Since these mixing products can fall directly on signal channels, proper FWM suppression is required to avoid significant interference between signal channels and FWM frequency components. When



all channels have the same input power, the FWM efficiency,  $\eta$ , can be expressed as the ratio of the FWM power to the output power per channel, and is proportional to:

$$\eta \propto \left[ \frac{n_2}{A_{eff} D (\Delta \lambda)^2} \right]^2 \dots\dots\dots (2.7)$$

where  $A_{eff}$  is the effective area of fiber.

Equation (2.7) indicates that FWM of a fiber can be suppressed either by increasing channel spacing or by increasing dispersion. Large dispersion can cause unacceptable power penalties especially in high bit rate systems. However, careful design of the dispersion map (often called *dispersion management*) which allows large local dispersion but limits the total average dispersion to be below a certain level is found to be very effective to combat both dispersion and FWM induced degradations. There is a rich collection of literature on dispersion management, and a few examples can be found in [50-51].

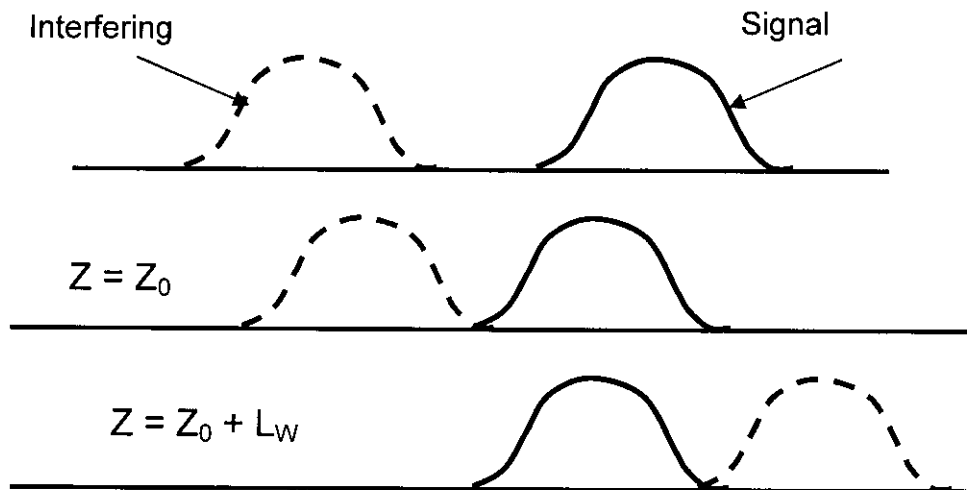


Figure 2.6 Illustration of Walk-off Distance

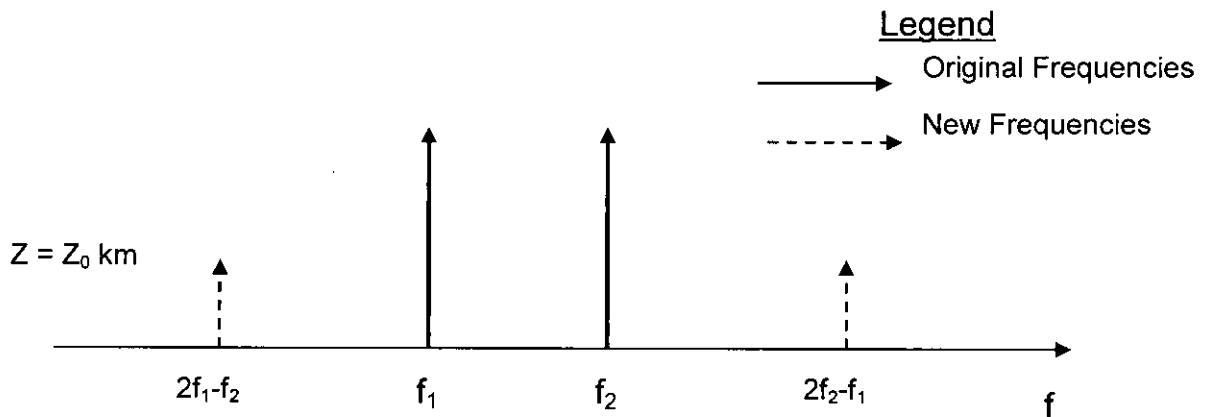


Figure 2.7 Illustration of Side-Bands Generation due to FWM in Two-Channel Systems

Three different effects from the nonlinear refractive index, namely, SPM, XPM, and FWM have been discussed. However, in a real system, especially in a DWDM system where channels are packed very closely to each other, the broadened spectrum due to the three nonlinear effects is usually indistinguishable. The system performance degradations by fiber nonlinearities are, in general, assessable by solving the nonlinear Schrödinger equation (NLSE). The NLSE and a numerical algorithm to solve the NLSE – the split-step Fourier method – will be introduced in Chapter 5.

## 2.4 Summary

This chapter describes briefly the optical transmission system including various nonlinear characteristics. The linear characteristics such as loss and dispersion parameters are not discussed here. Emphasis was put on the nonlinear parameters. It is evident from the discussion that the limitations offered by nonlinear parameters in optical fiber communication become more and more a detrimental with the increase of distance and bit rate, and decrease in the channel spacing.



## CHAPTER 3

### Theoretical Analysis of Optical Line Coding

#### 3.1 Introduction

The rapid worldwide growth of data and internet traffic in telecommunication networks results in a sharp increase in the demand for transmission capacity. Efficient utilization of the existing optical fiber network is an answer to this growing demand. It also provides the solution from the economical point of view. An important step to this end is the introduction of optical communication systems with terabits per second capacity, which are based on DWDM technology. Thus for the first time bandwidth efficiency, which is an important feature in wireless communication has appeared as an important issue in fiber optics.

There are several approaches to achieve overall bandwidth efficiency. Amongst them are improved modulation format, line-coding techniques, management of chromatic and polarization mode dispersion including equalization, wideband optical amplifiers, improved WDM multiplexers and demultiplexers. Modeling of the WDM optical channel including nonlinear effects is necessary in order to investigate the impact of the various methods. For practical reasons it is important (to avoid high complexity algorithms) to end up with structures that are realizable at these high frequencies.

Therefore research engineers focus mainly on bandwidth efficient modulation formats at channel data rates 40 Gbps. By saving bandwidth both the dispersion problems and the channel density are improved. A promising approach is multilevel signal line coding.

Optical systems by and large use RZ and NRZ modulation format. RZ and NRZ modulations are suitable for long haul systems in which the dispersion in the single mode fiber is compensated for by another fiber with negative dispersion. But it is not the best choice for uncompensated single mode fiber. Optical line codes are more resilient to dispersion and are found superior to NRZ modulation for the uncompensated optical fiber channel.

The popular line coding formats such as RZ and NRZ worked well up to 10 Gbps per channel in long haul high-speed optical communication networks. Recent analysis and investigations have shown that RZ turned out to be superior compared to conventional NRZ systems, at least as long as standard single mode fibers are used as transmission media. The RZ format has been reported to be effective against self phase modulation (SPM) in standard single mode fiber links. SPM and XPM resulting from fiber non-linearity effects caused by group velocity dispersion (GVD) lead to waveform distortion that limits the maximum transmission distance and capacity of high-speed optical links. Thus tolerance with respect to SPM, XPM and GVD are essential for reliable network operation. On the other hand, because of the narrower optical spectrum of NRZ format, NRZ enables higher spectral efficiency in wavelength division multiplexing (WDM) systems compared to RZ in the linear region. However the tolerable dispersion range is limited in both RZ and NRZ modulation formats. In addition, they limit the potential transmitted distance of the signal due to the non-linearity effects of fiber, when they are used in terabit capacity optical communication networks.

In this section generation of multilevel coding formats such as duobinary and novel optical coding are discussed in detail. In section 3.2 duobinary coding is discussed in detail, while in section 3.3 a detail description of novel optical line coding of order one is presented along with its generation example.

### **3.2 Duobinary Line Code**

Duobinary signal is a pseudo-binary coded signal in which a "0" bit is represented by a zero level electric current or voltage; a "1" bit is represented by a positive level current or voltage if the quantity of '0' bits since the last "1" bit is even, and by a negative level current or voltage if the quantity of '0' bits since the last "1" bit is odd [52]. In this scheme  $R$  bits/sec can be transmitted using less than  $R/2$  Hz of bandwidth. In order to realize practical transmitting and receiving filters for zero inter symbol interference (ISI) fulfilling Nyquist rate, minimum  $R/2$  Hz of bandwidth is required to transmit  $R$  bits/sec. The condition of zero ISI may be relaxed to achieve a symbol transmission rate of  $r$  bits/sec. By allowing for a controlled amount of ISI so that it can be subtracted out to recover the original signal values, we can achieve this symbol rate. This result implies that duobinary pulses will have ISI.

Let the transmitted signal be

$$x(t) = \sum_{k=-\infty}^{\infty} d_k q(t-kT), \quad d_k = 0, 1 \dots\dots\dots (3.1)$$

Here,  $\{d_k\}$  are the data bits,  $q(t)$  is the transmitted pulse and  $T = 1/R$  is the bit period. The pulse  $q(t)$  is usually chosen such that there is no ISI at the sampling instances ( $t = kt, k = 0, \pm 1, \dots\dots$ , are the sampling instances):

$$q(kT) = \begin{cases} 1 & k=0 \\ 0 & k \neq 0 \end{cases} \dots\dots\dots (3.2)$$

NRZ is one such scheme that requires a bandwidth of  $R$  Hz to transmit  $R$  bits/sec. This is twice as large as the Nyquist bandwidth of  $R/2$  Hz. The simplest duobinary scheme transmits pulses with ISI as follows:

$$q(kT) = \begin{cases} 1 & k=0, 1 \\ 0 & \text{otherwise} \end{cases} \dots\dots\dots (3.3)$$

For a channel with bandwidth  $W$  and with controlled ISI for  $T = \frac{1}{2W}$ , we get from Equation (2.2),

$$X(f) = \begin{cases} \frac{1}{2W} \left[ 1 + e^{-j\frac{f\pi}{W}} \right], & |f| < W \\ 0, & \text{otherwise} \end{cases}$$

$$X(f) = \begin{cases} \frac{1}{W} e^{-j\frac{f\pi}{2W} \cos\left(\frac{f\pi}{2W}\right)}, & |f| < W \\ 0, & \text{otherwise} \end{cases} \dots\dots\dots (3.4)$$

Therefore,  $x(t)$  is given by

$$x(t) = \text{sinc}(2Wt) + \text{sinc}(2Wt - 1) \dots\dots\dots (3.5)$$

It is evident from Equations 3.1 to 3.5 that at the sampling instance  $kT$ , the receiver does not recover the data bit  $d_k$ , but rather  $(d_{k-1} + d_k)$ . However this scheme allows for pulses with a smaller bandwidth. By allowing some ISI, the transmitted pulse  $q(t)$  can be made longer in the time domain. Thus its spectrum becomes narrower in the



frequency domain. With a narrower spectrum the distortion effects of the channel are also fewer. This outcome is one of the reasons why duobinary modulation is resilient to dispersion.

One way of generating duobinary signals is to digitally filter the data bits with a two-tap finite impulse response (FIR) filter with equal weights and then low-pass filter the resulting signal to obtain the analog waveform with the property in (3.3) as in Figure 3.1. When the input to the FIR filter is binary (let these binary values be -1 and 1), then the output can take one of these values:  $0.5*(-1+-1) = -1$ ;  $0.5*(-1+1) = 0$ ; or  $0.5*(1+1) = 1$ . Hence the duobinary signal is a three-level signal.

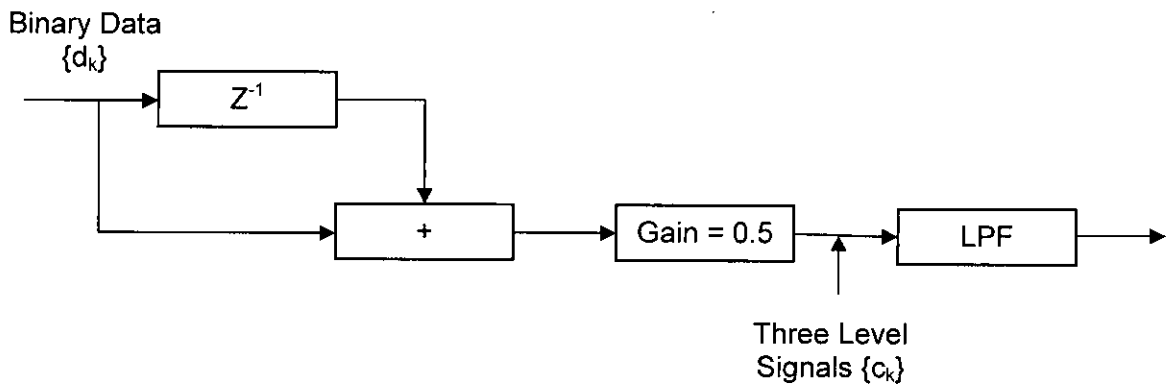


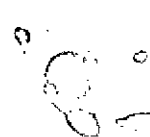
Figure 3.1 Duobinary Encoder

### 3.2.1 Differential Encoding

The ISI introduced at the transmitter can be revealed at the receiver by differential decoding. At each sampling instance  $kT$ , the receiver assumes the value of  $x_k = (d_k + d_{k-1})$  where  $x_k = x(kT)$  and  $x(t)$  satisfies Equation (3.3). If the previous decision at the output of the receiver is  $\hat{d}_{k-1}$ , this decision can be subtracted from the sampled value to obtain  $\hat{d}_k$ :

$$\hat{d}_k = x_k - \hat{d}_{k-1} \dots\dots\dots (3.6)$$

However, a single error at the receiver will propagate for ever, causing a catastrophic decoding error. To avoid this catastrophic error propagation, it is better to differentially pre-code the data at the transmitter. The data bits  $d_k$  are differentially encoded as follows:



$$c_k = c_{k-1} \oplus d_k \quad (\oplus \text{ is modulo 2 subtraction}) \dots\dots\dots (3.7)$$

The transmitted signal is now

$$x(t) = \sum_{k=-\infty}^{\infty} c_k q(t - kT) \dots\dots\dots (3.8)$$

with  $q(t)$  satisfying (3.3). Hence at the sampling instance  $kT$ , the receiver samples the value:

$$c_k \oplus c_{k-1} = c_{k-1} \oplus d_k \oplus c_{k-1} = d_k \dots\dots\dots (3.9)$$

### 3.2.2 Differential Encoder

Differential encoder can be implementing using an exclusive-OR (XOR) gate as in Figure 3.2. However, it can be difficult to implement the 1-bit delay in the feedback path at high data rates such as 10 Gb/sec.

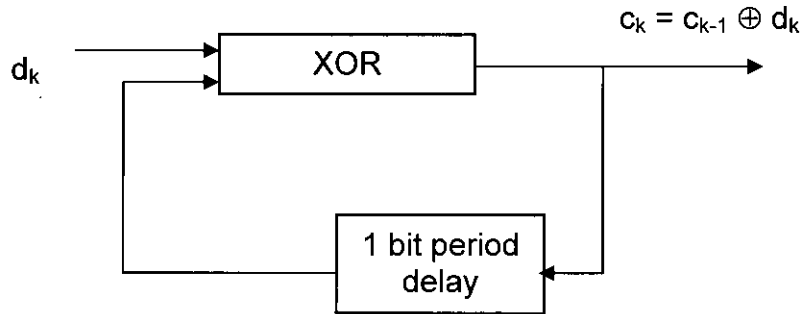


Figure 3.2: Differential Encoder with an XOR Gate

Another circuit that does not involve the in the feedback path is shown in Figure 3.3. Here, a divide-by-2 counter has a clock gated with the data. When the data is high, the counter changes state, which is equivalent to adding a 1 modulo 2. When the data is low, the counter state remains the same, which is equivalent to adding a 0 modulo 2.

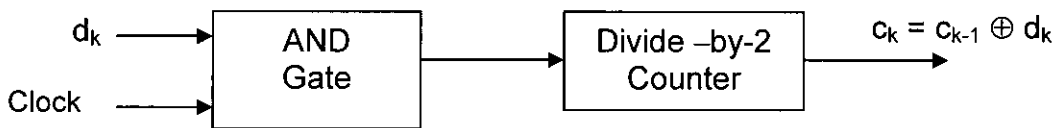


Figure 3.3: Differential Encoder with a Divide-by-2 Counter

### 3.2.3 Optical System for Duobinary Modulation

The final step is to modulate the light with the three-level duobinary signal, which implies a three-level optical signal. This result is achieved with a Mach-Zehnder (MZ) modulator biased at its null point. With a zero input, no light is transmitted, but with the +1 and -1 inputs are transmitted as +E and -E electrical fields. While this is a three level signal in terms of the electrical field, it is a two-level signal in terms of optical power. This choice significantly reduces the complexity of the receiver.

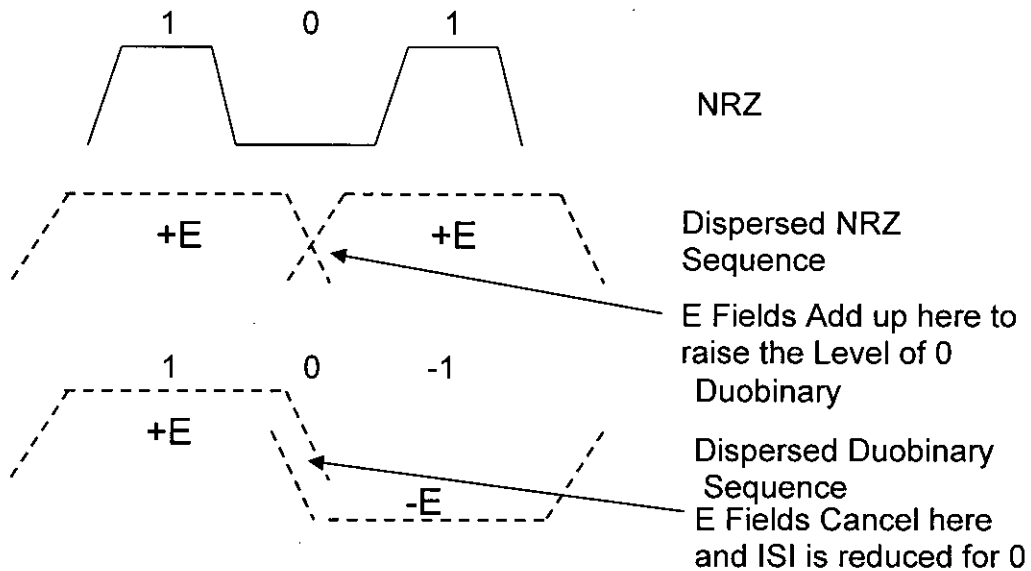


Figure 3.4: Effect of Dispersion on NRZ and Duobinary Sequences

The combination of the duobinary encoder and the above mapping to electric fields help further reduce the effects of dispersion in the fiber. As the pulses travel down the fiber, they spread out in time owing to dispersion. In an NRZ scheme, a data sequence of {1 0 1} is mapped onto the optical domain as {+E 0 +E}. In the encoded duobinary sequence, a {1 0 1} sequence cannot occur, but a {1 0 -1} does occur, which is mapped as {+E 0 -E} in the optical domain. The effect of dispersion in the two cases is shown in Figure 3.4. It depicts why the resulting dispersion is less in duobinary modulation.

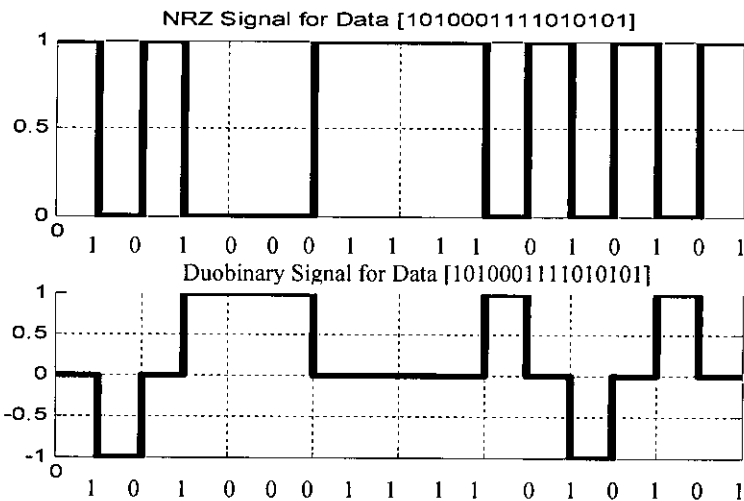
The same receiver that is used for a NRZ modulation scheme can be used for the duobinary modulation. The power detector squares the electric field to detect power and hence +E and -E outputs of the fiber get mapped to the same power level and are



detected as logical 1s. Figure 3.5 shows an example of the transformation of data in a duobinary system and its electrical modulating signal.

K	-1	0	1	2	3	4	5	6	7	8	9	10	11	12	13	14	15
$d_k$	0	1	0	1	1	1	0	0	0	0	1	0	1	0	1	0	
$\hat{d}_k$	1	0	1	0	0	0	1	1	1	1	0	1	0	1	0	1	
Diff Encoder	0	1	1	0	0	0	0	1	0	1	0	0	1	1	0	0	1
Bit to Voltage	-1	1	1	-1	-1	-1	-1	1	-1	1	-1	-1	1	1	-1	-1	1
Duobinary Encoder	0	1	0	-1	-1	-1	0	0	0	0	-1	0	1	0	-1	0	
Electric Field	0	+E	0	-E	-E	-E	0	0	0	0	-E	0	E	0	-E	0	
Optical Power	0	E <sup>2</sup>	0	E <sup>2</sup>	E <sup>2</sup>	E <sup>2</sup>	0	0	0	0	E <sup>2</sup>	0	E <sup>2</sup>	0	E <sup>2</sup>	0	
Received Bits	0	1	0	1	1	1	0	0	0	0	1	0	1	0	1	0	

(a)



(b)

Figure 3.5: (a) An Example Showing the Transformation of Data in a Duobinary System and (b) NRZ and Duobinary Signal for Data Sequence [1 0 1 0 0 0 1 1 1 1 0 1 0 1 0 1]

### 3.3 A Multi-Level Novel Optical Line Code

Novel optical line coding is similar to conventional Miller coding with the difference being that two of them are scaled by a factor  $\alpha < 1$  and transmitted in sequence according to the duobinary logic. Novel optical codes are ranging from order 1, 2 .....n and here only order one novel optical codes are used.

### 3.3.1 First Order Code

The first order code uses four wave forms  $s_i(t)$ , and the state diagram is shown in the Figure 3.6, where  $\Sigma_1, \Sigma_2$  are the code states, the elementary signals are  $s_i(t)$ , where  $i = 1, 2, 3, 4$ .

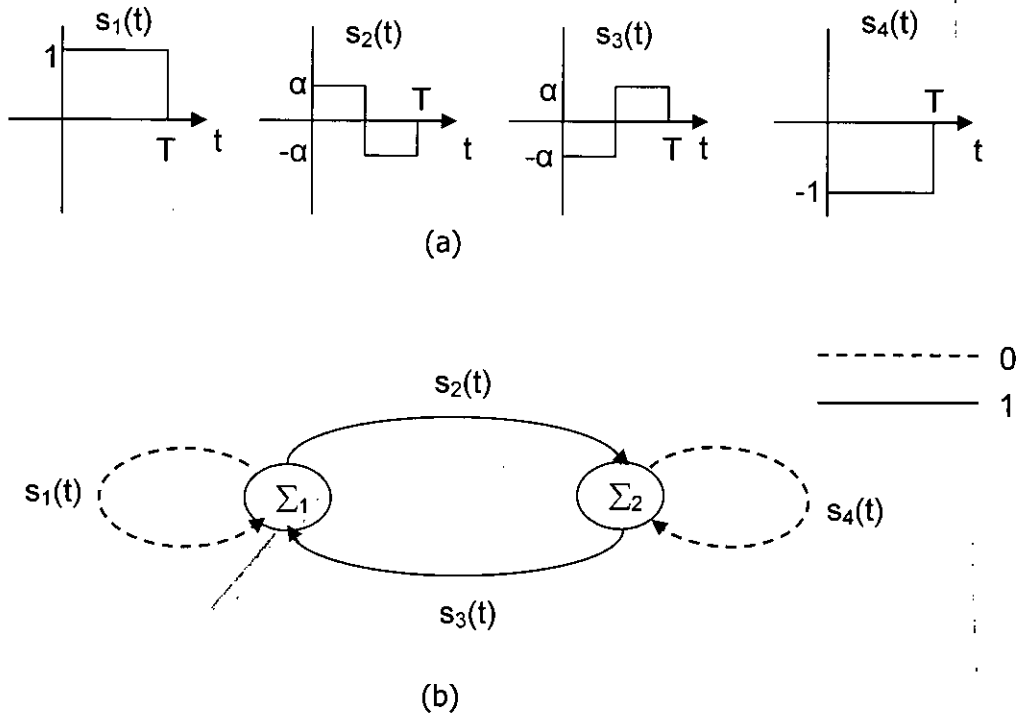


Figure 3.6: (a) Elementary Signals and (b) Code State Diagram for Novel Multilevel Optical Line Code of Order one [35].

Elementary signals form two pairs with  $s_1(t) = -s_4(t)$  and  $s_2(t) = -s_3(t)$ . In addition two of the elementary signals [ $s_2(t)$  and  $s_3(t)$ ] are scaled by  $\alpha$ . In this thesis  $\alpha$  is chosen as 0.5 to produce best spectral shape. The information sequence  $\{u_k\}$  is encoded as shown in Figure 3.7 to form the signal:

$$x_e(t) = \sum_{k=-\infty}^{\infty} g_1(\sigma_k) s_e(t - kT; u_k) \dots \dots \dots (3.10)$$

where  $\sigma_k$  stands for the generic encoder state and  $g_1(\sigma_k)$  is a coefficient defined by the following rule:

$$g_1(\sigma_k) = \begin{cases} 1, & \text{if } \sigma_k = \Sigma_1 \\ -1, & \text{if } \sigma_k = \Sigma_2 \end{cases} \dots \dots \dots (3.11)$$

where  $\sum_1$  and  $\sum_2$  indicate the states allowed to the encoder, and  $s_e(t; u_k)$  is one of the two elementary signals  $s_1(t)$  or  $s_2(t)$  selected in accordance to the following rule:

$$s_e(t; u_k) = \begin{cases} s_1(t), & \text{if } u_k = 0 \\ s_2(t), & \text{if } u_k = 1 \end{cases} \dots\dots\dots (3.12)$$

Hence, the actual elementary signal output from the encoder will be one of  $s_1(t)$  or  $s_2(t)$  or their negatives [ i.e.,  $s_4(t)$  or  $s_3(t)$  respectively] depending on the value of  $g_1(\sigma_k)$  as shown in Figure 3.6. The sequence of the encoder is defined by the following rule:

$$\sigma_k + 1 = g_2(u_k, \sigma_k) \dots\dots\dots (3.13)$$

where the value of the function  $g_2$  is described by the following map:

$u_k \backslash \sigma_k$	$\sum_1$	$\sum_2$
0	$\sum_1$	$\sum_2$
1	$\sum_2$	$\sum_1$

It may noticed that for  $\alpha = 0$ ,  $s_2(t) = s_3(t) = 0$ , and the code reduces to duobinary code. The above coding rule for order 1 code is summarized in Table-3.1.

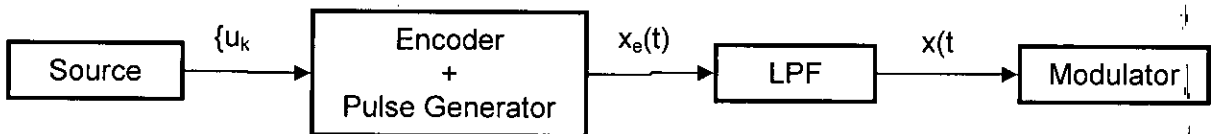


Figure 3.7: Transmitter Model of an optical system

Table-3.1: Encoding Rule of Novel Optical Line Code (Order 1)

Data Sequence $\{u_k\}$	Generic Encoder State $(\sigma_k)$	State of the Encoder $(g_2)$	Encoded Signal $x_e(t)$
0	$\sum_1$	$\sum_1$	$s_1(t)$
0	$\sum_2$	$\sum_2$	$-s_1(t) = s_4(t)$
1	$\sum_1$	$\sum_2$	$s_2(t)$
1	$\sum_2$	$\sum_1$	$-s_2(t) = s_3(t)$

The power spectral density of the signal  $x_e(t)$  in (3.10), coded in accordance to the state diagram of Figure 2.6 is given as [41]

$$G_e(f) = \frac{1}{T} |S_1(f)|^2 \cos^2(\pi f T) + \frac{1}{T} |S_2(f)|^2 \sin^2(\pi f T) + j \frac{1}{T} S_1(f) S_2^*(f) \sin(2\pi f T) \dots \quad (3.14)$$

where  $S_1(f)$  and  $S_2(f)$  are the Fourier transforms of the elementary signals  $s_1(t)$  and  $s_2(t)$  respectively. Elementary signals of order one code can be generated by expressing four elementary signals of Figure 3.6 as linear combinations of the rectangular pulses of duration  $T/2$ .

$$p(t) = \begin{cases} 1, & 0 < t < T/2 \\ 0, & \text{elsewhere.} \end{cases} \quad \dots \quad (3.15)$$

In this case, we get, for the elementary signals  $s_i(t)$ , and  $i = 1, 2, 3, 4$  the following expressions:

$$\begin{aligned} s_1(t) &= p(t) + p(t-T/2) \\ s_2(t) &= a[p(t) + p(t-T/2)] \\ s_3(t) &= -s_2(t) \\ s_4(t) &= -s_1(t) \end{aligned} \quad \dots \quad (3.16)$$

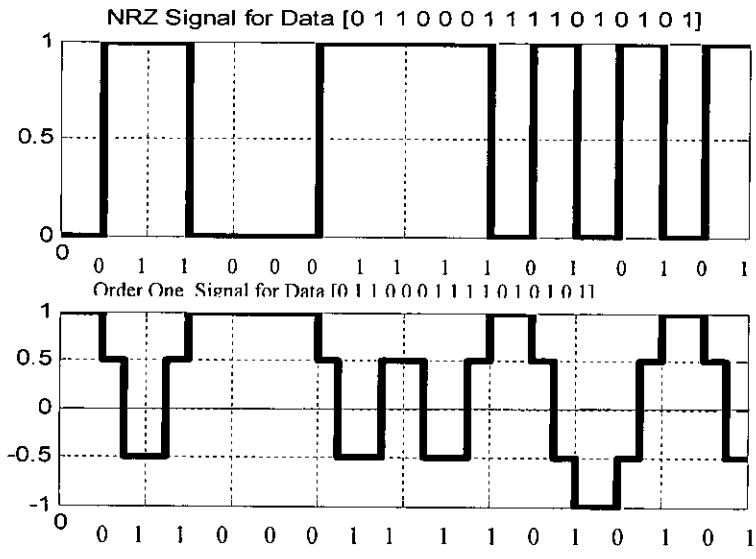


Figure 3.8: An Example Showing NRZ and Duobinary Signals for Data Sequence [0 1 1 0 0 0 1 1 1 1 0 1 0 1 0 1]

### **3.4 Summary**

Duobinary and Novel optical line codes described in this chapter will be applied in a modeled optical system in the later chapter. In this chapter, the methods of generating the line codes along with examples are described. These methods will be applied in this study in the subsequent chapters. However there are other multilevel line codes like alternate block inversion (ABI), monospaced mark inversion (MMI), etc. which are not discussed here in this study. Subsequent chapters are dedicated mainly to find out the effectiveness of these line codes in combating the nonlinear effects. Efforts will also be taken to quantify such effectiveness in terms realizable practically following several approaches.

## **CHAPTER 4**

### **Theoretical Analysis of XPM on a WDM System**

#### **4.1 Introduction**

This chapter starts by introducing an illustration of the system block diagram including its principles of operation. The WDM transmission employs intensity modulation direct detection (IM/DD) modulation scheme.

This chapter is organized into three sections. First, the input and output power are described taking into consideration of in-line amplifications and filters. In the second section, the derivation of total XPM induced phase shift in a single segment transmission line is presented. Finally an approach on calculating the BER is presented.

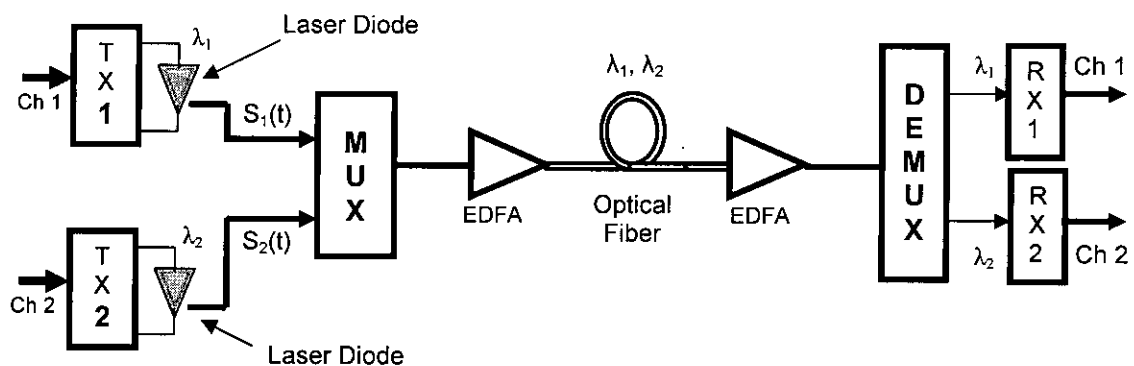
#### **4.2 Block System Diagram**

There are two major detection schemes widely used at present; coherent and direct detection schemes. The term coherent refers to any technique employing nonlinear mixing between two optical waves. To send information, one can modulate the amplitude, frequency or phase of the carrier. In direct detection system, electrical signal coming into the transmitter amplitude-modulates the optical power level of the light source. Thus, the optical power is proportional to the signal current level.

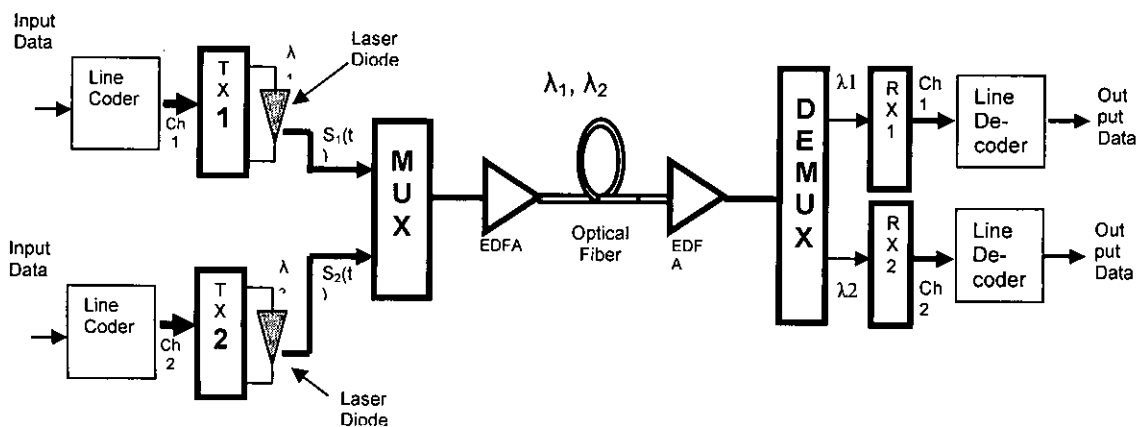
Coherent system offers improved receiver sensitivity and channel selectivity over direct detection technique. Advantages of coherent optical communication schemes are a nearly ideal receiver sensitivity (20 dB over direct detection) and high degree of frequency selectivity. Selectivity of coherent system is due to the fact that narrow band electronic filters pick out the neighbouring channels like broadband optical filters.

The operation of IM-DD is simple as depicted in Figure 4.1. At the transmitter, the information signal is obtained by modulating an optical source either through direct

detection or external modulation. The transmitted field from the laser is coupled to the fiber and is attenuated during propagation towards the fiber far end. At the receiver, the optical signal is directly detected by one or more photodiodes to obtain base-band electric currents. Since the generated current is normally low, the electrical front end should comprise of a wideband, low-noise amplifier, able to provide sufficient gain to drive the clock recovery circuit and the threshold comparator. Upon amplification, the base-band current is sampled in the middle of each bit interval to obtain the decision variable. The decision variable is then compared with a threshold to estimate the transmitted bit. If the decision variable exceeds the threshold, an "ON" state is estimated; otherwise an "OFF" state is assumed as shown in Figure 4.2.



(a)



(b)

Figure 4.1 Block system diagram (IM-DD): (a) without line coder (b) with line coder

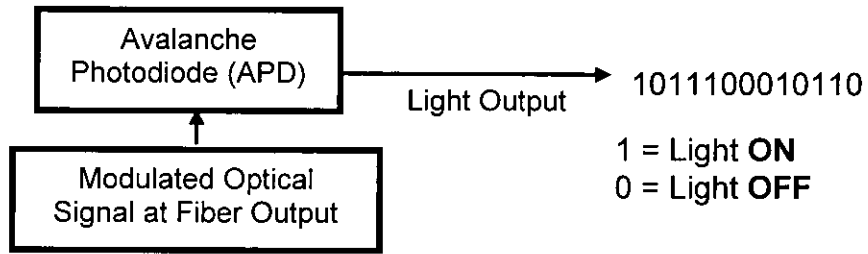


Figure 4.2 Direct detection optical receiver system

To synchronize the sampling, the digital signal clock must be recovered at the receiver by means of a base band phase locked loop. The advantage of IM-DD is that it offers system simplicity and low cost but suffers from the limited sensitivity and does not take full advantage of band width capabilities of the fiber.

The choice of modulation and detection schemes determines the fundamental receiver sensitivity. Receiver sensitivity in terms of SNR is proportional to received optical signal power. Receiver sensitivity for various coherent and direct detection techniques has been described in terms of the average number of photons required to achieve  $10^{-9}$  BER.

### 4.3 Theoretical Analysis of XPM

In theoretical analysis of XPM, a mathematical model is presented to quantify the XPM in a two channel optical system. An approach is adopted here to isolate in this effect from other nonlinear effects of optical fiber.

#### 4.3.1 Input and Output Power Representation

XPM occurs in systems having at least two channels. The group velocity dispersion (GVD) converts the XPM induced phase modulation (PM) to IM. Here, the analytical model to study the effects of XPM in DWDM transmission is based on in an IM/DD system. The two input channels considered in the system are sent to the



transmitter where the electrical signals modulate the optical output. Channel 1 or probe is a continuous wave (CW) and channel 2 is the pump channel which is sinusoidally modulated. The intensity modulated input pump signal has an angular frequency  $\omega$ . Considering a small section of fiber length where fiber nonlinearity and dispersion are assumed to act independently, the XPM induced phase shift in probe channel when optical pulse in pump channel traveled a distance  $z$  from fiber input can be expressed by [15-16]:

$$\phi_{xpm,1}(z, \omega) = -2\gamma_1 P_2(z, \omega) \dots\dots\dots (4.1)$$

where

$$P_2(z, \omega) = P_2(0, \omega) \cos(qz) \exp(-az) \exp(-j\omega z/v_{g2}) \dots\dots\dots (4.2)$$

Equation (4.2) represents the pump power fluctuation after propagating at distance  $z$  from the fiber input that modulates the phase of the probe signal through XPM.  $P_2(0, \omega)$  is a complex amplitude of pump signal power at fiber input and it is given by  $P_2(0, \omega) = P_{20} e^{j\theta}$ . Here,  $q = (\omega^2 D \lambda_2^2)/(4\pi c)$  with  $D$  is the fiber dispersion coefficient,  $\lambda_2$  is the wavelength of pump signal and  $c$  is the speed of light. The total XPM induced phase shift of probe signal after propagating a distance  $L$  is given by [53]:

$$\phi_{xpm,1}(L, \omega) = \int_0^L \phi_{xpm}(z, \omega) \partial z = |H(\omega)| P_2(z, \omega) \cos\left(\frac{\omega L}{v_{g1}} + \angle P_2(z, \omega) + \angle H(\omega)\right) \dots (4.3)$$

Equation (4.3) shows that XPM is a phase modulation process with the frequency response given by [53]:

$$H(\omega) = 2\gamma_1 P_1 \sqrt{\eta_{xpm}(\omega)} L_{eff} \exp(j\phi(\omega)) \dots\dots\dots (4.4)$$

Without the phase term of equation (3.4), the equation is known as XPM index:

$$\Delta\phi_1 = 2\gamma_1 P_1 \sqrt{\eta_{xpm}(\omega)} L_{eff} \dots\dots\dots (4.5)$$

In (4.4) and (4.5),  $L_{eff}$  is the effective length of the fiber,  $\phi(\omega)$  is the phase retardation factor,  $\eta_{xpm}$  is the XPM efficiency and  $\gamma_1$  is the nonlinear coupling coefficient of the optical signal. These parameters are defined as:

$$L_{\text{eff}} = (1 - \exp(-\alpha L)) / \alpha \quad \dots\dots\dots (4.6)$$

$$\varphi = -\arg(-\alpha + j \omega d) + \arg[-(1 - \exp(-\alpha L)) \cos(\omega d L) + j \exp(-\alpha L) \sin(\omega d L)] \dots (4.7)$$

$$\eta_{\text{XPM}} = \frac{\alpha^2}{\omega^2 d^2 + \alpha^2} \left[ 1 + \frac{4 \sin^2(\omega d L / 2) \exp(-\alpha L)}{(1 - \exp(-\alpha L))^2} \right] \dots\dots\dots (4.8)$$

In (4.6-8),  $\alpha$  is the attenuation coefficient of the fiber,  $L$  is the fiber length,  $d$  is the walk-off parameter defined as:

$$d_{12} = D \Delta \lambda \quad \dots\dots\dots (4.9)$$

where  $\Delta \lambda$  is the wavelength separation between channel 1 ( $\lambda_1$ ) and channel 2 ( $\lambda_2$ ), and  $D$  is the dispersion coefficient of the fiber. The nonlinear coupling coefficient is defined as:

$$\gamma_1 = \frac{2 n_2 \pi}{\lambda_1 A_{\text{eff}}} \quad \dots\dots\dots (4.10)$$

where  $n_2$  is the nonlinear refractive index of the fiber.  $A_{\text{eff}}$  is the effective core area of the fiber expressed as:

$$A_{\text{eff}} = \pi r^2 \quad \dots\dots\dots (4.11)$$

where  $r$  is the radius of the fiber. The total XPM induced phase shift in time domain can be obtained by taking the real part of inverse Fourier Transform of equation (4.3)

$$\phi_{\text{XPM}}(L, t) = \text{Re} \left( \frac{1}{\pi} \int_0^{\infty} \phi_{\text{XPM}}(L, \omega) \exp(-j \omega t) \partial \omega \right) \dots\dots\dots (4.12)$$

Equation (4.12) represents the XPM induced phase shift in probe signal at fiber output after propagating at distance  $L$ . This XPM induced phase shift will be converted to XPM induced intensity modulation (IM) by GVD effect [46, 54]. In order to determine the

strength of XPM induced IM in probe channel, the expression of power fluctuations on probe signal at fiber output induced by XPM at infinitesimal distance  $z$  from fiber input is given by [16]:

$$P_{xpm,1}(z, \omega) = -2P_1(z)\exp(-\alpha(L-z))\exp(-j\omega(L-z)/v_{g1})\sin(b(L-z))\phi_{xpm,1}(z, \omega) \dots (4.13)$$

Here  $P_1(z) = P_1(0)\exp(-\alpha z)$  is the average power of probe channel at distance  $z$ ,  $P_1(0)$  is the average power of probe channel at fiber input and  $b$  is defined as  $b = \omega^2 D \lambda_1^2 / (4\pi c)$ . The total XPM induced IM at probe channel at fiber output is the sum of the XPM induced IM at infinitesimal section  $z$  along the fiber with length with length  $L$  is given by:

$$P_{xpm}(\omega) = 2\gamma_1 P_1(0) P_2(\omega) \exp(-\alpha L) \exp(-j \omega L / v_{g1}) \cdot \left\{ \frac{1}{a^2 + (b + q)^2} [a \cdot \sin(bL) - (b + q) \cdot \cos(bL) + [a \cdot \sin(qL) + (b + q) \cdot \cos(qL)] \exp(-\alpha L)] \right. \\ \left. \frac{1}{a^2 + (b - q)^2} [a \cdot \sin(bL) - (b - q) \cdot \cos(bL) + [-a \cdot \sin(qL) + (b - q) \cos(qL)] \exp(-\alpha L)] \right\} \dots (4.14)$$

Here  $a = \alpha - j\omega d_{12}$ . In a nonzero dispersion region  $d_{12} \approx D_1 \cdot \Delta\lambda_{12}$  where  $\Delta\lambda_{12} = \lambda_1 - \lambda_2$  is the wavelength separation between channel 1 and 2. From equation (4.14) the magnitude and phase responses of XPM induced IM can be easily found out as shown in Figure 6.1. The normalized magnitude response induced by XPM in the probe channel, called normalized IM index is given by [36]:

$$m_{IM}^{XPM} = \left| P_{xpm}(\omega) / (P_2(z, \omega) \cdot \exp(-\alpha L)) \right| \dots (4.15)$$

On the other hand the phase response is given by

$$\phi_{IM}^{XPM}(\omega) = \arg \left[ P_{xpm}(\omega) / (P_2(z, \omega) \cdot \exp(-j\omega L / v_{g1})) \right] \dots (4.16)$$

The total XPM induced IM in the time domain at probe channel at fiber output is obtained by inverse Fourier transform of equation (4.14)

$$P_{xpm}(L, t) = \left| \frac{1}{\pi} \int_0^{\infty} P_{xpm}(\omega) \exp(-j\omega t) \delta t \right| \dots\dots\dots (4.17)$$

### 4.3.2 Bit Error Rate (BER) Derivation

The demultiplexed optical signals are then sent to the receiver. The photo-detector in the receiver senses the varying optical intensity falling upon it and converts them into varying electric current, using the direct detection method. The photo-detector output current is given by:

$$i(t) = R_d |E|^2 + i_n(t) = R_d |S_{out}(t)|^2 + i_n(t) = 2R_d P_s G L \cos(\Delta\phi_{xpm}(L, t)) + i_n(t) \dots\dots (4.18)$$

$R_d$  is the bias or load resistance,  $P_s$  is the receiver power.  $G$  and  $L$  are the gain and loss of the transmission link respectively.  $\Delta\phi_{xpm}(L, t)$  represents the random phase distortion introduced by XPM which can be obtained from (4.12).  $i_n(t)$  is the sum of the various noises considered in the system. The noise considered in this system are the receiver shot noise, thermal noise and beat noise due to beating of the spontaneous emission of the amplifier.

Considering the thermal noise to be predominant, it is assumed that the noise for transmitted "1" and "0" are of same magnitude. The total noise variance is obtained by summing the variances of the individual noise components:

$$\sigma_n^2 = \sigma_{shot}^2 + \sigma_{thermal}^2 + \sigma_{s-sp}^2 \dots\dots\dots (4.19)$$

The variance of the shot noise is given by:

$$\sigma_{shot}^2 = 2eR_d P_1 B_e \dots\dots\dots (4.20)$$

where  $R_d$  is the bias or load resistance of the photo-detector receiver,  $B_e$  is the bandwidth of the photo-detector and  $P_T$  is the received optical power at the photo-detector. The variance of the thermal noise is:

$$\sigma_{thermal}^2 = I_{th}B_e \dots\dots\dots (4.21)$$

where  $I_{th}$  is the thermal noise current generated by the detector bias resistance in the photo-detector receiver. The variance of the signal spontaneous noise is given by:

$$\sigma_{s-sp}^2 = n_{sp} (G-1)hv2R_d^2 P_T GLB_e \dots\dots\dots (4.22)$$

where  $G$  is the gain of the amplifier,  $\nu$  is the optical frequency and  $n_{sp}$  is the spontaneous emission factor or population inversion factor. Then the BER can be directly found out from [34]:

$$BER = 0.5\text{erfc} \left[ \frac{2R_d P_s GL \cos(\bar{\phi}_{xpm})}{\sqrt{\sigma_n^2 + \sigma_{xpm}^2}} \right] \dots\dots\dots (4.23)$$

Here  $\bar{\phi}_{xpm}$  is the mean phase shift due to XPM,  $\sigma_{xpm}^2$  is the mean amplitude fluctuation of the probe signal due to XPM.

#### 4.4 Applying Line Coding Schemes

For applying the line coding, the input data are passed through the line coder as in Figure 4.1(b). Then the data will have the form as shown in Equation (4.1) or (4.4). These data are then passed to the transmitter. The mathematical representation of the line coded data  $\bar{P}_2(0, \omega)$  replaces  $P_2(0, \omega)$  of Equation (4.2). The subsequent procedures are the same as given in Equation (4.14)

##### 4.4.1 Applying Duobinary Line Coding Schemes

For duobinary line coding scheme the expression for the input power is expressed as:

$$\bar{P}_i(0, \omega) = X_i(0, \omega) \cos(qz) \exp(-az) \exp(-j\omega z/v_{g2}) \dots \quad (4.24)$$

where  $X_i(0, \omega)$  is the power spectrum of the  $i$ th channel and is defined as following with  $W$  as the bandwidth [55]:

$$X_i(f) = \begin{cases} \frac{1}{2W} \left[ 1 + e^{-j\frac{f\pi}{W}} \right], & |f| < W \\ 0, & \text{otherwise} \end{cases}$$

$$X_i(f) = \begin{cases} \frac{1}{W} e^{-j\frac{f\pi}{2W} \cos\left(\frac{f\pi}{2W}\right)}, & |f| < W \\ 0, & \text{otherwise} \end{cases}$$

#### 4.4.2 Applying Novel Optical Line Coding Schemes

The input power of a system with Novel optical coding is expressed as

$$\bar{P}_2(0, \omega) = P_2(z, \omega) = G_e(f) \cos(qz) \exp(-az) \exp(-j\omega z/v_{g2}) \dots \quad (4.25)$$

where  $G_e(f)$  is defined in Equation (3.14).

#### 4.5 Summary

The quantified expression of XPM and its effect in terms of BER as expressed in Equations 4.4, 4.14 and 4.23 will be applied in the simulation in subsequent chapters. The IM Index and phase response on XPM as shown in Figure 4.3 is a reproduction of the graph as given in [16] which confirms the correctness of the approach. This result helps the author to go forward to apply the line codes.

## CHAPTER 5

### Simulation Methods

#### 5.1 Introduction

The nonlinear Schrodinger equation (NLSE) given in equation (5.1) governs the propagation of optical pulses inside single mode fibers. The NLSE is a partial differential equation that does not generally lend itself to analytical solutions except some specific cases in which the inverse scattering method can be employed. A numerical approach is often necessary for an understanding of the interplay between group velocity dispersion Kerr effects of optical fibers. The method that has been used extensively to solve the pulse propagation in nonlinear dispersive media is the split step Fourier method. The relative speed of this method compared with most finite-difference methods can be attributed in part to the use of the fast Fourier transform (FFT) algorithm.

#### 5.2 Split Step Fourier Method

Pulse propagation in optical fiber is simulated by applying the split-step Fourier method to numerically solve the NLSE, which includes the effect of first order and second order GVD, self phase modulation (SPM) and cross phase modulation (XPM) due to fiber nonlinearity and fiber attenuation. This is a well established mathematical model and is extensively modeled for all fibers in the transmission system, i.e. for DSF and DCF. Considering a slow varying pulse envelope  $A(z,t)$  which can be the envelop of a summation of a number of optical channels of the WDM system, which propagates inside a nonlinear dispersive optical fiber in the following manner:

$$\frac{\partial A}{\partial z} + \frac{\alpha}{2} A + \frac{j}{2} \beta_2 \frac{\partial^2 A}{\partial T^2} - \frac{1}{6} \beta_3 \frac{\partial^3 A}{\partial T^3} = j\gamma_k \left[ |A_k|^2 + \sum_{i=1, i \neq k}^N 2|A_i|^2 \right] A_k \dots\dots (5.1)$$

where  $\alpha$  is the fiber loss,  $\beta_2$  and  $\beta_3$  are the second and third order GVD factors respectively,  $\gamma$  is the nonlinearity parameter, and  $T = t - z/v_g$  is a frame of reference

moving with the pulse at group velocity  $v_g$ . The first and second terms on the right hand side account for self phase modulation and cross phase modulation of the optical field with the  $N-1$  adjacent channels respectively. If we consider a two channel system what is considered in this paper, then the field propagation can be expressed as the coupled NLSE [36]:

$$\frac{\partial A_1}{\partial z} + \frac{j}{2} \beta_{21} \frac{\partial^2 A_1}{\partial T^2} + \frac{\alpha}{2} A_1 = j \gamma_1 \left[ |A_1|^2 + 2|A_2|^2 \right] A_1 \dots\dots\dots (5.2.a)$$

$$\frac{\partial A_2}{\partial z} + d \frac{\partial A_2}{\partial T} + \frac{j}{2} \beta_{22} \frac{\partial^2 A_2}{\partial T^2} + \frac{\alpha}{2} A_2 = j \gamma_2 \left[ |A_2|^2 + 2|A_1|^2 \right] A_2 \dots\dots\dots (5.2.b)$$

The walk-off parameter  $d = v_{g2}^{-1} - v_{g1}^{-1}$  where  $v_{gj}$  is the group velocity of channel  $j$ . The walk-off parameter can also be expressed in terms of the dispersion coefficient  $D$ . Then,

$$d = \int_{\lambda_1}^{\lambda_2} D(\lambda) d\lambda = D |\lambda_2 - \lambda_1| = D \Delta\lambda$$

### 5.2.1 Light Waves Beam Propagation Method using Split Step Model

The instantaneous pulse envelope  $A(z,t)$  propagating inside the fiber is calculated by solving equation (5.1) numerically using the split-step Fourier method. Expressing equation (56) as

$$\frac{\partial A}{\partial z} = (\hat{D} + \hat{N})A \dots\dots\dots (5.3)$$

where  $\hat{D}$  is the dispersion differential operator and  $\hat{N}$  is the nonlinearity operator.  $\hat{D}$  and  $\hat{N}$  are defined by:

$$\hat{D} = -\frac{\alpha}{2} - \frac{j}{2} \beta_2 \frac{\partial^2}{\partial T^2} + \frac{1}{6} \beta_3 \frac{\partial^3}{\partial T^3} \dots\dots\dots (5.4.a)$$



$$\hat{N} = j\gamma_k \left[ |A_k|^2 + \sum_{i=1, i \neq k}^N 2|A_i|^2 \right] \dots\dots\dots (5.4.b)$$

As these two operators appear to add by superposition, dispersive and nonlinear effects can be considered to act independently. That is, the two effects split. Next consider dividing the fiber length into small steps of length h. The exact solution of (5.1) describes the pulse envelope in segment z+h relative to its shape in the preceding segment z:

$$A(z+h, T) = \exp(h\hat{D})\exp(h\hat{N})A(z,T) \dots\dots\dots (5.5)$$

where the exponential operator  $\exp(h\hat{D})$  is evaluated in the Fourier domain by replacing the differential operator by  $\frac{\partial}{\partial T}$  by  $(j\omega)$ :

$$\exp(h\hat{D})B(z,T) = F^{-1}\{\exp[h\hat{D}(j\omega)]F(B(z,T))\} \dots\dots\dots (5.6)$$

This equation is numerically solved using the Finite-Fourier-Transform (FFT) algorithm. To improve the accuracy of the split-step Fourier method, the pulse is made to propagate in the following pattern:

$$A(z+h,T) = \exp\left(\frac{h}{2}\hat{D}\right) \exp\left(\int_z^{z+h} \hat{N}(z')dz'\right) \exp\left(\frac{h}{2}\hat{D}\right)A(z,T) \dots\dots (5.7)$$

Intuitively, this equation says that a pulse emerges out of the preceding fiber segment and enters the current segment would propagate in a purely dispersive medium in the first half of the segment, then stops at middle of the segment and picks up all nonlinear effects in that segment, then set off to complete the remaining half of the purely dispersive segment. The pulse would then propagate through the subsequent segments in the same manner until it reaches the receiving end of the fiber.

The self-phase-modulation SPM refers to the nonlinear phase shift in the optical wave caused by the optical field itself. Such effect is generally negligible at low power levels (normally below 10 mW) but becomes significant when the peak intensity of the pulse is sufficiently high to cause appreciable change in the refractive index of silica fiber [56]. This intensity induced index variation, referred to as the Kerr nonlinearity, produces a nonlinear phase shift in the carrier wave and leads to spectral broadening of the pulse. For WDM systems, the nonlinear effects are expected to further enhance with the phase shift for a channel depends not only on the power of that channel but also on the power in the adjacent channels, the so called cross phase modulation (XPM).

In general, dispersion and nonlinearity act together along the length of the fiber. The Split Step Method obtains an approximate solution by assuming that in propagating the optical field over a small distance  $h$ , the dispersive and nonlinear effects can be pretended to act independently. More specifically, propagation from  $z$  to  $z+h$  is carried out in two steps as shown in Figure 5.1. The algorithm for this model is implemented in MATLAB.

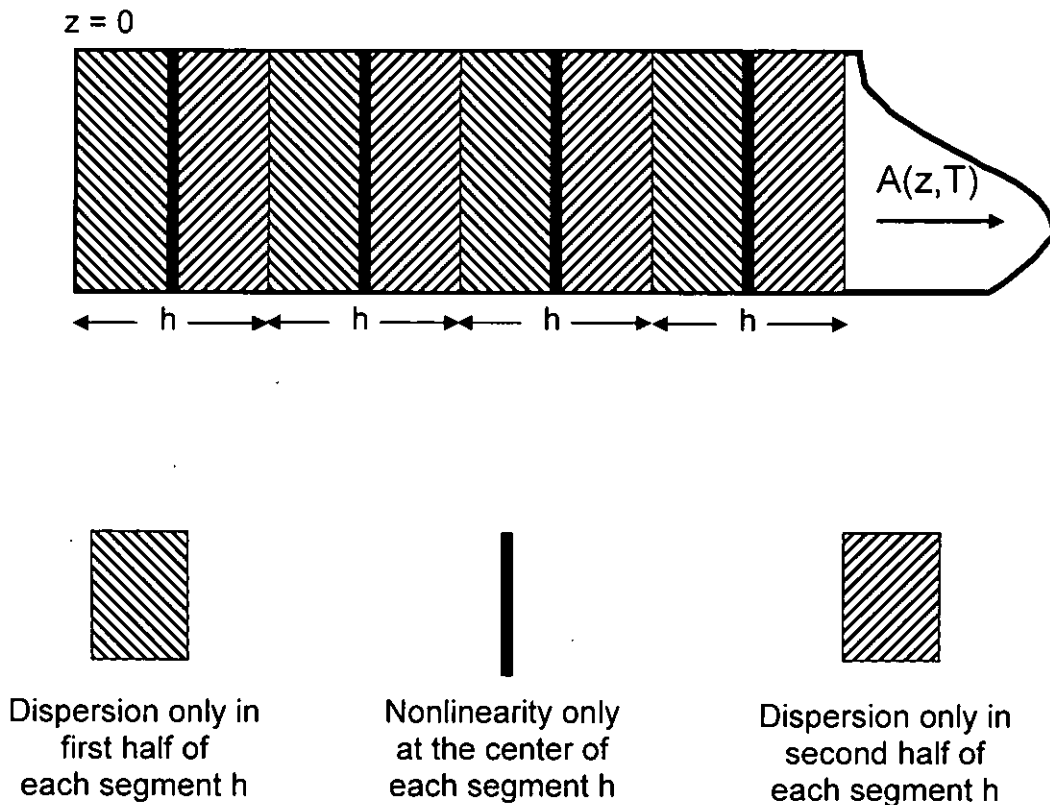


Figure 5.1 Schematic Illustration of Symmetrized Split Step Model

### 5.2.2 Algorithm for the Split Step Model

This algorithm is developed to synthesize the Split Step Model using the numerical methods. The algorithm is developed for the MATLAB platform.

Step 1: This step corresponds to the first half dispersion only region shown in Figure 5.1. In this process, only the dispersion (the linear operator part) acts alone and nonlinearity = 0. Thus, we have

$$A_{D1}(z+\frac{h}{2}, T) = F^{-1} \left[ \exp\left(\frac{h}{2} \tilde{D}(j\omega)\right) \cdot F\{A_0(0, T)\} \right] \dots\dots\dots (5.8)$$

where F is the Fast Fourier Transform and  $A_0(0, T)$  is the optical multiplexed signals of the optical channels of different carriers or that of a single channel. The WDM signals is in fact a summation of all the electric fields representing the optical intensity channels propagated along the optical fiber transmission line. The linear operator  $D(j\omega)$  is obtained by replacing differential operator by  $(j\omega)$  where  $\omega$  is the Fourier frequency. Thus, the equation is given by

$$\tilde{D}(j\omega) = \frac{j}{2} \beta_2 \omega^2 - \frac{j}{6} \beta_3 \omega^3 - \frac{\alpha}{2} \dots\dots\dots (5.9)$$

Step 2: The Split Step Model can be expressed in the following expression:

$$A(z+h, T) = \exp\left(\frac{h}{2} \tilde{D}\right) \exp\left(\int_z^{z+h} \tilde{N}(z') dz'\right) \exp\left(\frac{h}{2} \tilde{D}\right) A(z, T) \dots\dots\dots (5.10)$$

where the integral has to be evaluated more accurately by employing the trapezoidal rule and the approximated integral is given by

$$\left( \int_z^{z+h} \tilde{N}(z') dz' \right) \approx \frac{h}{2} \left\{ \tilde{N}(z) + \tilde{N}(z+h) \right\} \dots\dots\dots (5.11)$$

However, the implementation of (5.11) is not simple since  $\tilde{N}(z+h)$  is unknown at the mid-segment located at  $z+h/2$  as marked by thick black line in Figure 5.1. It is necessary to follow an iterative procedure that is initiated by replacing  $\tilde{N}(z+h)$  by  $\tilde{N}(z)$ . Equation (5.10) is then used to estimate  $A(z+h,T)$  which in turn to calculate the new value of  $\tilde{N}(z+h)$  from (5.7). Thus, the overall algorithm of Step 2 can be expressed in the following steps:

$$A_{D1}(z + \frac{h}{2}, T) = F^{-1} \left[ \exp\left(\frac{h}{2} \tilde{D}(j\omega)\right) F\{A(z, T)\} \right] \dots\dots\dots (5.12)$$

$$A_{N1}\left(z + \frac{h}{2}, T\right) = \exp\left[\frac{h}{2} \left\{ \tilde{N}(z) + \tilde{N}(z+h) \right\}\right] A_{D1}\left(z + \frac{h}{2}, T\right) \dots\dots (5.13)$$

$$A_{D1+N1}\left(z + \frac{h}{2}, T\right) = F^{-1} \left[ \exp\left(\frac{h}{2} \tilde{D}(j\omega)\right) F\{A_{N1}(z + \frac{h}{2}, T)\} \right] \dots (5.14)$$

Hence, the predicted  $\tilde{N}(z+h)$  is found to be:

$$\tilde{N}(z+h) = jY \left\{ \left| A_{D1+N1}\left(z + \frac{h}{2}, T\right) \right|^2 \right\} \dots\dots\dots (5.15)$$

The predicted  $N(z+h)$  will be substituted into (5.13) in order to get a more accurate prediction of (5.15). Thus, this process is done iteratively.

Step 3: The predicted  $N(z+h)$  would then be used to calculate the lumped region which is shown in Figure 5.1. In this process, only the nonlinear (nonlinear operator part) acts alone and  $D = 0$ .

$$A_{N2}\left(z + \frac{h}{2}, T\right) = \exp\left\{\frac{h}{2} \left( \tilde{N}(z) + \tilde{N}(z+h) \right)\right\} A_{D1}\left(z + \frac{h}{2}, T\right) \dots\dots (5.16)$$

Step 4: This step corresponds to the second half dispersion only region shown in Figure 5.1. In this process, only the dispersion (linear operator part) acts alone and  $\hat{N} = 0$ . Thus, we have

$$A(z+h,T) = F^{-1} \left[ \exp\left(\frac{h}{2} \tilde{D}(j\omega)\right) F\left\{A_{N_2}\left(z + \frac{h}{2}, T\right)\right\} \right] \dots\dots\dots (5.17)$$

Step 5: Repeat Step 1 by substituting  $A(z+h,T)$  from equation (4.17) into  $A_0(0,T)$  of (5.8) for further propagation into the next segment defined in Figure 5.1.

### 5.3 Eye-opening Penalty

In a digital communication link, bit error rate (BER) is the most important parameter to measure the performance of the communication link between a transmitter and a receiver. In an optical fiber communication system, BER may often be measured only experimentally. This is because the high quality performance of a conventional optical fiber communication link ( $BER = 10^{-9}$ ) requires an extremely large number of bits to evaluate BER, which makes numerical simulation of BER generally impractical. BER is often evaluated indirectly using Q-factor, which is commonly used to measure system performance. Another simpler way of estimating performance is to observe eye-opening. The eye-opening is quantified by measuring the minimum value between the sampled values of marks (ones) and spaces (zeros) in the received bit sequence,  $r(t)$ . The eye opening is a useful system performance metric when signal distortion is a more limiting factor than noise. Mathematically, it is defined as below [53].

$$\text{Eye-opening} = \frac{\min(r_j(t_j, b = 1)) - \max(r_j(t_j, b = 0))}{\sqrt{P_0}} \dots\dots\dots (5.18)$$

where  $t_j$  represents the sampling instant of the  $j$ th-bit interval and  $P_0$  is the peak power of  $r(t)$ . The first term in the numerator represents the minimum value at the sampling instant when a mark is transmitted, and the second term is the maximum value when a space is transmitted. In this chapter, the sampling instant of the received signal is assumed to be at the center of each bit period.

To assess system performance degradation due to signal transmission through the fiber, eye-opening penalty (EOP) is often used. EOP is the measure of the relative eye opening after transmission compared to eye opening in the back-to-back case (no transmission effect). That is,

$$\text{EOP(dB)} = -10\log\left[\frac{\text{EOAT}}{\text{EOBB}}\right] \dots\dots\dots (5.19)$$

where EOAT and EOBB denote eye-opening after transmission (with fiber) and eye-opening back-to-back (without fiber) respectively. EOP will be used in this paper to quantify the system performance.

#### 5.4 Filter Design

There are several methods commonly used to design filter, such as Butterworth, Chebyshev and Elliptic filter designs. Amongst these, Butterworth response is normally called the "maximally flat" response with minimum ripple in the passband and stopband region. Its magnitude squared function is defined by:

$$|H_{LP}(j\omega)|^2 = \frac{1}{1 + \left(\frac{\omega}{\omega_c}\right)^{2N}} \dots\dots\dots (5.20)$$

N is the order of the filter and  $\omega_c$  is the cutoff frequency where the filter magnitude is  $1/\sqrt{2}$  times the dc gain at  $\omega = 0$ , which is also 3 dB cutoff. For a cutoff or critical frequency of 1, the result is called a normalized prototype lowpass filter. Cutoff frequency of 1 is used in the simulations of this paper. For Butterworth filter responses, the poles of  $H_{LP}(s)H_{LP}(-s)$  are the roots of:

$$(-1)^N s^{2N} = -1 = e^{j(2k-1)\pi} \quad k = 0, 1, 2, \dots, 2N-1 \dots\dots\dots (5.21)$$

Therefore, the poles of  $S_k$  are given by

$$S_k = e^{j[(2k+N-1)/2N]\pi} \quad k = 0, 1, 2, \dots, 2N \quad \dots \quad (5.22)$$

$S_k$  is also expressed as  $S_k = \sigma_k + j\omega_k$ , where the real and imaginary parts are given by:

$$\sigma_k = \sin\left(\frac{2k-1}{N}\right)\frac{\pi}{2}, \quad \omega_k = \cos\left(\frac{2k-1}{N}\right)\frac{\pi}{2} \quad \dots \quad (5.23)$$

With (5.22) and (5.23), the transfer function of the Butterworth lowpass prototype response for specific order could easily be found out. The magnitude and phase response of a Butterworth lowpass filter with  $N = 2$ ,  $f_c = 1$  and sampling frequency of  $1000 \times f_c$  are shown in Figure 5.2 and Figure 5.3.

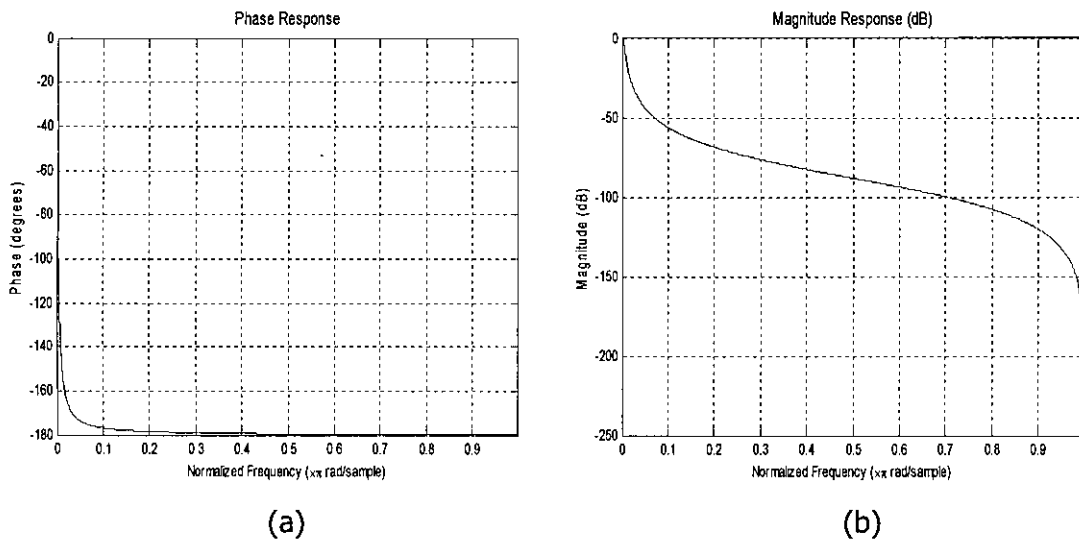


Figure 5.2 (a) Frequency and (b) Magnitude Response of a Butterworth Lowpass Filter

## 5.5 Summary

In this chapter, the numerical analysis technique is described that is followed in this work. Since there is no analytical solution for NLSE, we solved it using the split step Fourier transform method using the FFT algorithm as described in this chapter. During the transmission of an optical pulse and during its detection within the receiver different noise mechanisms degrade the actual pulse shape. Therefore, signal-to-noise ratio (SNR) is an important parameter for any transmission system. The system performance can be judged from the value of BER and eye-power penalty.

## CHAPTER 6

### Simulation Results and Discussions

#### 6.1 Introduction

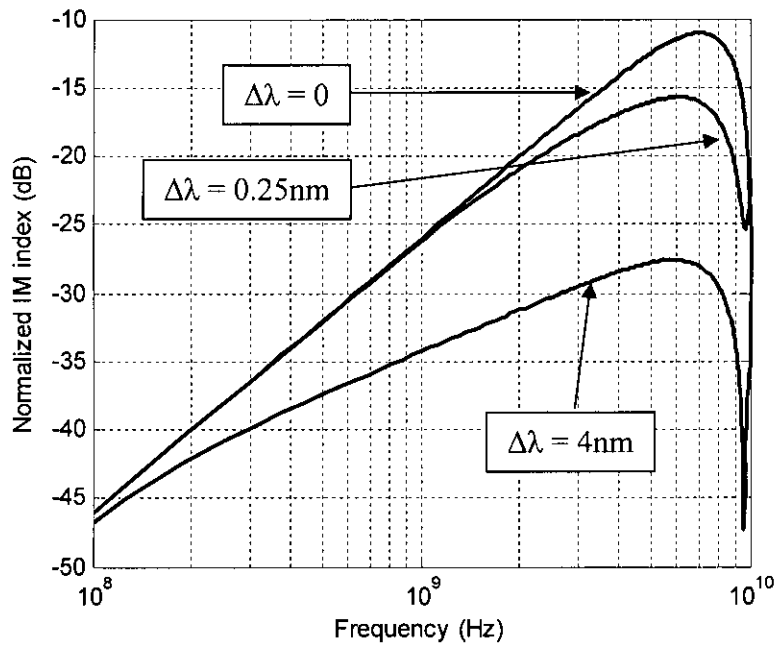
In this chapter, first, the reader is introduced to the effect of XPM induced phase shift considering the pump-probe approach. The XPM effects will be shown for different probe power, pump power, distance, channel separation and bit rates. Then line code will be applied for the same parameters to visualize its effect on XPM. Thereafter the allowable probe and pump power will be found out for the BER of  $10^{-9}$  with and without line code to quantify the improvement in power penalty achieved by the application of the line code. At last a two channel DWDM system will be examined to verify the effects of XPM by applying 1024 bit sequence with and without line code where eye penalty will be applied to verify the effect of the XPM.

#### 6.2 Simulation Results for XPM in the DWDM System

For a consistent and gradual development of the study some of the parameters are kept unchanged. The bit pattern used is PRBS 512 bits, nonlinear refractive index ( $n_2$ ) is  $2.6 \times 10^{-20} \text{ m}^2/\text{W}$  and fiber core effective area ( $A_{\text{eff}}$ ) is  $5.28 \times 10^{-11} \text{ m}^2$ . According to Equation (4.17) that the XPM induced power depends on factors such as probe power, pump power, distance, channel separation, bit rate, etc. Normalized IM index and phase response due to XPM for the channel separations of 0, 0.25 and 4 nm; the average power per channel is 0 dBm,  $\lambda_1 = 1550 \text{ nm}$ ,  $D = 17 \text{ ps/km-nm}$ ,  $\gamma_1 = 1.18 \text{ W}^{-1} \cdot \text{km}^{-1}$ ,  $\alpha = 0.21 \text{ dB/km}$  and  $L = 80 \text{ km}$  are depicted in Figure 6.1.

Figure 6.2 and 6.3 shows the total XPM induced power for analytical and simulated approach in a lossless system. Figure 6.2 exhibits XPM induced power for a range of pump power with probe power  $P_1 = 0 \text{ dBm}$ . Bit rate = 10 GHz, channel spacing = 50 GHz and fiber length = 50, 100 and 150 km. Figure 6.3 exhibits XPM induced power for a range of probe power with probe power  $P_1 = 0 \text{ dBm}$ . Bit rate = 10 GHz, channel spacing = 50 GHz and fiber length = 50, 100 and 150 km. These two figures show that the XPM induced power increases proportionately with distance and input powers which conforms to the Equation (4.17).





(a)

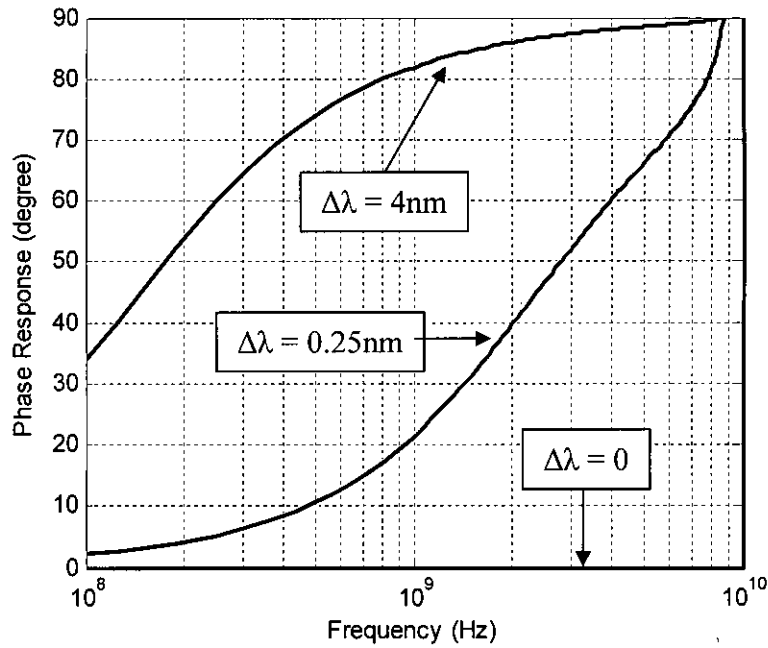


Figure 6.1 (a) Normalized IM index in dB and (b) phase response versus the pump modulation frequency for the channel separations of 0, 0.25 and 4 nm. The average power per channel is 0 dBm. Here  $\lambda_1=1550$  nm,  $D = 17$  ps/km-nm,  $\gamma_1 = 1.18$  W<sup>-1</sup>.km<sup>-1</sup>,  $\alpha = 0.21$  dB/km and  $L = 80$  km.

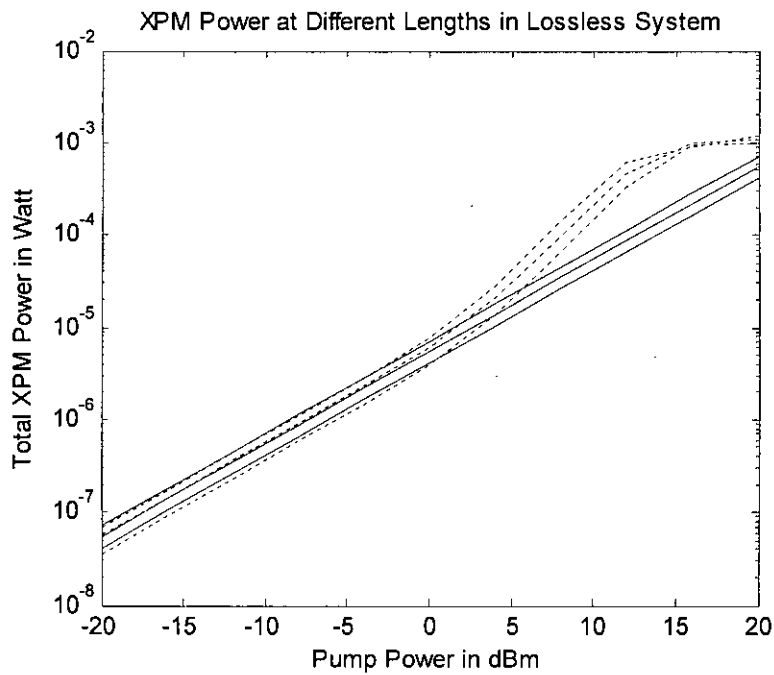
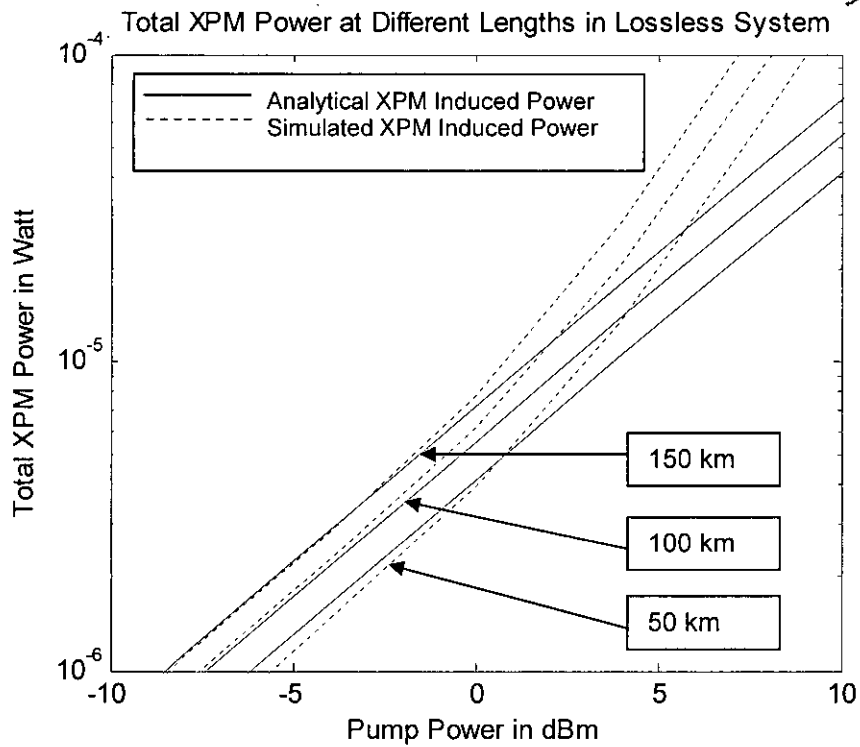
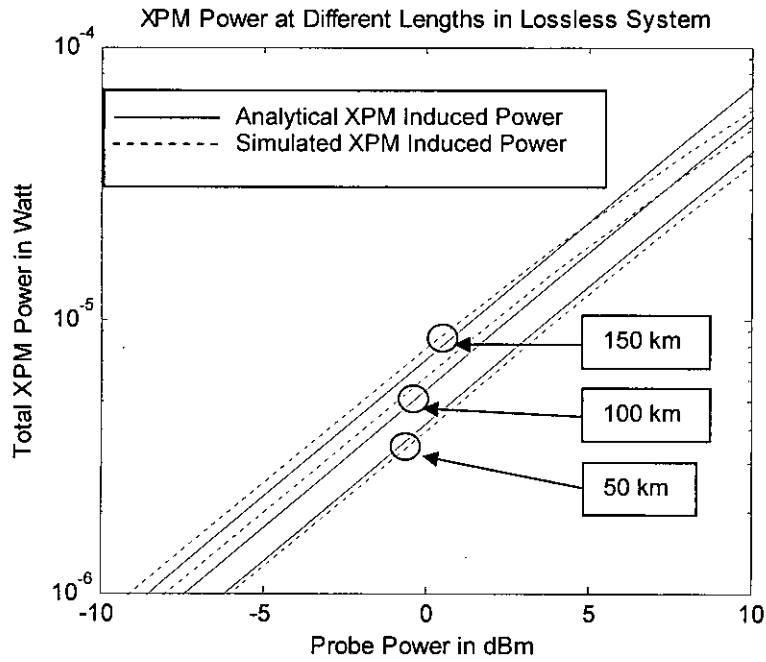
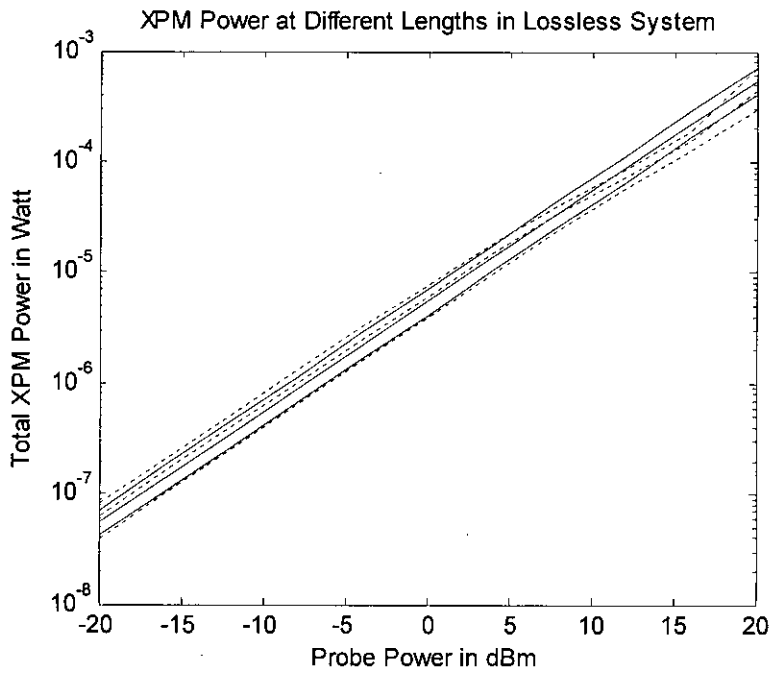


Figure 6.2 Total XPM induced power in a lossless system with probe power  $P_1 = 0$  dBm, bit rate = 10 GHz, channel spacing = 50 GHz and fiber length = 50, 100 and 150 km for pump power ( $P_2$ ) = (a) -20 to 20 and (b) -10 to 10 dBm.



(a)



(b)

Figure 6.3 Total XPM induced power in a lossless system with pump power  $P_2 = 0$  dBm, bit rate = 10 GHz, channel spacing = 50 GHz and fiber length = 50, 100 and 150 km for probe power ( $P_1$ ) = (a) -20 to 20 and (b) -10 to 10 dBm.

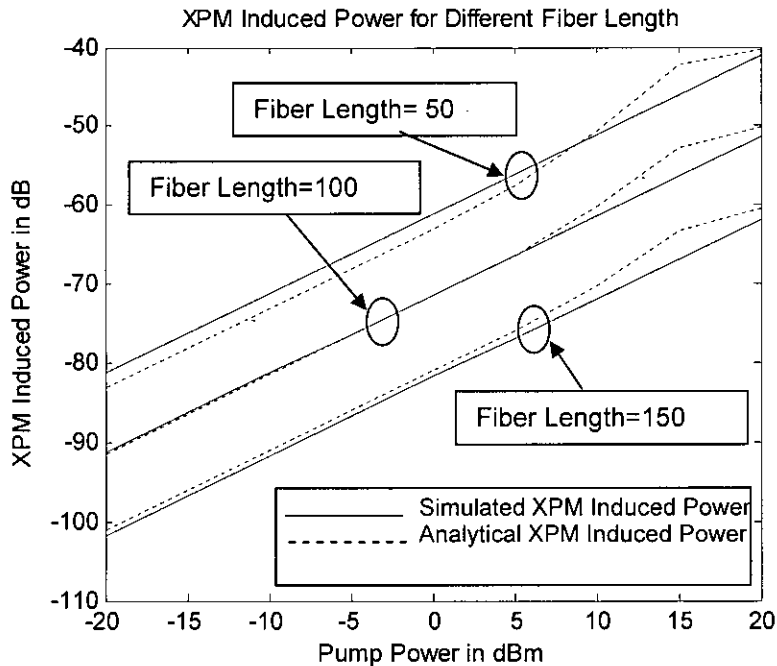
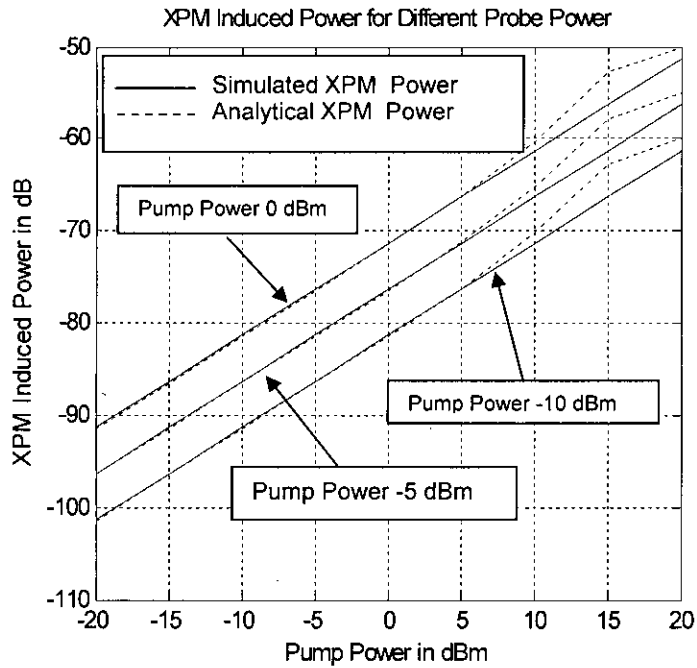


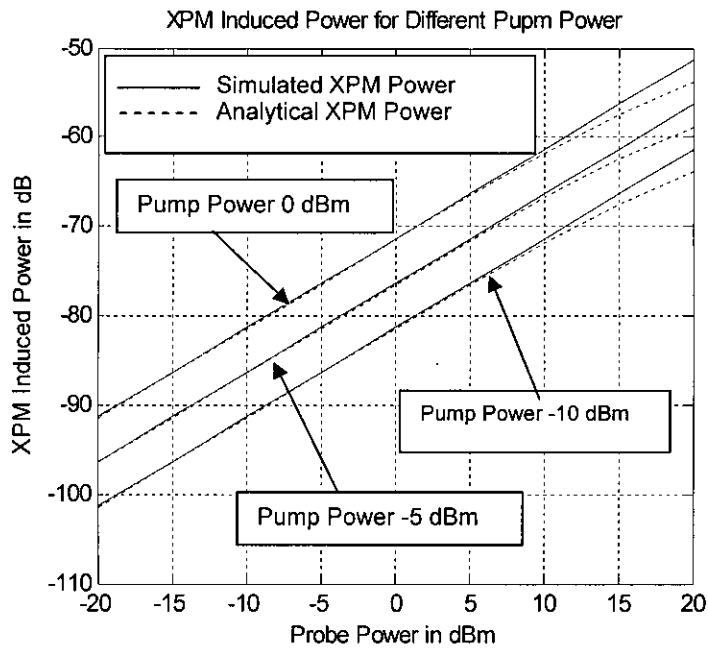
Figure 6.4 Total XPM induced power for a lossy system with probe power  $P_1 = 0$  dBm, bit rate = 10 GHz, channel spacing = 50 GHz and fiber Length = 50, 100 and 150 km.

Figure 6.4 shows analytical and simulated XPM power for a lossy system ( $\alpha > 0$ ) for different lengths with probe power  $P_1 = 0$  dBm, bit rate = 10 GHz and channel spacing = 50 GHz. This figure conforms to Figure 6.2 and 6.3 which was lossless, with the difference that total XPM induced power for a particular input pump power decreases proportionately with distance. This phenomenon is due to the reason that the input powers at higher distances gets decreased due to loss effect and so as to the induced XPM power due to those input powers.

Figure 6.5 shows total XPM power in dB for different probe and pump powers at 100 km, bit rate = 10 GHz and channel spacing = 50 GHz. Here also the figure conforms to the mathematical expression of Equation (4.17). The XPM induced power increases proportionately with input powers, the higher the input power either probe power or pump power the more is the XPM induced power.



(a)



(b)

Figure 6.5 Total XPM power in dB for different (a) probe powers (0, -5 and -10 dBm) and (b) pump powers (-10, -5 and 0 dBm) at 100 km

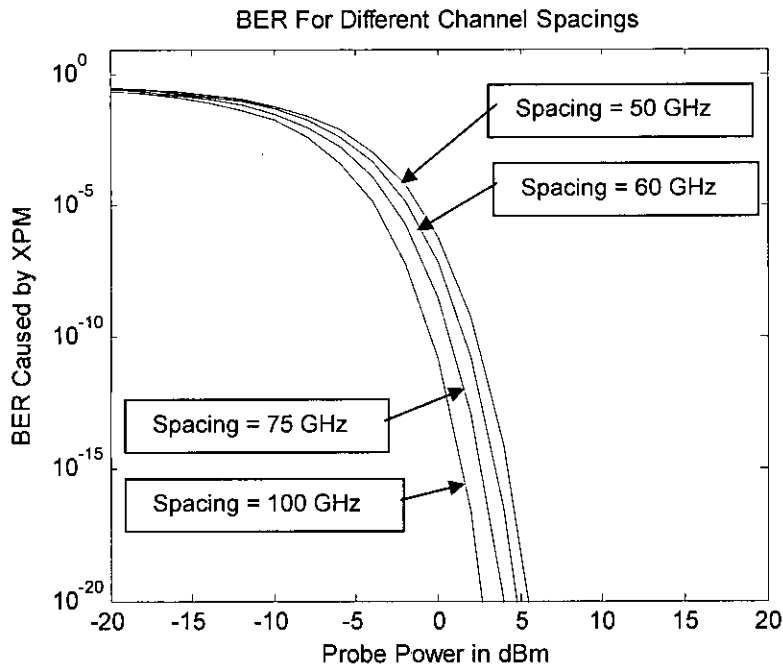


Figure 6.6 Plot of BER for channel spacing 50, 60, & 75 and 100 GHz with  $P_2 = 0$  dBm, fiber length = 100 km and bit rate = 10 GHz

Figure 6.6 shows the Plot of BER for channel spacing 50, 60, & 75 and 100 GHz with  $P_2 = 0$  dBm, fiber length = 100 km and bit rate = 10 GHz. The figure shows that with lower channel spacing the BER increases.

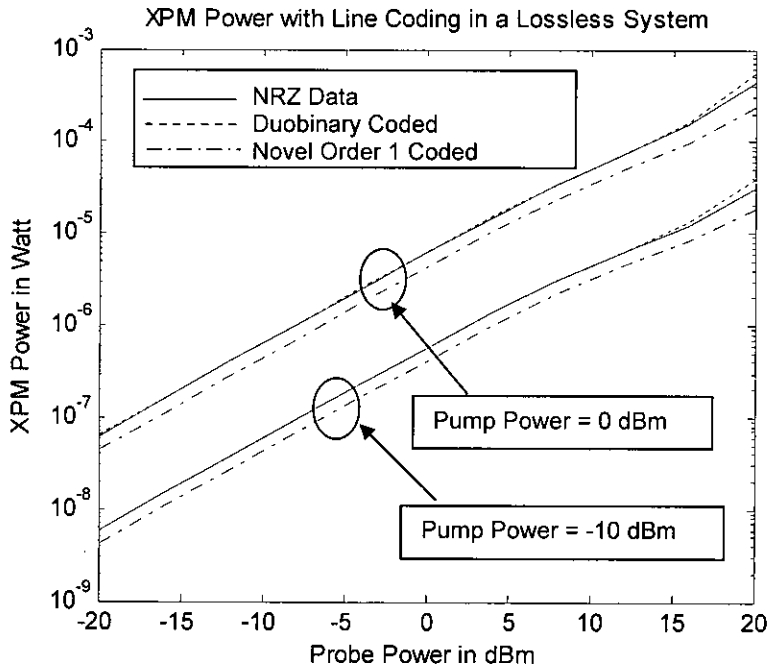
Figure 6.7 shows XPM Power with line coding for both analytical and simulated result for different pump and probe powers. Figure 6.7 shows a very important finding that the XPM induced power is less for Novel line coded scheme. Two coding schemes are applied in this simulation. It is evident from the plot that the application of duobinary coding does not reduce the XPM much but the Novel Order one coding scheme shows a remarkable reduction of XPM induced power.

In Figure 6.8 the analytical and simulated BER for different probe powers at 100 km with bit rate = 10 GHz and channel spacing = 50 GHz exhibits an important characteristics of XPM. It is evident from Equation (4.1) that the influence of pump power is more than the probe power. The analytical and simulated results show similar pattern of the curves in terms of shape and related values are also without much discrimination. It is very clear from the plot that when the probe power is low in comparison with the pump power, the BER is more. As the probe power is increased the BER also reduced. From this figure we can conclude that the BER due to XPM will be more if the probe power is less in comparison with the pump power.

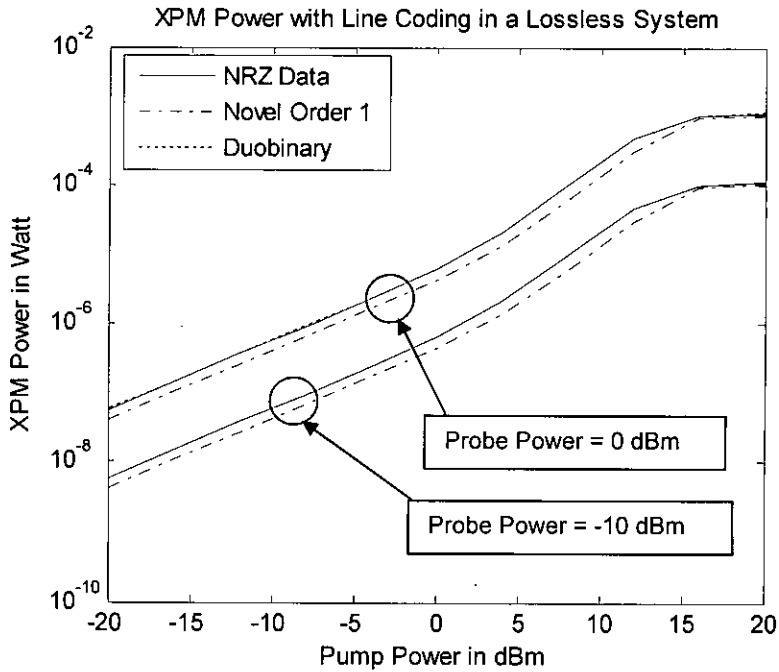
In Figure 6.9 the analytical and simulated BER for different pump powers at 100 km with bit rate = 10 GHz and channel spacing = 50 GHz exhibits another important characteristics of XPM induced power and the related effects. It is evident from Equation (4.1) that the probe power contributes directly to the XPM. Here also the analytical and simulated results show similar pattern of the curves in terms of shape and related values are also without much disagreement. It is very clear from the plot that when the pump power is low in comparison with the probe power, the BER is also low. As the pump power is increased the BER also increases. From this figure we can conclude that the BER due to XPM will be more if the pump power is more in comparison with the probe power.

Figure 6.10 shows the effect of the application of line coding scheme in a DWDM system with bit rate of 10 GHz, channel spacing of 50 GHz and fiber length of 100 km. XPM induced power and BER caused by XPM with for different probe powers for NRZ data, Duobinary code and Novel Order 1 code shows that Novel Order 1 code could successfully reduce the XPM induced power and in the same token the BER also reduced. Figure 6.11 shows exhibits the same characteristics for different pump powers.

100898



(a)



(b)

Figure 6.7 XPM Power with line coding, (a) analytical result for pump power = -10 and 0 dBm and (b) simulated result for probe power = -10 and 0 dBm with fiber length = 100 km, bit rate = 10 GHz and channel spacing = 50 GHz.



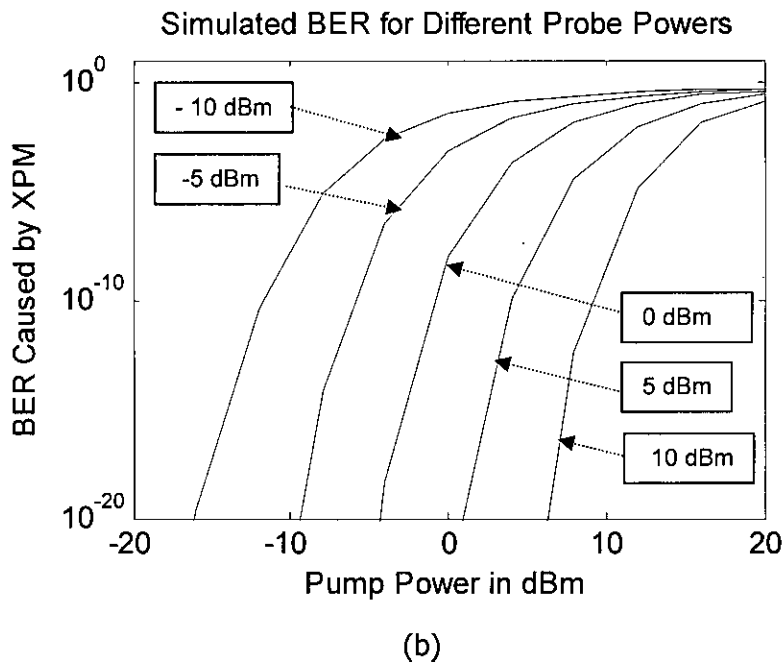
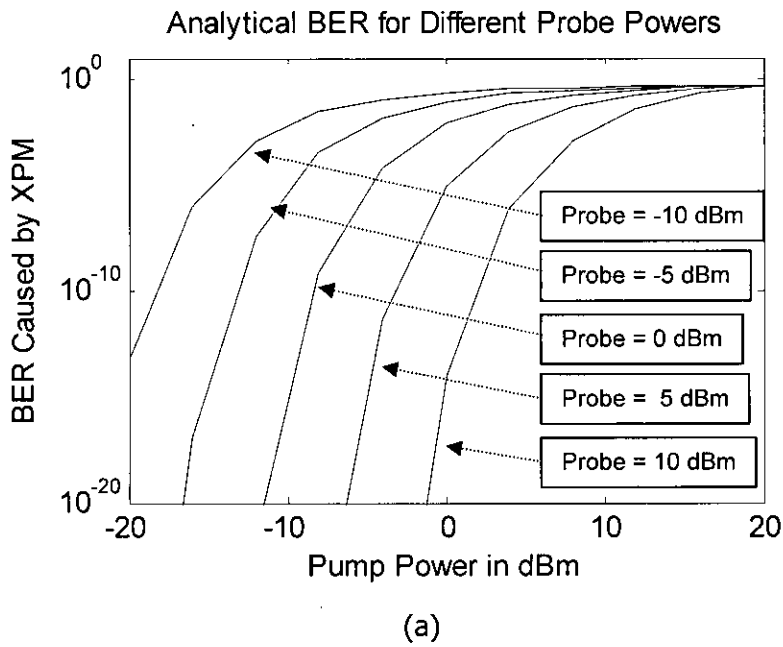
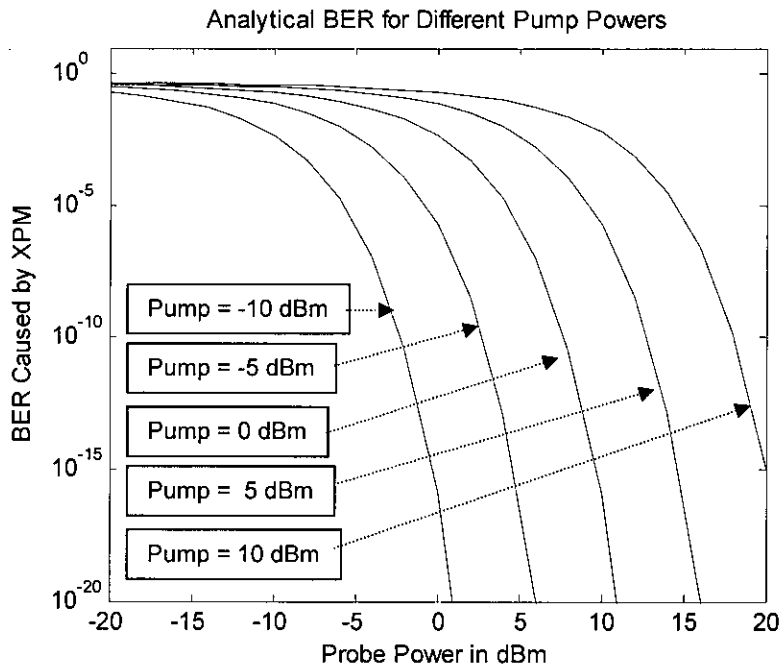
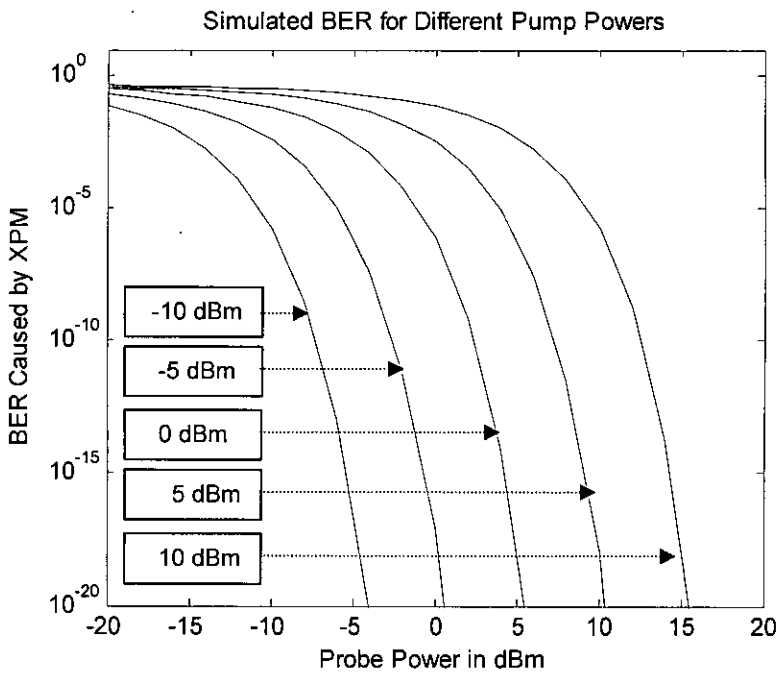


Figure 6.8 (a) Analytical (b) Simulated BER for different probe powers -10, -5, 0, 5 and 10 dBm at 100 km with bit rate = 10 GHz and channel spacing = 50 GHz.

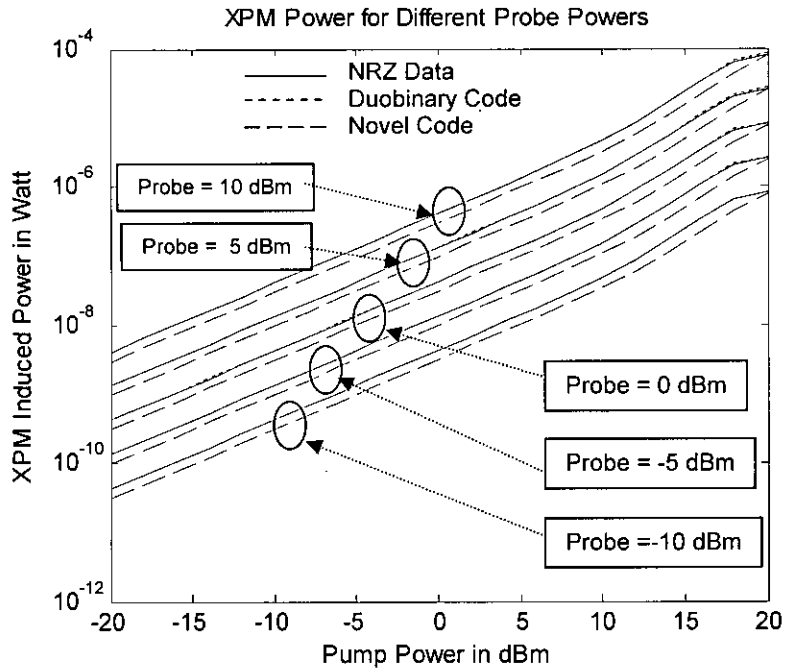


(a)

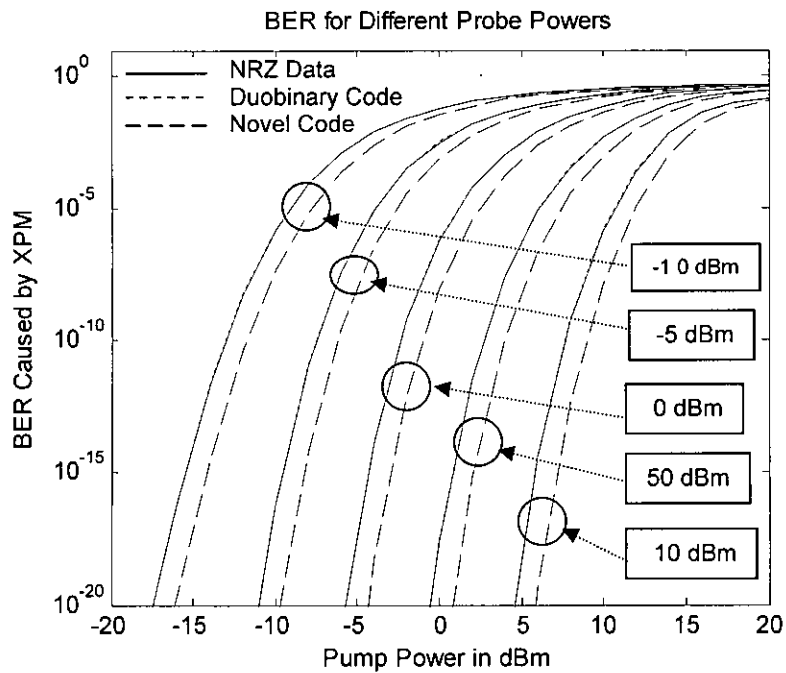


(b)

Figure 6.9 (a) Analytical (b) Simulated BER for different pump powers -10, -5, 0, 5 and 10 dBm at 100 km

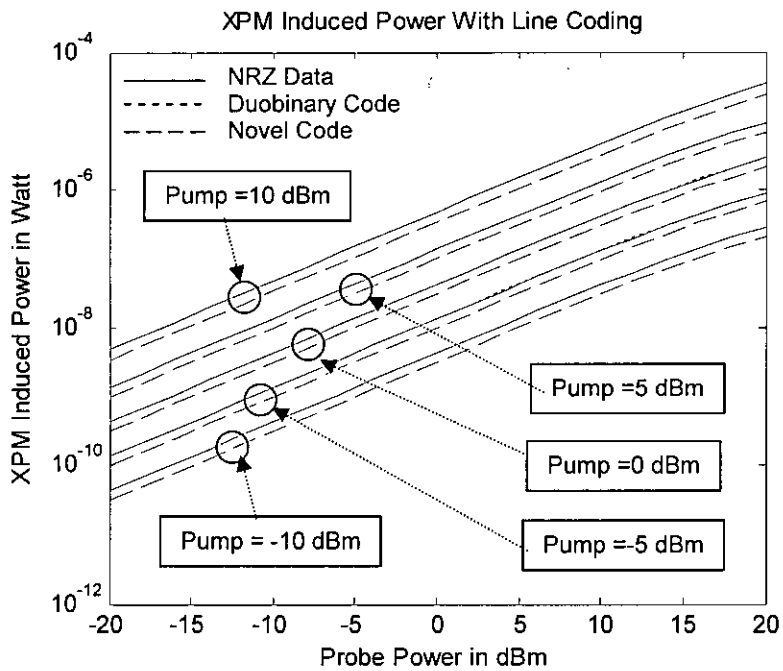


(a)

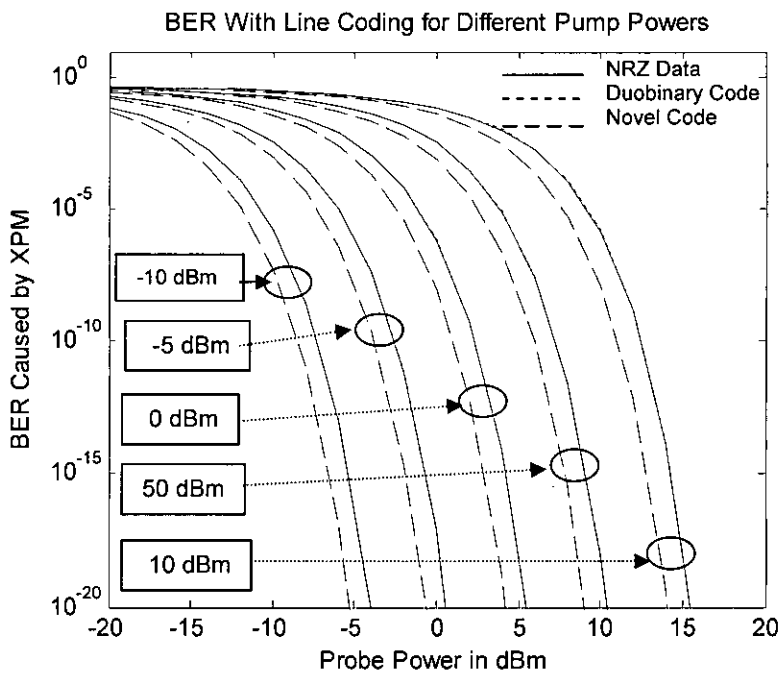


(b)

Figure 6.10 Plot of (a) XPM induced power and (b) BER caused by XPM with NRZ data, Duobinary and Novel Order 1 Code for probe power -10, -5, 0, 5 and 10 dBm for 100 km fiber.



(a)



(b)

Figure 6.11 Plot of (a) XPM induced power and (b) BER caused by XPM with NRZ data, Duobinary and Novel Order 1 Code for pump power -10, -5, 0, 5 and 10 dBm for 100 km fiber.

Figure 6.12 shows the allowable pump power at different distances applying line codes. Table 6.1 quantifies the allowable pump power. It is evident from Figure 6.12 that with Novel Order 1 code, the allowable pump power is more for the same BER. Table 6.1 shows that the improvement is about 1.27 dB. This improvement is the main finding of this study.

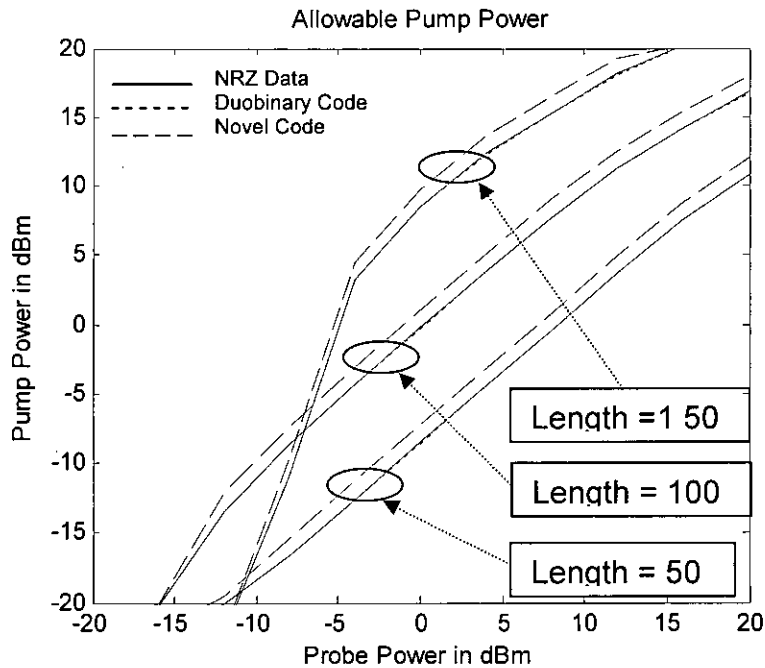


Figure 6.12 Plot of allowable pump power for BER of  $10^{-9}$  at 50, 100 and 150 km

Table 6.1: Improvement in allowable pump power in dB by applying Novel line code in comparison with NRZ data for BER of  $10^{-9}$  at different lengths

Length km	Probe Power in dBm										
	-20	-16	-12	-8	-4	0	4	8	12	16	20
50	0	0	0.5630	1.2900	1.2910	1.2902	1.2892	1.2884	1.2842	1.2715	1.2540
100	0	0.2380	1.2930	1.2918	1.2913	1.2902	1.2871	1.2814	1.2660	1.2530	1.2300
150	0	0	0	1.2859	1.2884	1.2824	1.2710	1.2490	1.2000	0	0

Figure 6.13 shows the allowable probe power at different distances applying line codes. Table 6.3 quantifies the allowable probe power. It is evident from Figure 6.13 that with Novel Order 1 code, the allowable probe power is decreased for the same BER. Table 6.2 shows that the improvement is about 1.3 dB. It is also evident that the improvement is not the same for all the combinations of power. This improvement is also the main finding of this study. Figure 6.14-16 shows the simulated eye diagram of probe channel for 512 PRBS data.

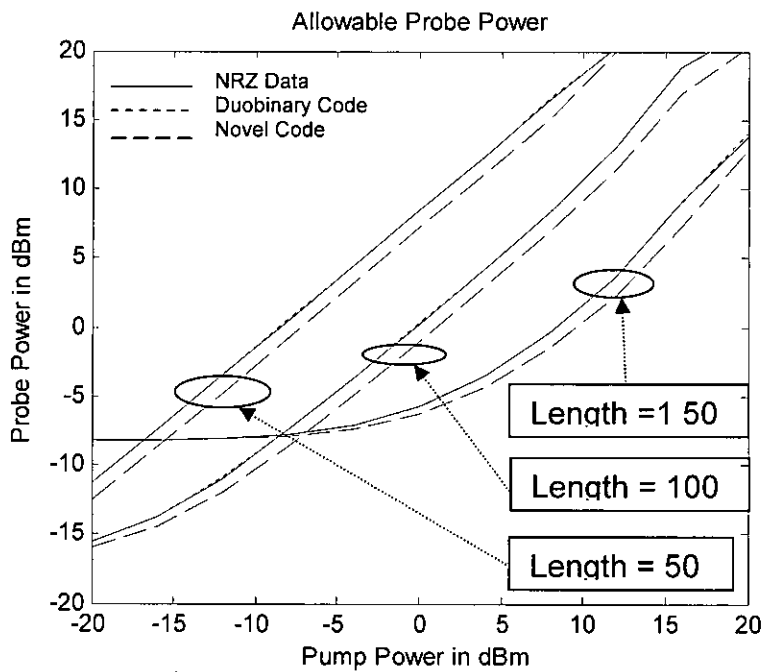
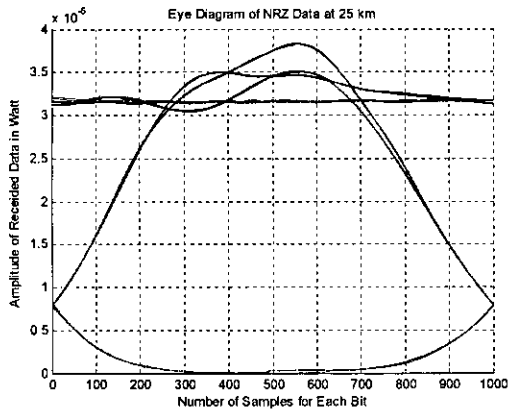


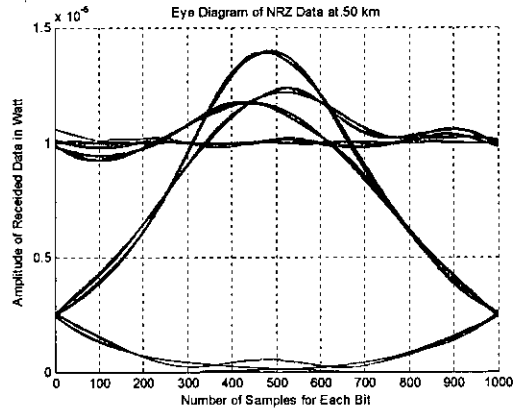
Figure 6.13 Plot of allowable probe power for BER of  $10^{-9}$  at 50, 100 and 150 km

Table 6.2: Improvement in allowable probe power in dB by applying Novel line code in comparison with NRZ data for BER of  $10^{-9}$  at different lengths

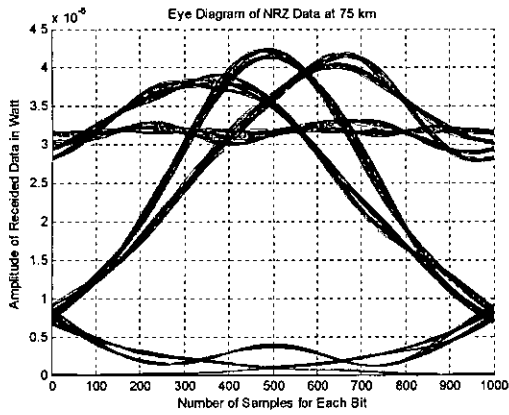
Length (km)	Pump Power in dBm										
	-20	-16	-12	-8	-4	0	4	8	12	16	20
50	1.1930	1.2667	1.2832	1.2854	1.2797	1.2698	1.2660	1.3870	0.4440	0	0
100	0.3760	0.6980	1.0000	1.1683	1.2402	1.2683	1.2823	1.3363	1.5950	1.8910	1.3470
150	0.0085	0.0217	0.0533	0.1268	0.2761	0.5248	0.8203	1.0909	1.4219	1.8162	0.9470



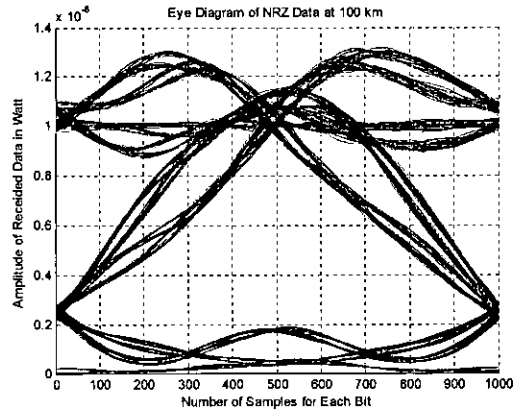
(a)



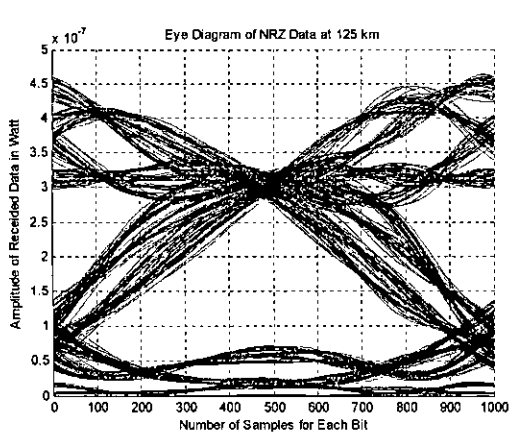
(b)



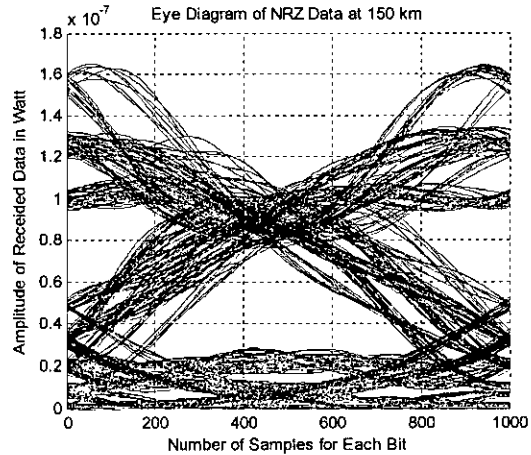
(c)



(d)

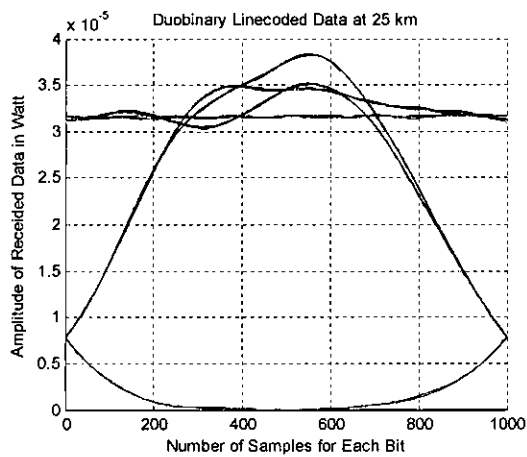


(e)

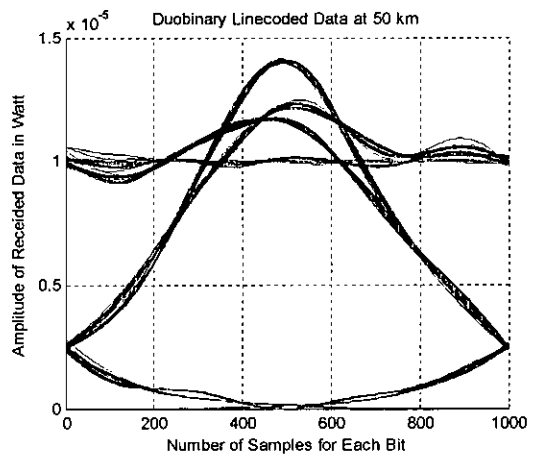


(f)

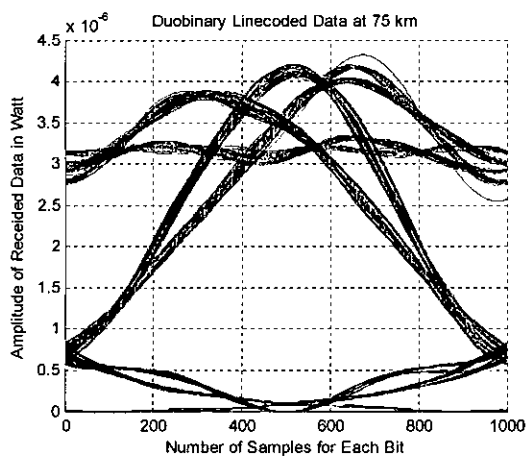
Figure 6.14 Plot of 512 bit (PRBS) eye-power penalty of NRZ data for 25, 50, 75, 100, 125 and 150 km



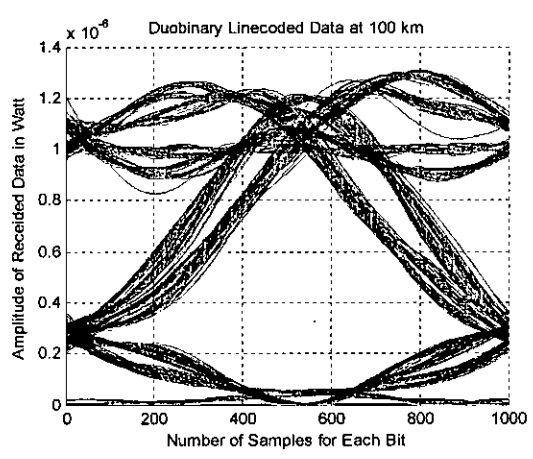
(a)



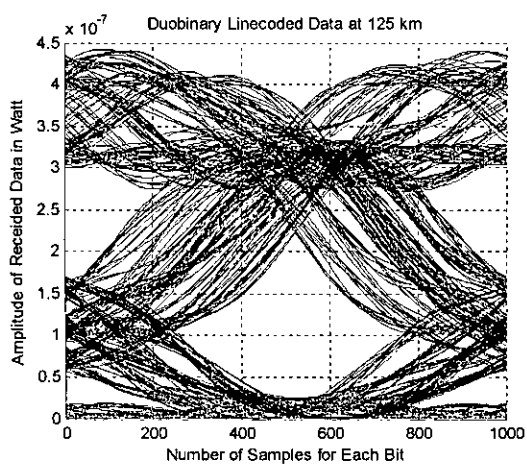
(b)



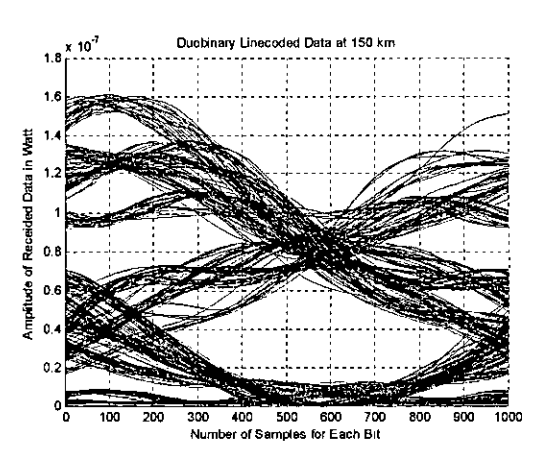
(c)



(d)



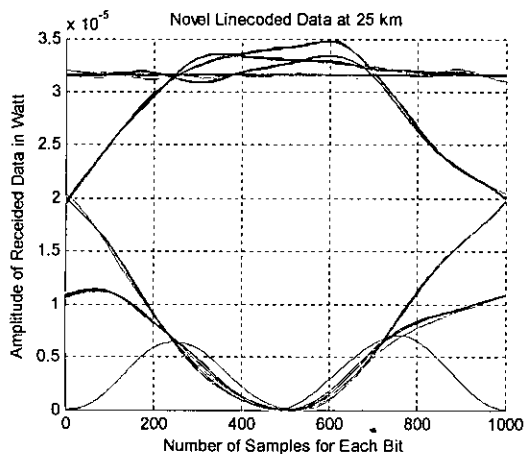
(e)



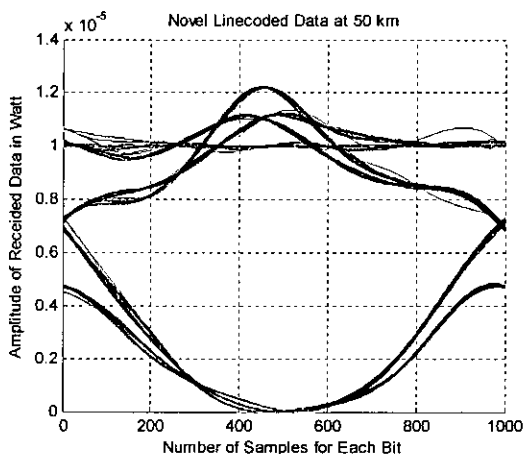
(f)

Figure 6.15 Plot of 512 bit (PRBS) eye-power penalty of Duobinary coded data for 25, 50, 75, 100, 125 and 150 km

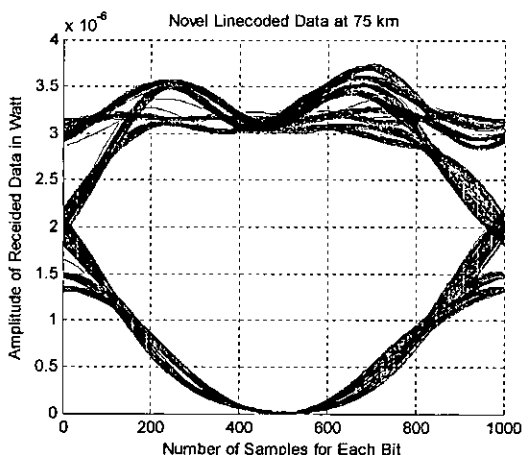




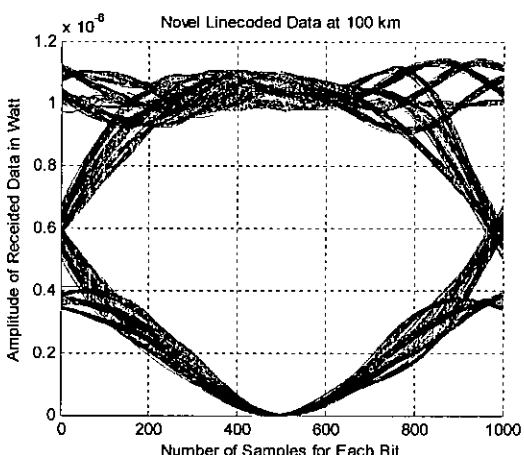
(a)



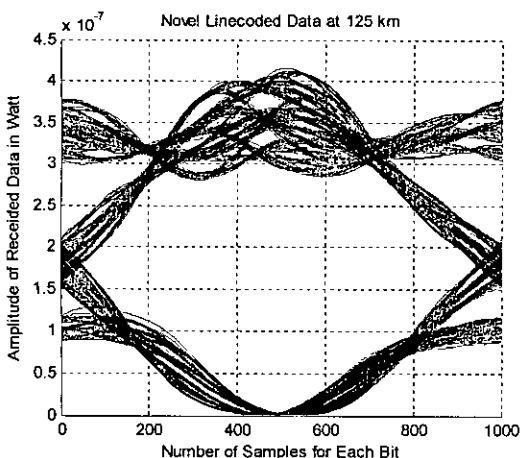
(b)



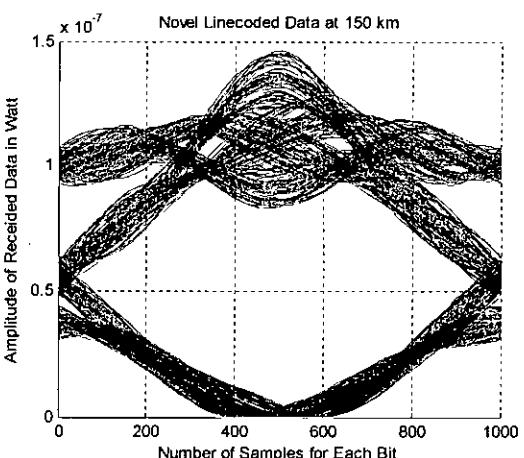
(c)



(d)



(e)



(f)

Figure 6.16 Plot of 512 bit (PRBS) eye-power penalty of Novel Optical coded data for 25, 50, 75, 100, 125 and 150 km

Table 6.3: Eye power penalty for pump power of 0 dBm and probe power of -10 dBm

	Length of Fiber in km					
	25	50	75	100	125	150
NRZ Data	4.6257	9.3113	14.5882	20.0822	25.5588	30.8877
Duobinary	4.6157	9.2144	14.5235	19.7558	25.3566	30.8043
Novel Code	4.8264	9.5936	15.0597	19.8245	24.5400	29.5663

Table 6.3 also shows that the improvement obtained by using the Novel Order 1 code, is about 1.3 dB which conforms to the allowable probe and pump power improvement. Thus we can conclude here that the application of multilevel optical line code especially the Novel Optical code is effective in combating the effect of XPM. It gives an improvement of about 1.3 dB in terms of pump or probe power.

Cartaxo [16] showed that XPM-induced IM in fiber links with multiple optical amplifiers can be enhanced or reduced by properly arranging the dispersion characteristics in each fiber segment of a multiple segment fiber system. In a non-dispersion compensated amplified link and for weak walk-off effect, the total XPM induced IM increases approximately with the square of the number of fiber segments and of modulation frequency. However, if the dispersion is compensated for within each fiber segment the total XPM induced IM increases proportionately to the number of fiber segments and to the square frequency.

Figure 6.17 (taken from [16]) shows the theoretical normalized IM index versus pump modulation frequency for a two-channel system with average power per channel of 0 dBm and channel separation of 0.8 nm. 10 and 20 periodically amplified fiber segments of DSF with  $\lambda_1 = -1.7$  ps/(nm-km),  $dD/d\lambda = 0.065$  ps/(nm<sup>2</sup>-km),  $\gamma_1 = 2.2$  W<sup>-1</sup>km<sup>-1</sup>,  $\alpha = 0.21$  dB/km and  $L = 80$  km are considered. As can be seen from this figure, at low frequency the difference of the normalized IM index corresponding to 20 and 10 fiber segments is about 6 dB resulting from the increase of the IM index proportionally to the

number of segments. At higher frequencies, the walk-off effect is noticeable and such difference becomes smaller. Comparing with the non-DC case a reduction of more than 10 dB is observed when distributed DC with 10 fiber segments is used and a reduction of more than 15 dB is achieved for 20 fiber segments, at low and moderate frequencies.

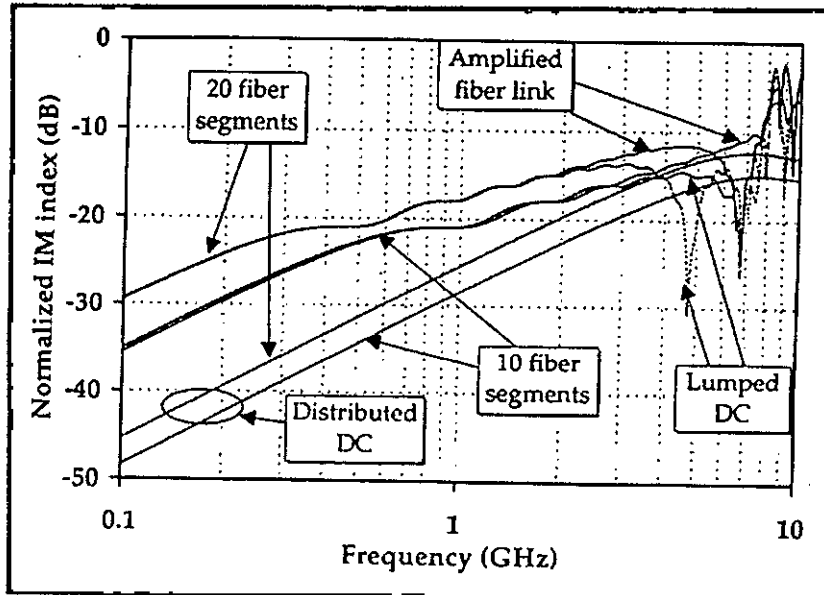


Figure 6.17 Plot of Theoretical normalized IM index in dB as a function of the pump modulation frequency in 10 and 20 fiber segment fiber links of DSF without DC and with distributed and lumped DC. The average power per channel at fiber input is 0 dBm and the channel separation is 0.8 nm.

### 6.3 Discussions

There are many texts where efforts are taken to reduce optical nonlinear effects as a whole including FWM, SPM and XPM by managing the dispersion. But, to the best knowledge of this author, there is no text reported so far that directly quantifies the reduction of XPM effect alone in terms of BER and input powers. Cartaxo [16] discussed an approach to combat XPM by dispersion management in links with multiple fiber segments in terms of XPM index. The improvement in XPM index does not provide any indication about the power penalty or BER. But this paper addresses the XPM effect in a single segment by reducing it applying line coding schemes without dispersion

management. Hence, the findings of this paper could not be compared with the findings of similar kind which could help better establish the findings of this study.

## **6.5 Summary**

This chapter presented the simulated expressions of XPM in the MATLAB environment. Different parameters related to XPM are also presented. Parameters like the input powers in probe and pump channel, channel spacing and bit rate are discussed here showing their effects on XPM. Two line codes are applied here. They are duobinary and Novel optical coding. For performance evaluation two methods are applied. They are BER calculation and eye-power penalty determination. For calculating BER, the input in the probe channel was a CW signal and the input in the pump channel was spaces for "0" and rectangular pulses for "1". For calculating the eye-power penalty, both probe and pump channel inputs were spaces for "0" and rectangular pulses for "1". Finally the result shows that maximum 1.89 dB improvement can be achieved by using the Novel optical line code whereas the duobinary coding did not show mentionable improvement. However, the findings of this study could not be compared with the findings of same kind as such findings are not reported so far.

## CHAPTER 7

### CONCLUSION AND RECOMMENDATIONS FOR FUTURE WORK

#### 7.1 Conclusion of this Study

A rigorous analysis has been carried out to explain the optical line coding scheme, quantify the effect of XPM, modeling the system to apply the line coding scheme and finally to quantify the effect of the application of line coding scheme in a multiple channel DWDM scheme. The application of line coding in optical communication system exhibits promising features that will be useful for future high speed, long distance optical networks. The multilevel line coding schemes especially Novel Optical line code of order one show an improvement of about 1.3 dB at different lengths. The parameters of the optical communication system model discussed in this study conform to the real life optical systems. At longer distance, high bit rate and lower channel spacing the XPM effect become more dominant causing higher BER. It has been observed that the performance of conventional DWDM system without employing appropriate line coding show more ISI, the performance is further deteriorated when channel spacing is less and input power per channel is high. Line coding scheme is found an effective tool in combating the nonlinear effects by reducing the dispersion effects. Two line coding schemes; Duobinary and Novel Optical coding were described in detail. These schemes are implemented in the modeled system to combat the effect of XPM successfully. Out of these two schemes, Novel Optical line coding of order one is found more effective. A remarkable improvement in system performance can be achieved by this scheme. Maximum allowable input power per channel is much higher than that of a system without line coding. The balanced configuration of the system including the encoder, transmitter, amplifier, receiver and decoder yields a system with lower BER even at lower channel spacing and longer distance which enables larger link length at higher band width. Therefore, these schemes will also be attractive for DWDM networks.

## **7.2 Recommendations for Future Work**

In our work we have assumed that the fibers used in the transmission system are perfect without considering FWM, SRS, SBS, PMD, etc. Therefore, a study on how line coded DWDM system performs after considering those nonlinear effects is of immediate of interest. In the calculation of bit error rate (BER), we have not encountered the response of the optical filters and amplifier noise, and if fiber amplifiers are used, then FWM effect in these fibers will also have to be taken into account. Moreover, we have analyzed the systems considering only a repeater-less network. So there is an opportunity to analyze the multi-channel multi-repeater systems and the combined systems considering amplifier noise along with shot noise, thermal noise and FWM noise. Future studies may include dispersion management schemes with line coding schemes to combat the nonlinear effects.

## REFERENCES

- [1] Senior J. M., "Optical Fiber Communication"; 2<sup>nd</sup> Ed., New Delhi, Prentice-Hall of India, 2002.
- [2] Kao K. C. and Hockham G. A., "Dielectric Fiber Surface Waveguides for Optical Frequencies"; Proceedings of the IEE, vol. 133, pp.1151-1158, July 1966.
- [3] Trischitta, M. Colas, M. Green, G. Wuzniak, and J. Arena, "The TAT-12/13 cable network"; IEEE Communication Magazine, vol.34, no.2, pp.24-28, February 1996.
- [4] Barnett W. C., Takahira H., Baroni G. C., and Ogi., "The TPC-5 Cable Network"; IEEE Communication Magazine, vol.34, no.2, pp.36-40, February 1996.
- [5] Jamal S. and Cartledge J. C., "Variation in the Performance of Multispan 10 Gb/s Systems Due to the Group Delay Ripple of Dispersion Compensating Fiber Bragg Gratings"; IEEE Journal of Lightwave Technology, vol. 20, no. 1, pp. 28-35, January 2002.
- [6] Sharif M. and Alkhansari M. G., "On the Peak-to-Average Power OFDM Signals Based on Oversampling"; IEEE Transactions on Communications, Vol. 51, No. 1, pp 72-78, January 2004.
- [7] Bergano N. S., "Long-Haul WDM Transmission Using Optimum Channel Modulation: A 160 Gb/s (32x5 Gb/s) 9,300 km Demonstration"; Proceedings of Optical Fiber Communications Conferences, paper PD-21, February 1997.
- [8] Srivastava A. K., "L-Band 64 10 Gb/s DWDM Transmission over 500km DSF with 50GHz Channel Spacing"; ECOC'98, pp.73-75, September 1998.
- [9] Bergano N. S., "640 Gb/s Transmission of Sixty-four 10Gb/s WDM Channels Over 7200km With 0.33 (bits/s)/Hz Spectral Efficiency"; Proceedings of Optical Fiber Communications Conferences, paper PD2, February 1999.
- [10] Vareille G., "340Gb/s (34x10Gb/s, 50 GHz spacing DWDM) Straight Line Transmission Over 6380 km with Full System Implementation Assessment"; Proceedings of Optical Fiber Communications Conferences, paper PD18, February 1999.
- [11] Marcuse D., Chraplyvy A. R. and Tkach R. W., "Dependence of Cross-Phase Modulation on Channel Number in Fiber WDM Systems"; Journal of Lightwave Technology, vol.12, no.5, pp.885-890, May 1994.
- [12] Chiang T. K., "Cross-phase modulation in dispersive fibers: theoretical and experimental investigation of the impact of modulation frequency"; IEEE Photonics Technology Letters, vol.6, no.6, pp.733-736, June 1994.
- [13] Chiang T. K., "Cross-Phase Modulation in Fiber Links with Multiple Optical Amplifiers and Dispersion Compensators"; Journal of Lightwave Technology, vol.14, no.3, pp.249-259, March 1996.

- [14] Song K. and Premaratne M., "Effects of SPM, XPM and Four Wave Mixing in L-Band EDFAs on Fiber-Optic Signal Transmission"; IEEE Photonics Technology Letters, Vol 12, No 12, pp. 1630-1632, December 2000.
- [15] Cartaxo A. V. T., "Impact of Modulation Frequency on Cross Phase Modulation Effect in IM/DD WDM Systems"; IEEE Photonics Technology Letters, vol.10, no.9, , pp.1268-1270, September 1998.
- [16] Cartaxo A. V. T., "Cross Phase Modulation in Intensity Modulation – Direct Detection WDM systems with Multiple Optical Amplifiers and Dispersion Compensators"; Journal of Lightwave Technology, Vol. 17, No. 2, , pp. 178-190, February 1999.
- [17] Kim H., Han K. H. and Chuang Y. C., "Performance Limitation of Hybrid WDM Systems Due to Stimulated Raman Scattering"; IEEE Photonics Technology Letters, vol.13, no.10, pp 855-858 October 2001.
- [18] Djordjevic B. I., "Transmission Limitations of WDM Transmission Systems with Dispersion Compensated Links in the Presence of Fiber Nonlinearities"; IEEE Photonics Technology Letters, vol.1, no.2, pp. 496 – 499, March 2001.
- [19] Norimatsu S. and Yamamoto T., "Waveform Distortion Due to Stimulated Raman Scattering in Wide Band WDM Transmission Systems"; Journal of Lightwave Technology, vol.19, no.2, 226-236 February 2001.
- [20] Bellotti G., "Intensity Distortion Induced by Cross-Phase Modulation and Chromatic Dispersion in Optical-Fiber Transmissions with Dispersion Compensation"; IEEE Photonics Technology Letters, vol.10, no.12, pp.1745-1747, December 1998.
- [21] Kowalewski M., Marciniak M. and Sedlin A., "Nonlinear Interactions in Wavelength Multiplexed Optical Fiber Telecommunications Systems"; Journal of Optics, Pure Applications, pp 319-326, February 2000.
- [22] Lakoba T. I. and Agrawal G. P., "Optimization of the Average-Dispersion Range for Long-Haul Dispersion-Managed Systems"; Journal of Lightwave Technology, vol.18, no.11, pp 1504-1512 November 2000.
- [23] Ten S., Ennser K. M., Grochocinski J. M., Burtsev S. P. and Silva V. L., "Comparison of Four Wave Mixing and Cross Phase Modulation Penalties in dense WDM at 2.5 GBits/s"; Journal of Lightwave Technology, vol.19, no.5, pp 679-685 May 2000.
- [24] Betti S., Giacon M. and Nardini M., "Effect of Four Wave Mixing on WDM Optical Systems: A Statistical Analysis"; IEEE Photonics Technology Letters, vol.18, no. 8, pp.745-747, August 2003.
- [25] Thiele H. J., Killely R. I. and Bayvel P., "Pump-Probe Investigation of Cross Phase Modulation in Standard-Fibre, Dispersion Compensated WDM Recirculating Loop"; Conference on Lasers and Electro-Optics, pp.305-306, May, 1999.



- [26] Keang P. H., "Channel Capacity of WDM Systems Using Constant Intensity Modulation Formats"; Proceedings of Optical Fiber Communications Conferences, May 2002.
- [27] Hoon K., "Cross Phase Modulation Induced Nonlinear Phase Noise in WDM Direct Detection DPSK Systems"; Journal of Lightwave Technology, vol. 21, no. 8, pp 1126-1137 August 2003.
- [28] Sang S. L., Hyun J. L., Wanseok S. and Seung G. L., "Stimulated Brillouin Suppression Using Cross Phase Modulation Induced by an Optical Supervisory Channel in WDM Links"; IEEE Photonics Technology Letters, vol. 13, no. 7, pp.145-149, July 2001.
- [29] Wang Z., Bodtker E. and Jacobson G., "Effects of Cross Phase Modulation in Wavelength Multiplexed SCM Video Transmission Systems"; Electronic Letters, vol. 31, no. 10, pp 893-896 October 1995.
- [30] Bellotti G., Varani M., Francia C. and Bononi A., "Intensity Distortion Induced by XPM and Chromatic Dispersion in Optical Fiber Transmission with Dispersion Compensation"; IEEE Photonics Technology Letters, Vol 10, No 12, pp. 605-607, Dec 1998.
- [31] Hui R., Demarest K. R. and Allen C. T., "Cross Phase Modulation in Multispan WDM Optical Fiber Systems"; Journal of Lightwave Technology, vol. 17, no. 6, pp 1018-1026, June 1999.
- [32] Thiele H. J., Killy R. I. and Bayvel P., "Investigation of XPM Distortion in Transmission over Installed Fiber"; IEEE Photonics Technology Letters, Vol 12, No 6, pp 669 -671, June 2000.
- [33] Hui R., Wang Y., Demarest K. and Allen C., "Frequency Response of Cross Phase Modulation in Multispan WDM Optical Fiber Systems"; IEEE Photonics Technology Letters, Vol 10, No 9, pp 1271 -1273, September 1998.
- [34] Majumder S. P., Gangopadhyay R., Alam M. S. and Prati G., "Performance of Linecoded Optical Hetrodyne FSK Systems with Nonuniform Laser FM Response"; Journal of Lightwave Technology, Vol. 13, No. 4, pp. 628-638, April 1995.
- [35] Forestieri E. and Giancarlo P., "Novel Optical Line Codes Tolerant to Fiber Chromatic Dispersion"; Journal of Lightwave Technology, Vol. 19, No. 11, pp. 1675-1684, November 2001.
- [36] Agrawal G. P., Nonlinear Fiber Optics, Second Ed., Academic Press, San Diego, 1995. pp. 5-20, 267-288.
- [37] Aoki Y., Tajima K. and Mito I., "Input Power Limits of Single-Mode Optical Fibers Due to Stimulated Brillouin Scattering in Optical Communication Systems"; Journal of Lightwave Technology, vol.6, no. 5, pp. 710-719, May 1988.

- [38] Forghieri F., Tkach R. W. and Chraplyvy A. R., "Fiber Nonlinearities and Their Impact on Transmission Systems"; in *Optical Fiber Telecommunications IIIA*, Academic Press, 1997.
- [39] Chraplyvy, "Impact of Nonlinearities on Lightwave Systems"; *Optics and Photonics News*, vol.5, pp.16-21, May 1994.
- [40] Chraplyvy A. R. and Tkach R. W., "What is the Actual Capacity of Single-Mode Fibers in Amplified Lightwave Systems?"; *IEEE Photonics Technology Letters*, vol.5, no.6, pp.666-668, June, 1993.
- [41] Peckham D. W., Judy A. F. and Kummer R. B., "Reduced Dispersion Slope, Nonzero-Dispersion Fiber"; *Proceedings of European Conference on Optical Fiber Communication (ECOC '98)*, vol.2, pp.139-140, September 1998.
- [42] Shen S., Cheng-Chun C., Sardesai H. P., Binjrajka V. and Weiner A. M., "Effects of Self-Phase Modulation on Sub-500 fs Pulse Transmission over Dispersion Compensated Fiber Links"; *Journal of Lightwave Technology*, Vol. 17, No. 3, pp. 452-461, March 1999.
- [43] Kikuchi N. and Sasaki S., "Analytical Evaluation Technique of Self-Phase-Modulation Effect on the Performance of Cascaded Optical Amplifier Systems"; *Journal of Lightwave Technology*, Vol. 13, No. 5, pp. 868-878, May 1995.
- [44] Talukder M. A., "Analysis of Self-Phase Modulation Effect on Optical WDM System With Dispersion Compensation"; M. Sc. Thesis, Dept of EEE, BUET, 2004.
- [45] Kurtzke C., "Suppression of Fiber Nonlinearities by Appropriate Dispersion Management"; *IEEE Photonics Technology Letters*, vol.5, pp. 1250-1253, 1993.
- [46] Rongqing H., Kenneth R. D. and Christopher T. A., "Cross Phase Modulation in Multispan WDM Optical Fiber Systems"; *Journal of Lightwave Technology*, Vol. 17, No. 6, pp. 1018-1026, June 1999.
- [47] Faisal M., "Analysis of Wavelength Shift keying Technique with Dispersion Management Scheme to Reduce Four-Wave Mixing Effect in Optical WDM System"; M. Sc. Thesis, Dept of EEE, BUET, 2003.
- [48] Brandt-Pearce M., Jacobs I., Lee J. H. and Shaw J. K., "Optimal Input Gaussian Pulse Width for Transmission in Dispersive Nonlinear Fibers"; *Journal of Optical Society of America*, vol. 16, no.8, pp.1189-1196, August 1999.
- [49] Hayashi Y., "Verification of Four-Wave Mixing Suppression in WDM Transmission Experiments on the FSA Commercial System with Dispersion Managed Optical Fiber Cable"; *Optical Fiber Communications Conferences Technical Digest Paper*, pp.49-50, February, 1996.
- [50] Takahashi H. and Inoue K., "Cancellation of Four-Wave Mixing by use of Phase Shift in a Dispersive Fiber Inserted into a Zero-Dispersion Transmission Line"; *Optics Letters*, vol.20, no.8, pp.860-862, April 1995.

[51] Tkach R. W., "Four-Photon Mixing and High-Speed WDM Systems"; Journal of Lightwave Technology, vol.13, no.5, pp.841-849, May 1995.

[52] "Duobinary Code" at <http://www.inphi-corp.com/products/whitepapers/DuobinaryModulationForOpticalSyatems.pdf>

[53] Ezmir M. R. Majumder S. P. and Muhammad A. F., "Eye Penalty Due to Cross-Phase Modulation (XPM) in a Single Segment WDM IM/DD Transmission System"; Faculty of IT, Multimedia University, Malaysia.

[54] Pal B., Gangopadhyay R. and Prati G., "Analytical Evaluation of Transmission Penalty Due to Group Velocity Dispersion, Self-Phase Modulation and Amplifier Noise in Optical Heterodyne CPFSK Systems"; Journal of Lightwave Technology, Vol. 18, No. 4, pp. 530-539, April 2000.

[55] Proakis G. P. and Salehi M., *Communication System Engineering*, 2<sup>nd</sup> Ed., Pearson Education, Delhi, India, 2003.

[56] Binh L. N. and Perera D., "Modelling Platform for Ultra-Long Ultra-High-Speed Dispersion-Managed DWDM Optical Fibre Communication Systems"; Technical Report, MECSE-13-2003, Monash University.

